Observations of Dust in Space from Space

Takashi Onaka
(University of Tokyo)

UV observations (extinction & depletion)

X-ray observations (scattering & absorption)

IR observations (emission & absorption)

0.1 μm

Small particles produced by
Gas-evaporation method in the lab

Interstellar Extinction Curve

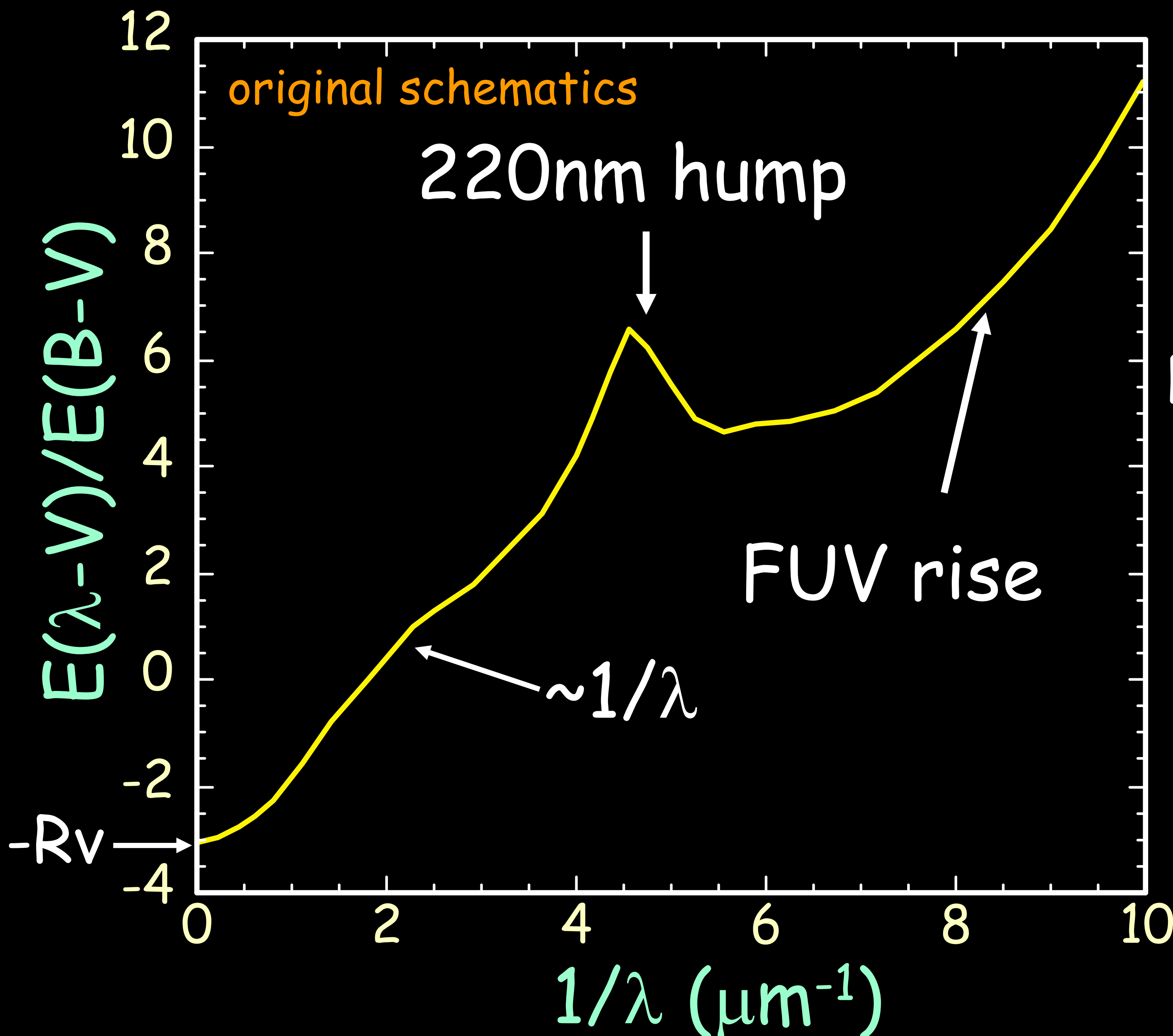

Tells us the dust size and compositions

Distinct feature at 220nm (UV)

Carbonaceous origin of the 220nm feature
Graphite?
PAH?

Mysteries of the 220nm hump

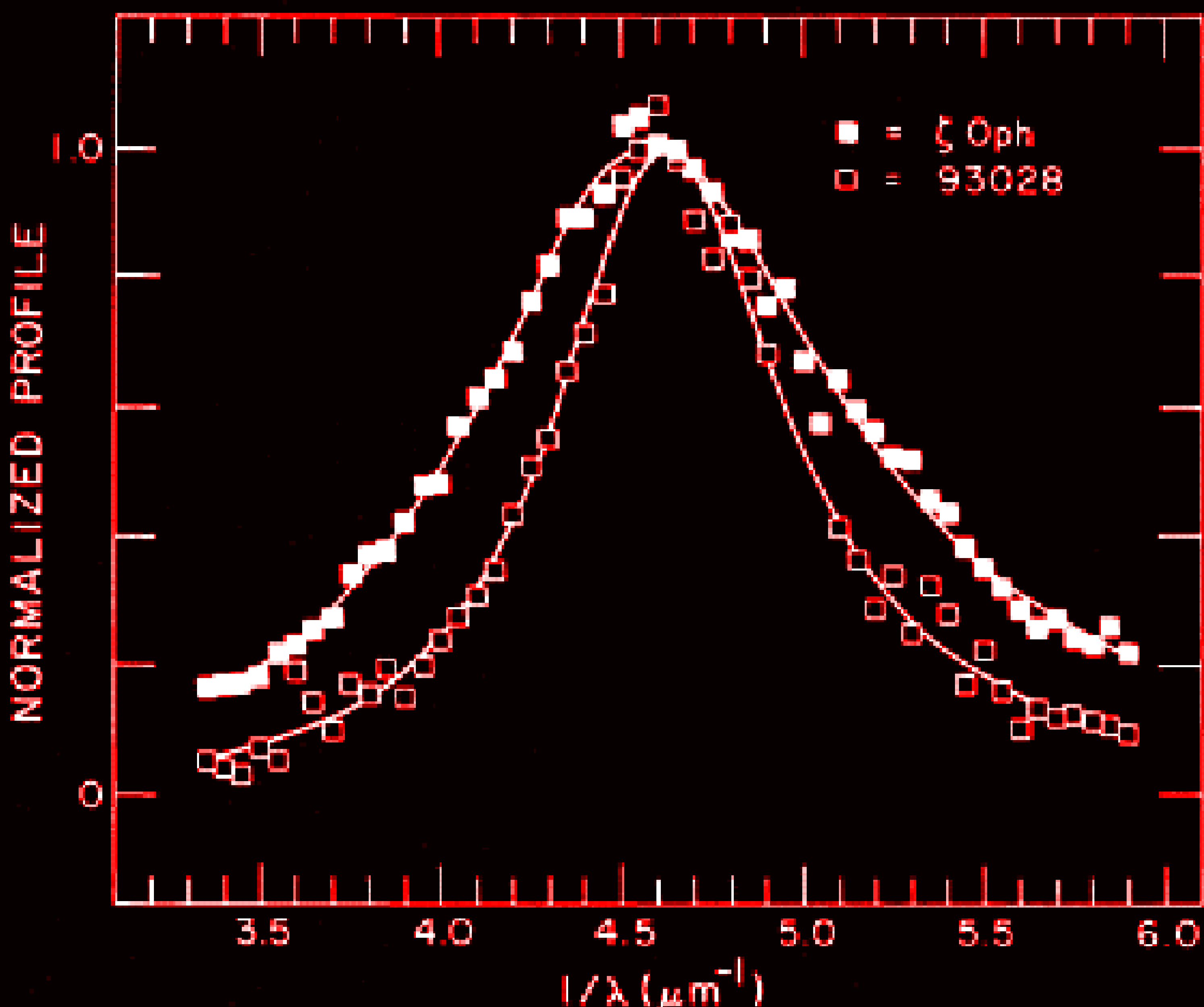

Constant peak wavelength against varying width

Fitzpatrick & Massa (1986) ApJ, 307, 286

No correlation between λ0 and γ

$$\sim 1/[\{1/\lambda - (\lambda/\lambda_0^2)\}^2 + \gamma^2]$$

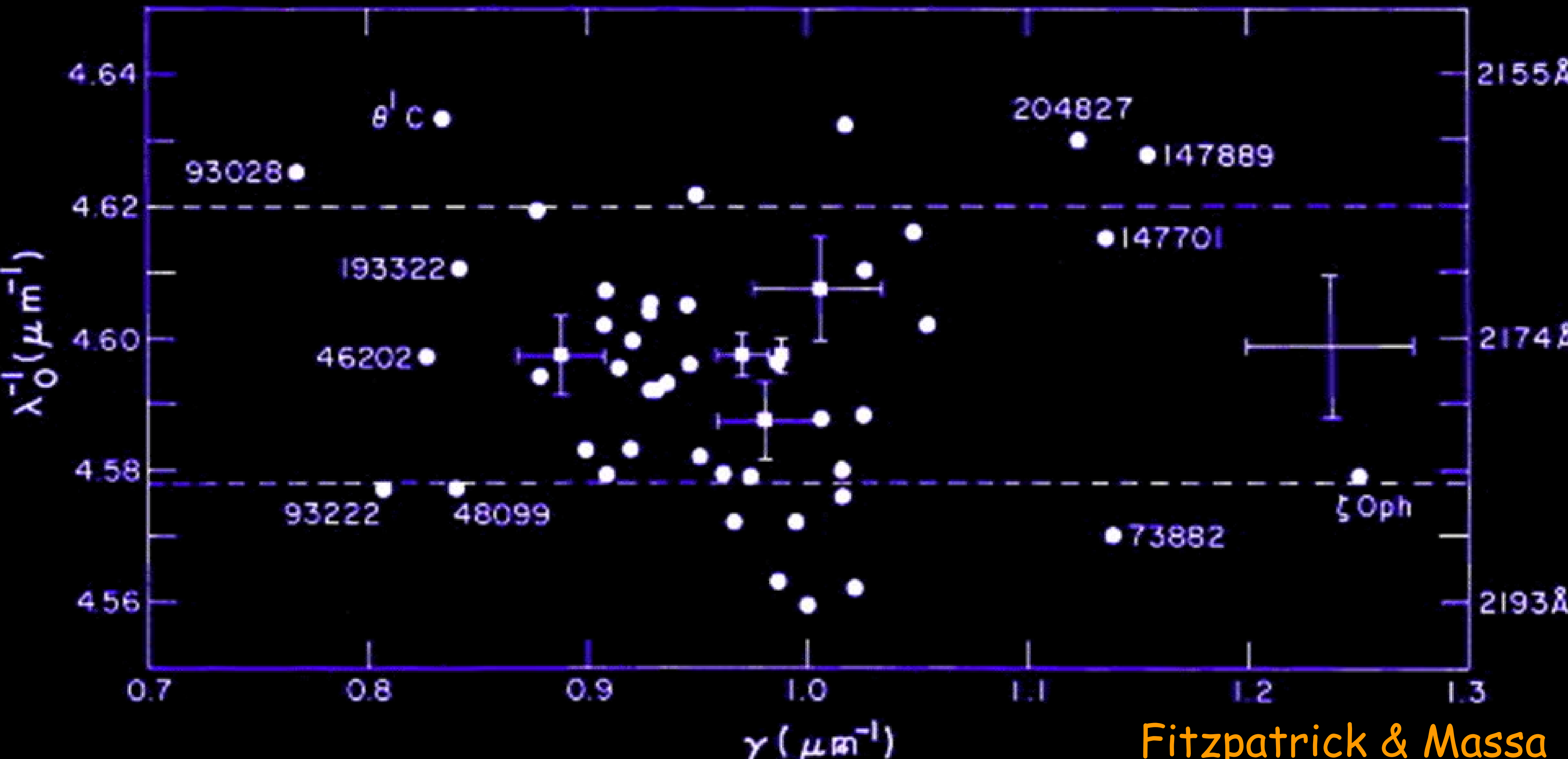

Fitzpatrick & Massa
1986 ApJ, 307, 286

Difficult to be interpreted by single component model

2 components for 220nm hump?

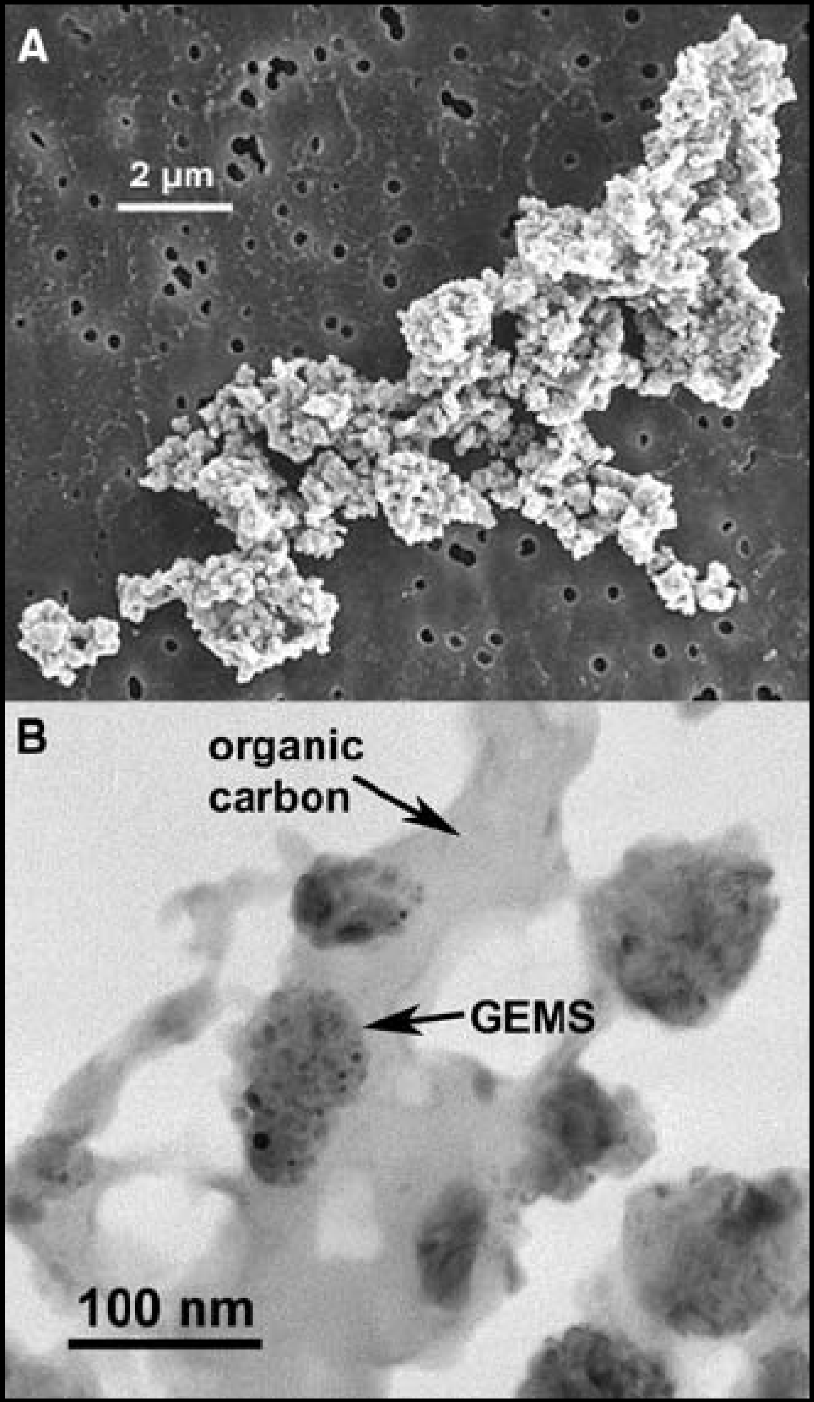

Interplanetary Dust Particles (IDPs)

GEMS (glass with embedded metal sulfides) an interstellar dust analogue?

Bradley et al. (2005) Science 307, 244

The 1st CPS International School of Planetary Sciences
Dust in Space
January 5 - 9, 2009
Kobe, Japan

220nm in IDPs

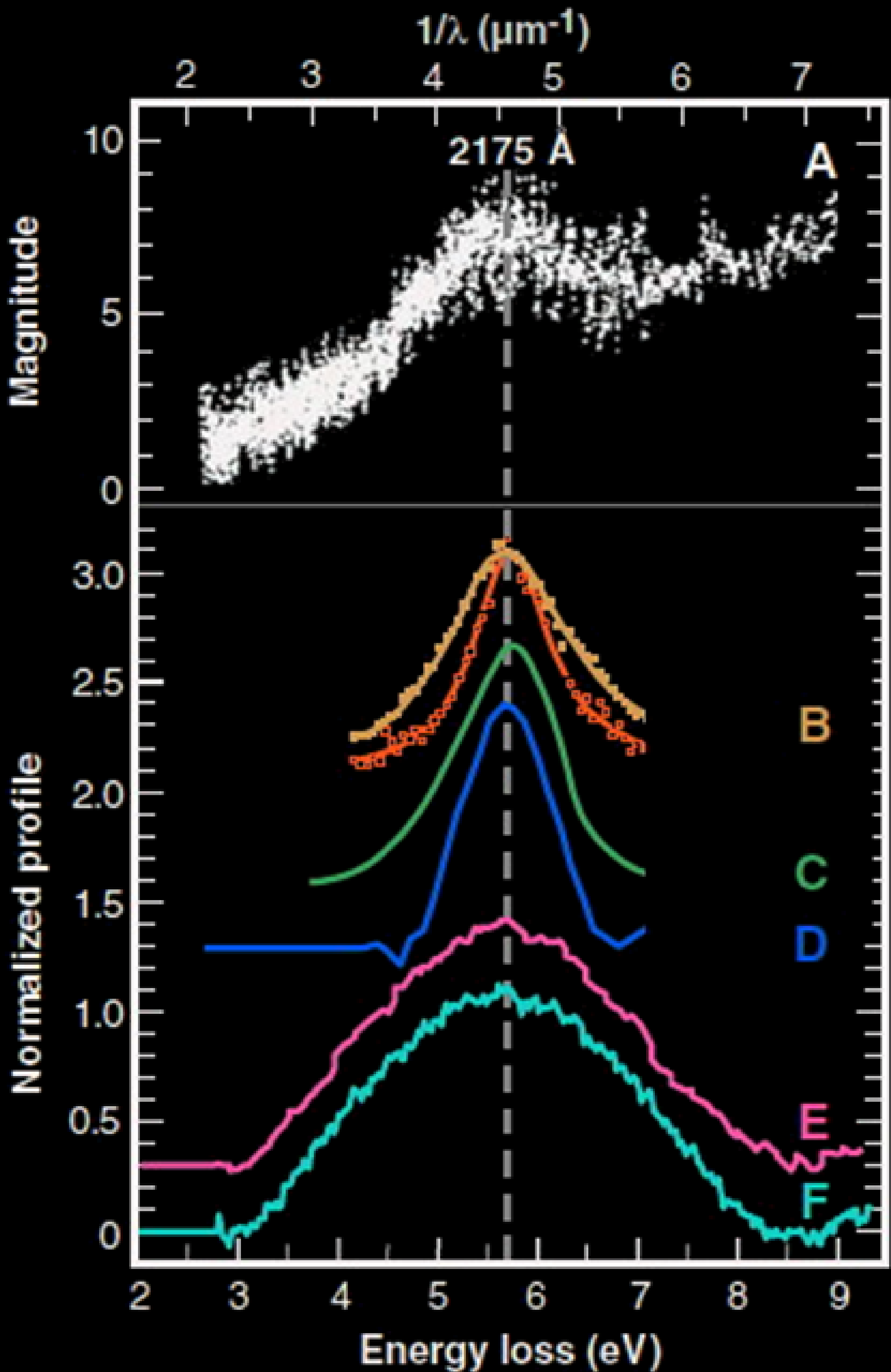

A, B: Observations
C, D: hydroxylated (OH-) Mg silicates
E: organic C in IDP
F: GEMS in IDP

OH-silicate has a feature at 220nm
(Steel & Duley 1987, ApJ, 315, 337)

Contribution of 2 components (carbonaceous and silicate) may account for the non-correlation of λo and γ

Interstellar Gas Depletion

Observations of interstellar gas absorption
➔ gas abundance in the ISM
[metal absorption lines are mostly in the UV]

Depletion = Log (gas abundance in the ISM
/reference abundance)

Reference abundance = generally solar abundance

Depleted elements are thought to reside in dust grains

➔Elemental depletion indicates the dust composition
(associated with the uncertainty
in the reference abundance)

UV absorption lines

Observations towards HD93521 HST/GHRS

Need high spectral resolution to resolve velocity components

Most metal lines are in the UV

Savage & Sembach (1996) ARAA 34, 279

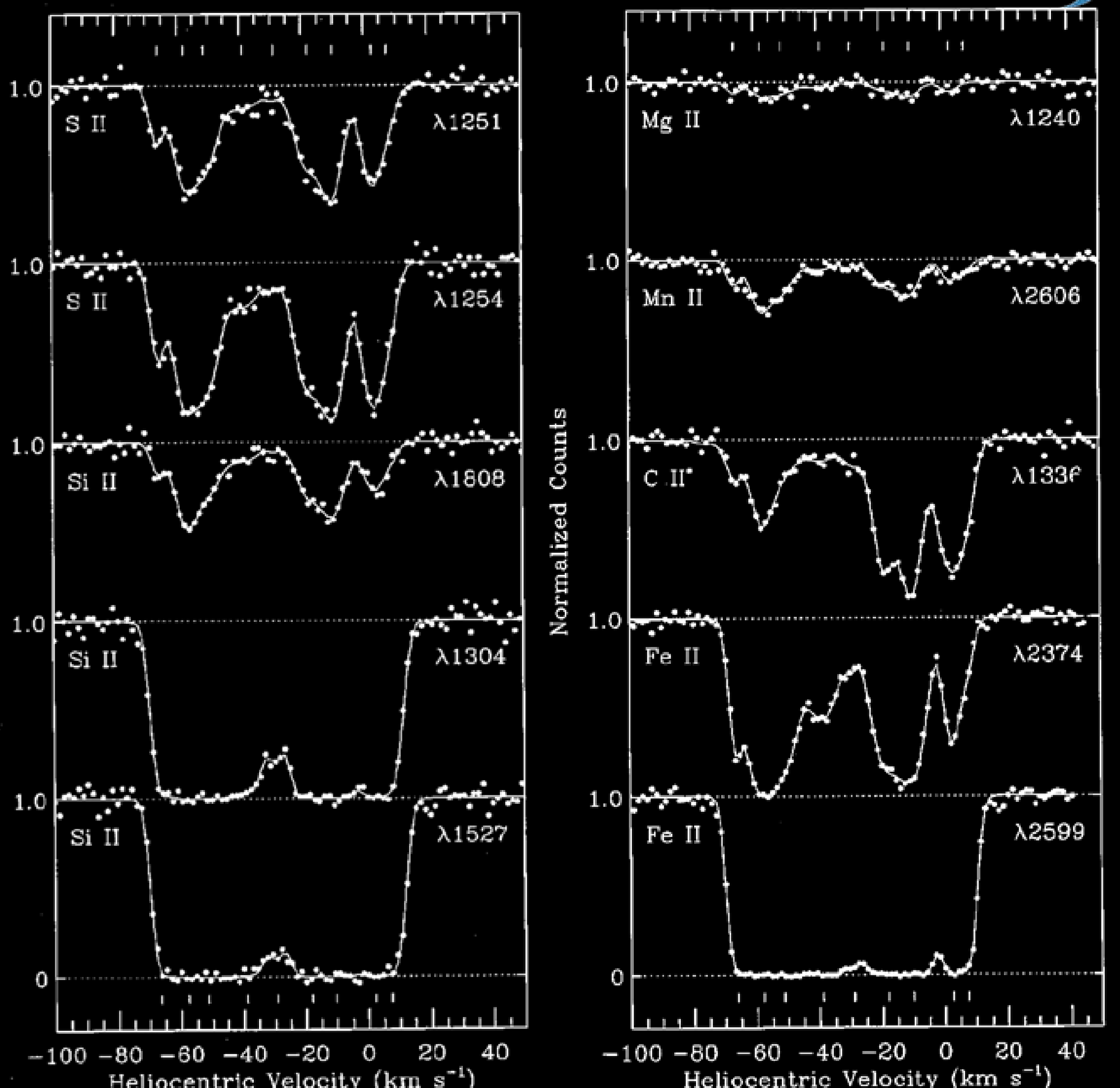

Interstellar Depletion

Depletion correlated with condensation Temperature T_d*

*temperature at which a half of the element in question will be condensed

Savage & Sembach (1996) ARAA, 34, 279

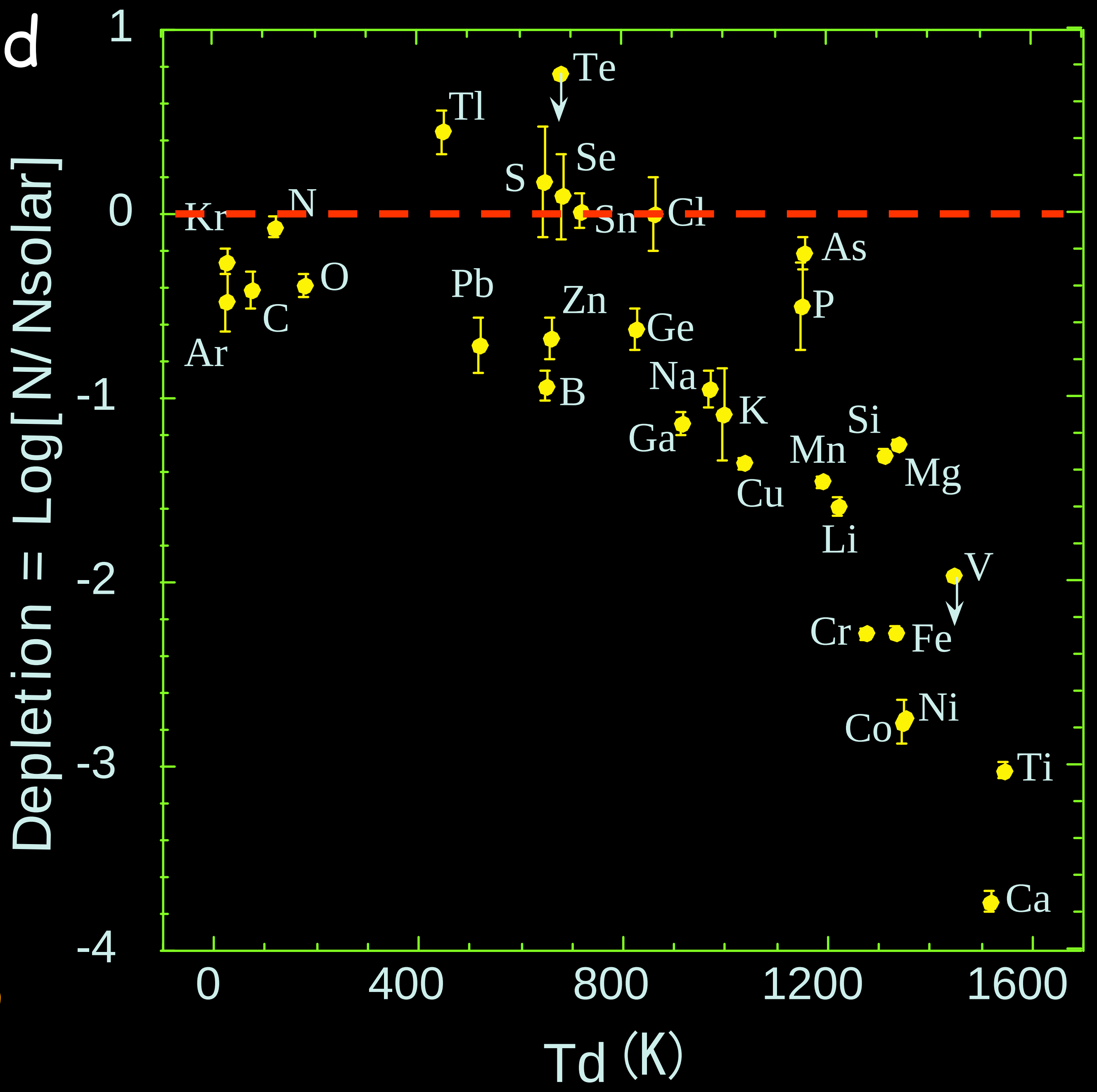

Depletion with abundance

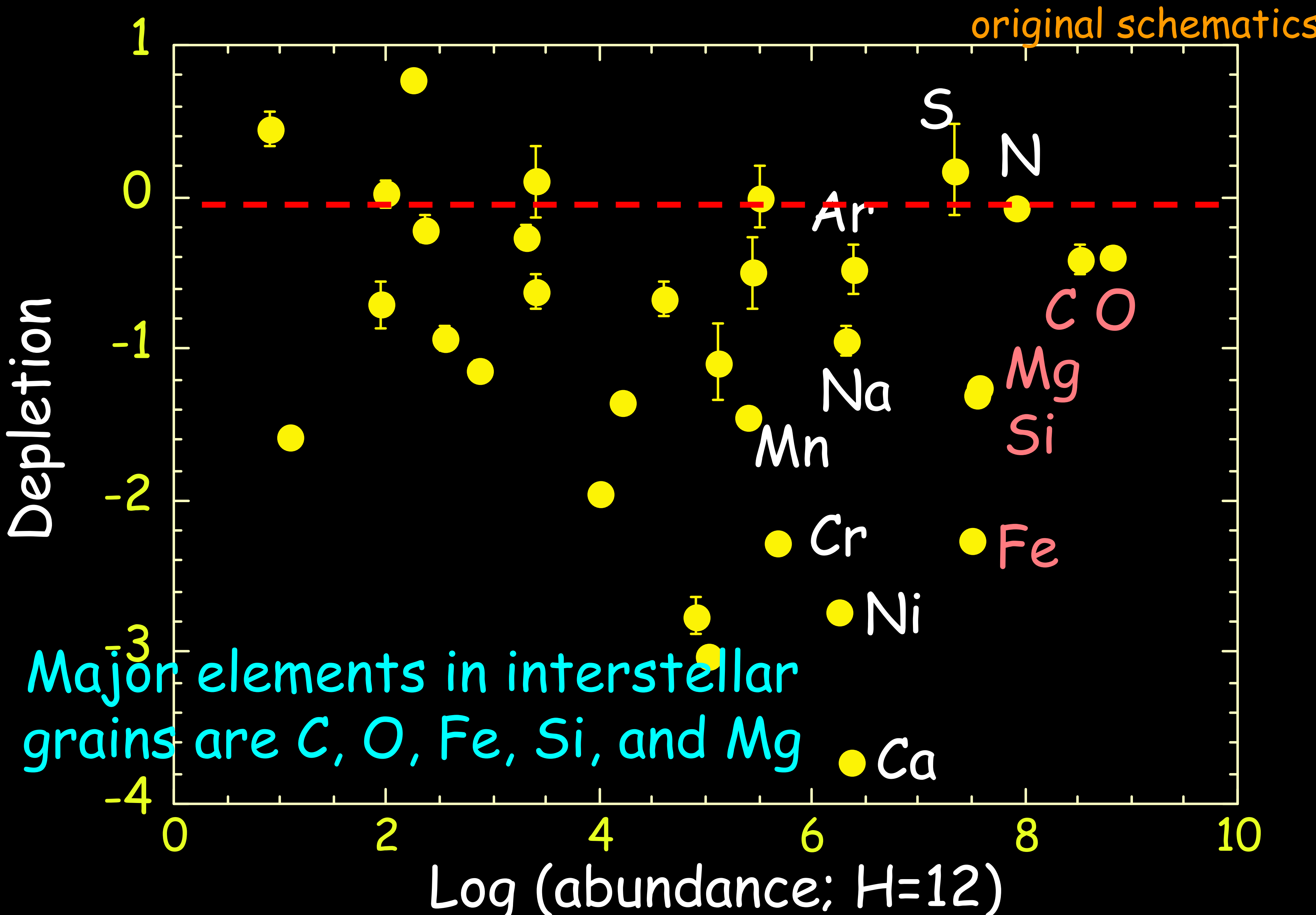

Major elements in interstellar grains are C, O, Fe, Si, and Mg

X-ray observations of interstellar dust

X-ray halo (angular scale ~1′)

Forward scattering by interstellar dust produces a halo around the X-ray source

e.g. Hayakawa (1970) Prog. Theor. Phys. 43, 1224
Mauche & Gorenstein (1986) ApJ, 302, 371
Predehl & Klose (1996) A&A, 306, 283

(2) X-ray spectroscopy of absorption edge & X-ray Absorption Fine Structure (XAFS)
($\Delta E \leq 10$eV)

Abundance estimate of elements in gas and solid phases without the reference abundance uncertainty

X-ray Halo

Forward scattering dominant

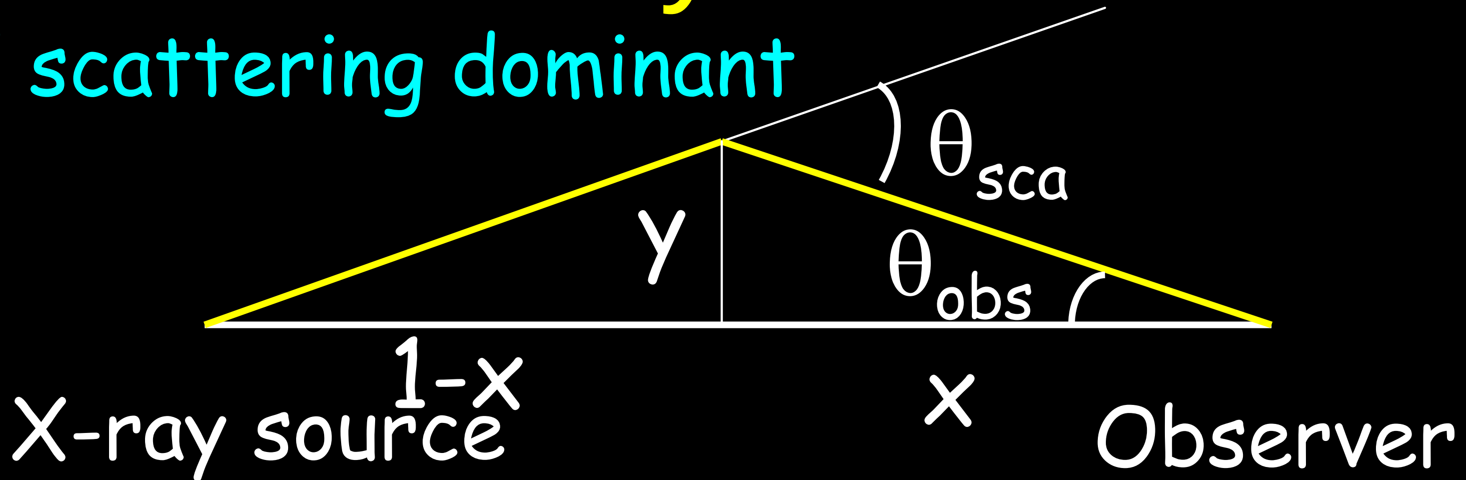

$$\theta_{sca} \sim \theta_{obs} + y/(1-x), \quad \theta_{obs} = y/x$$

$$= [1/(1-x)]\,\theta_{obs}$$

$$I(\theta_{obs}) = F_x N_H \int_{Emin}^{Emax} dE\, S(E) \int_{a(min)}^{a(max)} da\; n(a) \int_0^1 dx \frac{d\sigma}{d\Omega}(\theta_{sca}) \frac{f(x)}{(1-x)^2}$$

Fx: source flux, n(a): size distribution

f(x): spatial distribution;

$\sigma(\theta)$: scattering cross-section;

S(E): source spectrum

Scattering cross-section

$$\frac{d\sigma}{d\Omega}=1.1\times10^{-6}\left(\frac{2Z}{M}\right)^2\left(\frac{\rho}{3g\,cm^{-3}}\right)^2\left(\frac{a}{0.1\mu m}\right)^6\left(\frac{F(E)}{Z}\right)^2\exp\left(-\frac{\theta^2}{2\Delta'^2}\right)cm^2$$

$$\sigma=6.3\times10^{-11}\left(\frac{2Z}{M}\right)^2\left(\frac{\rho}{3g\,cm^{-3}}\right)^2\left(\frac{a}{0.1\mu m}\right)^4\left(\frac{1keV}{E}\right)^2\left(\frac{F(E)}{Z}\right)^2 cm^2$$

Δ' = 10.4 (1 keV/E) (0.1μm/a) arcmin

|m-1| <<1, 2πa|m-1|/λ << 1; Rayleigh-Gans approximation

[valid for E>1-2KeV]

F(E): atomic scattering factor ~ Z far from abs. edge

Mauche & Gorenstein (1986) ApJ, 302, 371

$\sigma_{sca} \sim a^4 \rho^2/E^2 \sim M^2/a^2/E^2$ ($\rho \propto M/a^3$)

Larger dust dominates in X-ray halo scattering

X-ray halo decreases with E^{-2}

Porous dust has less scattering per mass

-> information on the dust porosity/size

Observations by ROSAT(0.1-2.4keV)

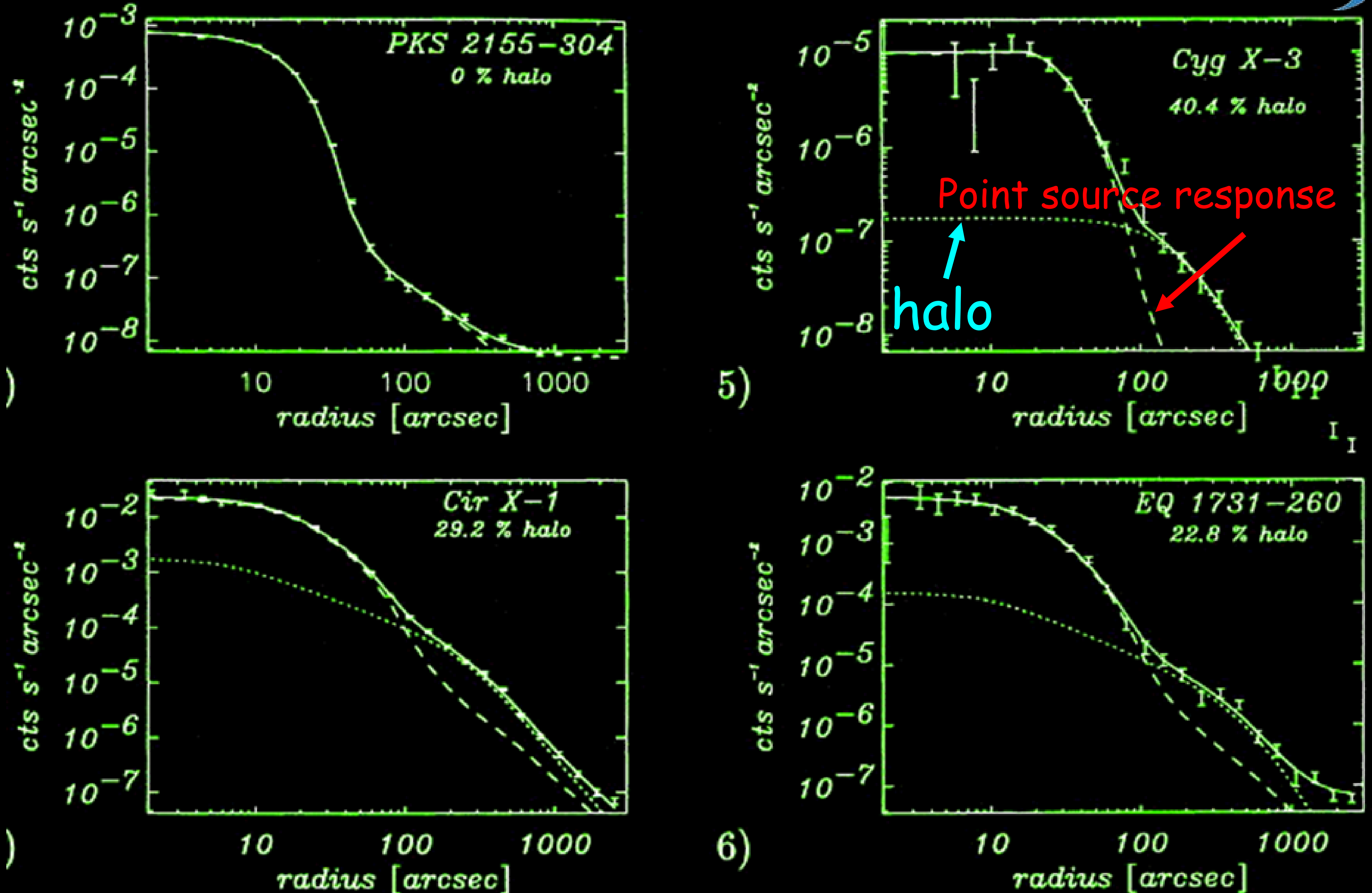

Predehl & Schmitt (1995) A&A, 293, 889

Correlation with Av

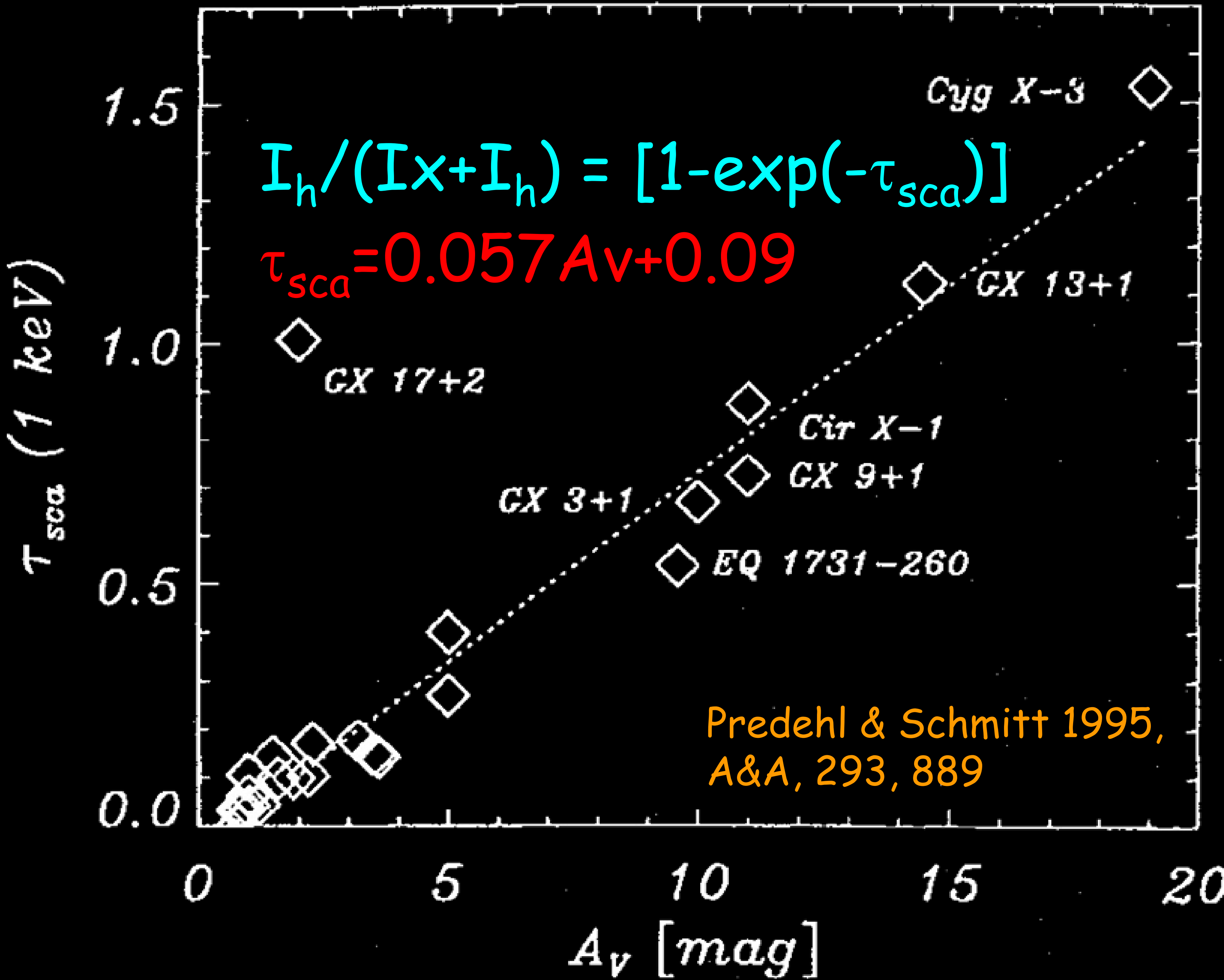

Correlation with N_H

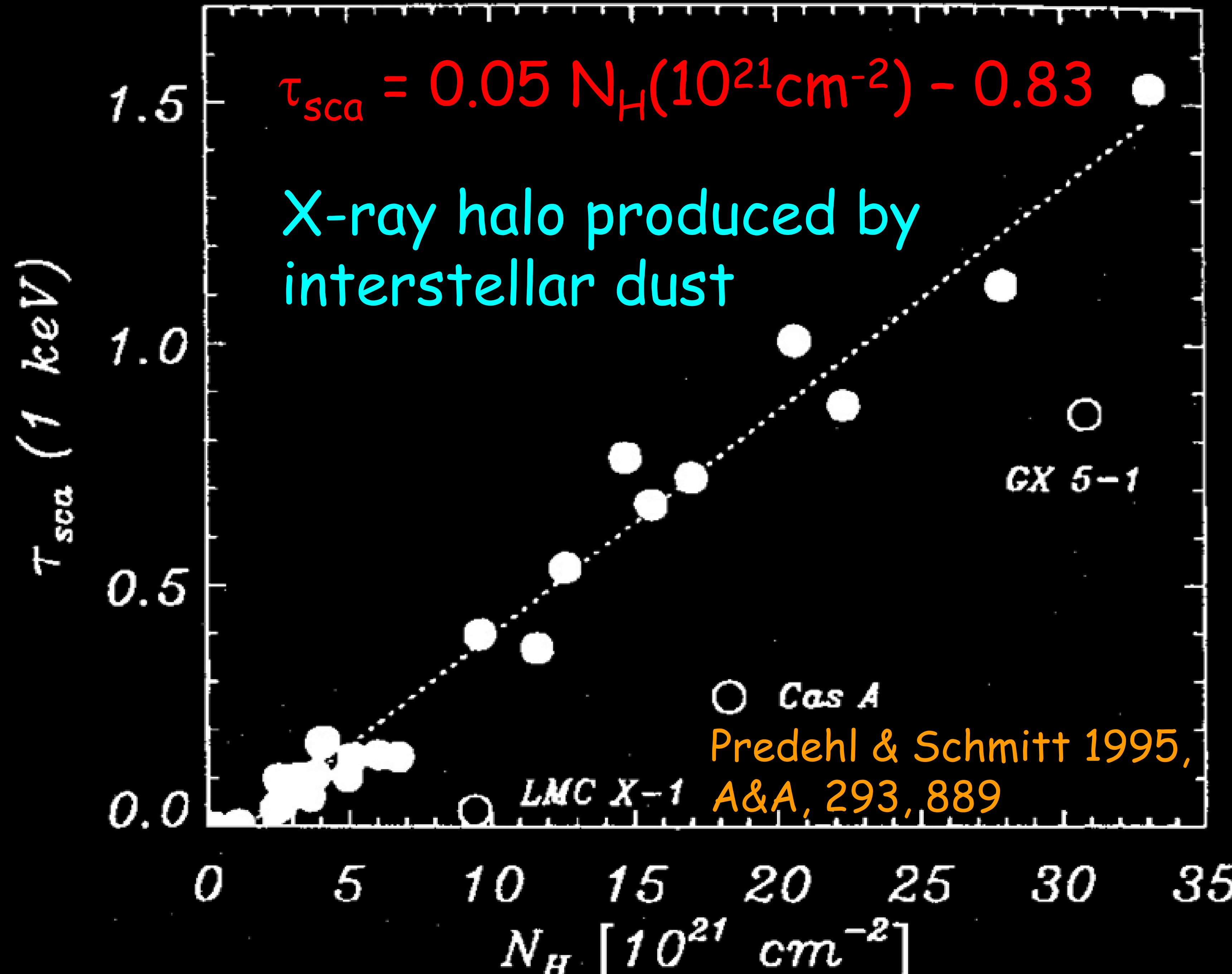

Observations of X-ray Absorption edge

Dispersion relation for f_1<->f_2 ($F = f_1 + if_2$)

$$f_1(E) = Z + \frac{2}{\pi}\int_0^{\infty} \frac{\varepsilon\, f_2(\varepsilon)}{E^2 - \varepsilon^2}\, d\varepsilon$$

Absorption edge

	L	K
C		0.28 keV
O		0.53 keV
Mg	~ 0.05 keV	1.3 keV
Si	0.1 keV	1.8 keV
Fe	~ 0.7 keV	7.1 keV

Absorption edge of Fe

Absorption edge

Fe

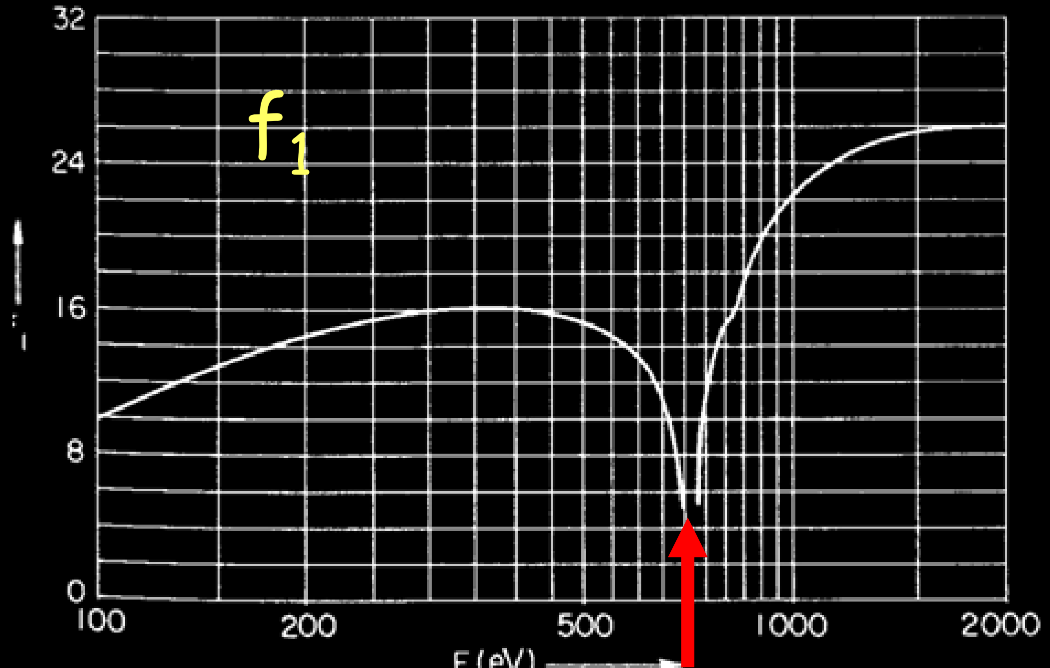

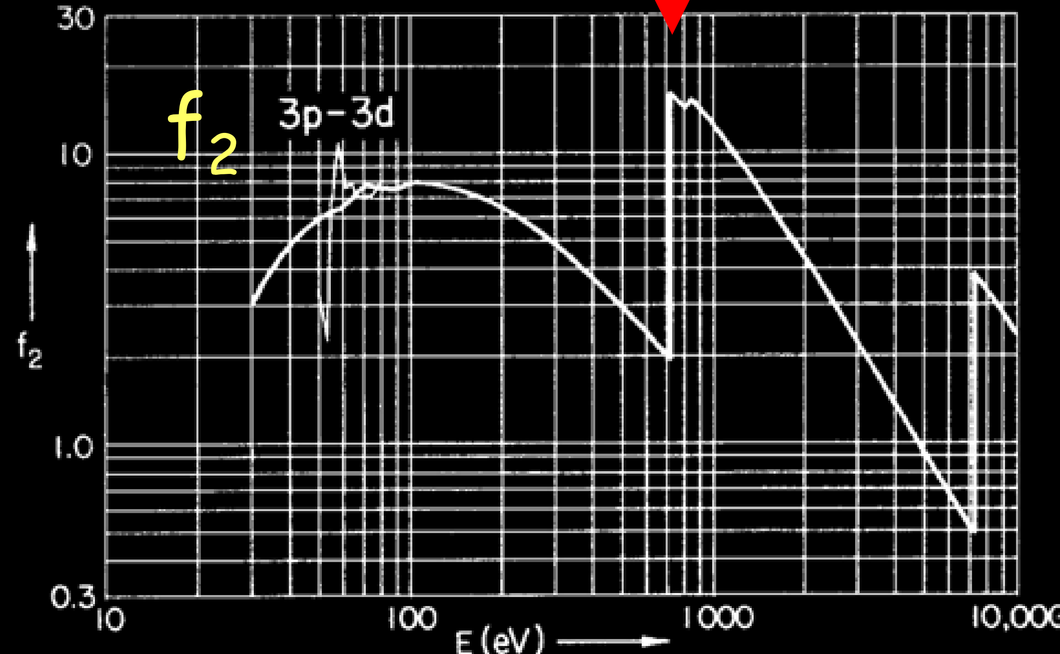

f_1 becomes a dip

Henke 1982 Atomic Data and Nuclear Data Tables 27, 1

Scattering cross-section decreases at the absorption edge

Absorption Features in σ_{sca}

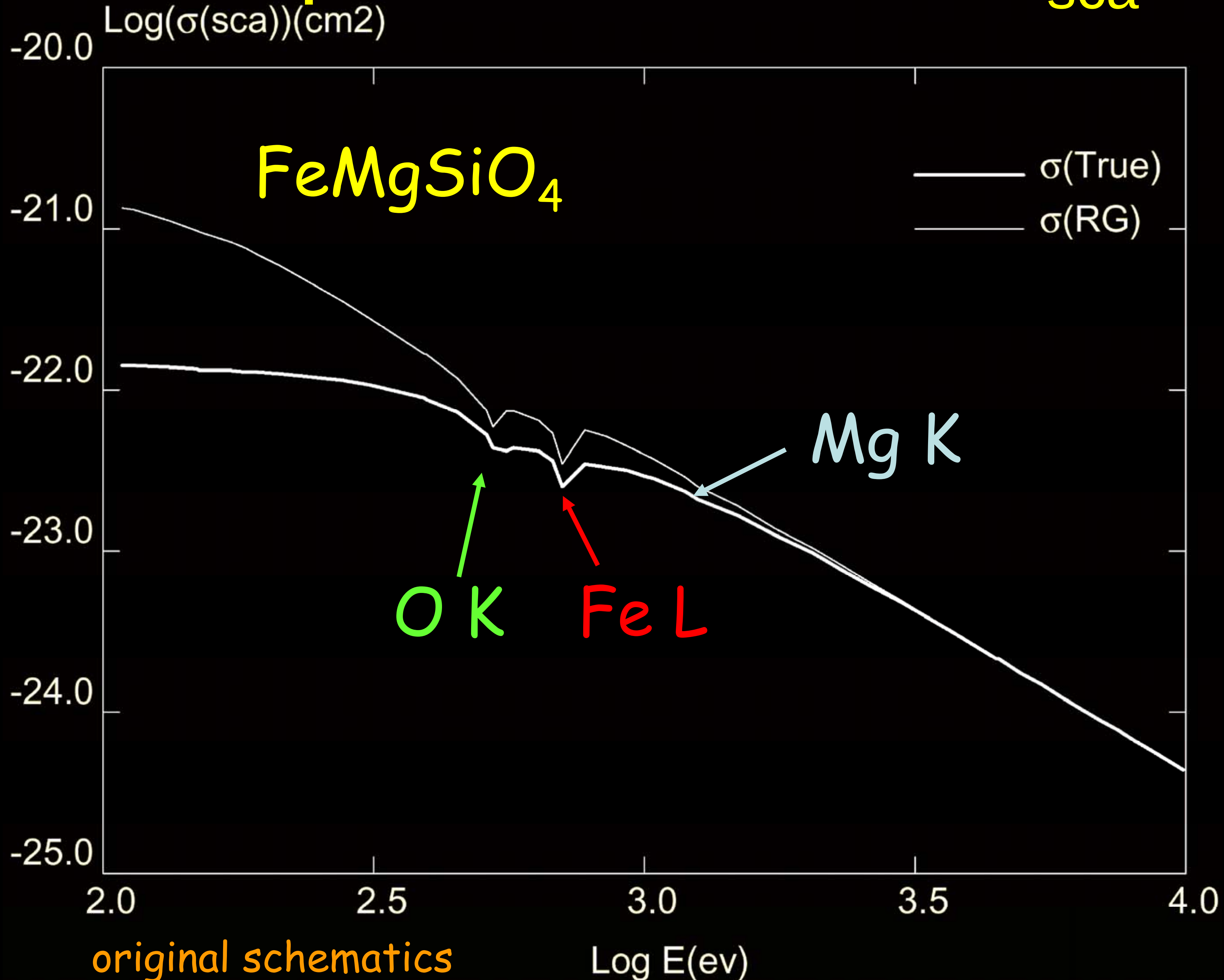

original schematics

The 1st CPS International School of Planetary Sciences
Dust in Space
January 5 - 9, 2009
Kobe, Japan

Observations of Cyg-2

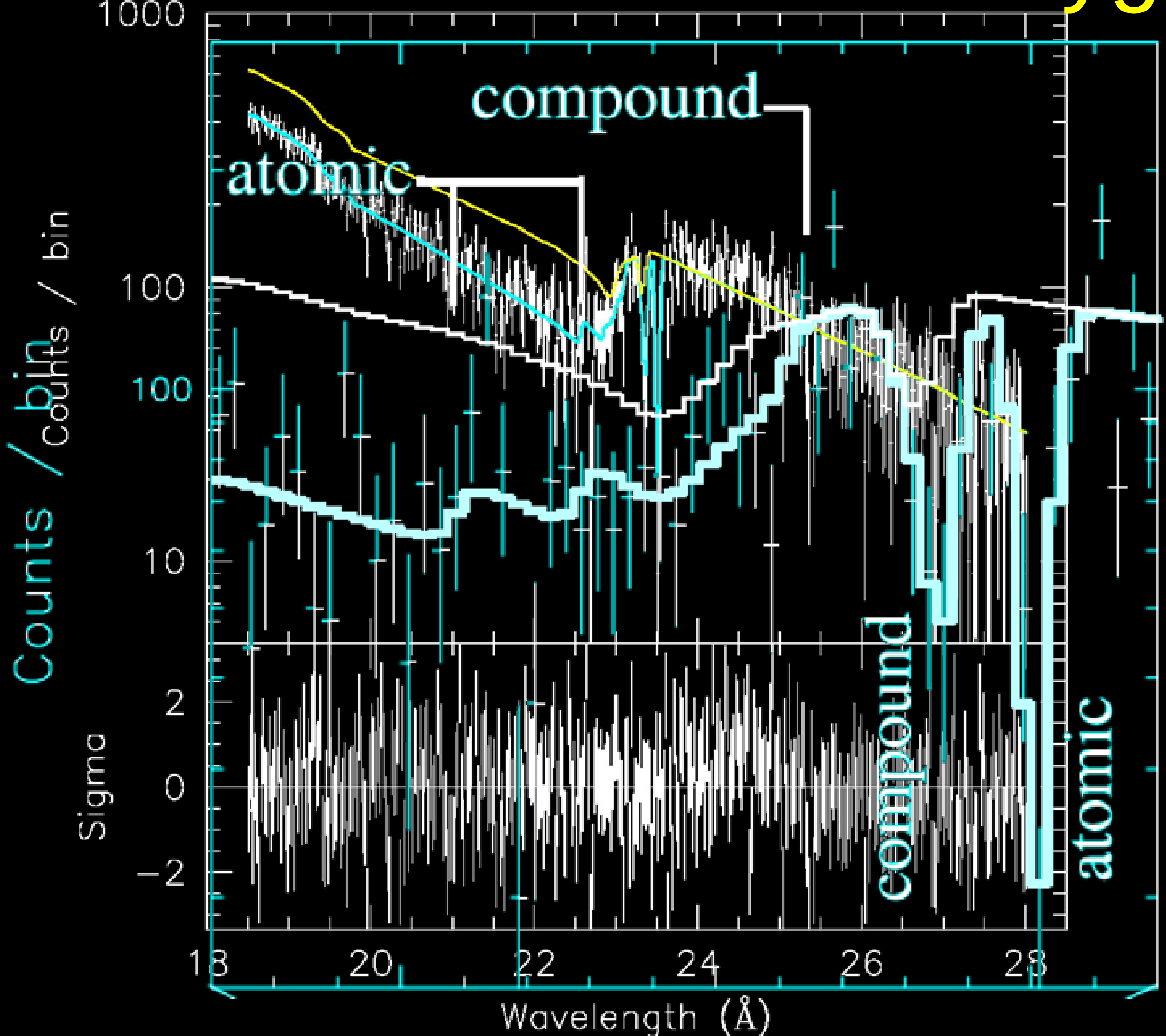

Chandra observations of Cyg X-2 around oxygen K-edge

Can be accounted for by a 3-edge model

Takei et al. (2002) ApJ, 581, 307

Alternative interpretation

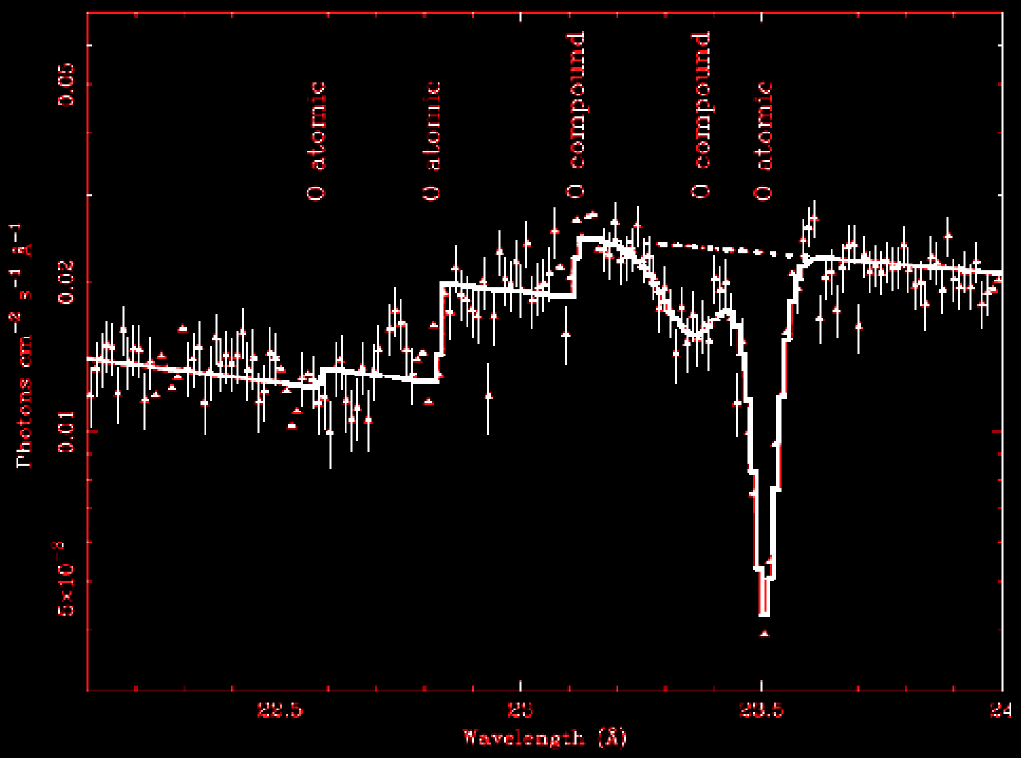

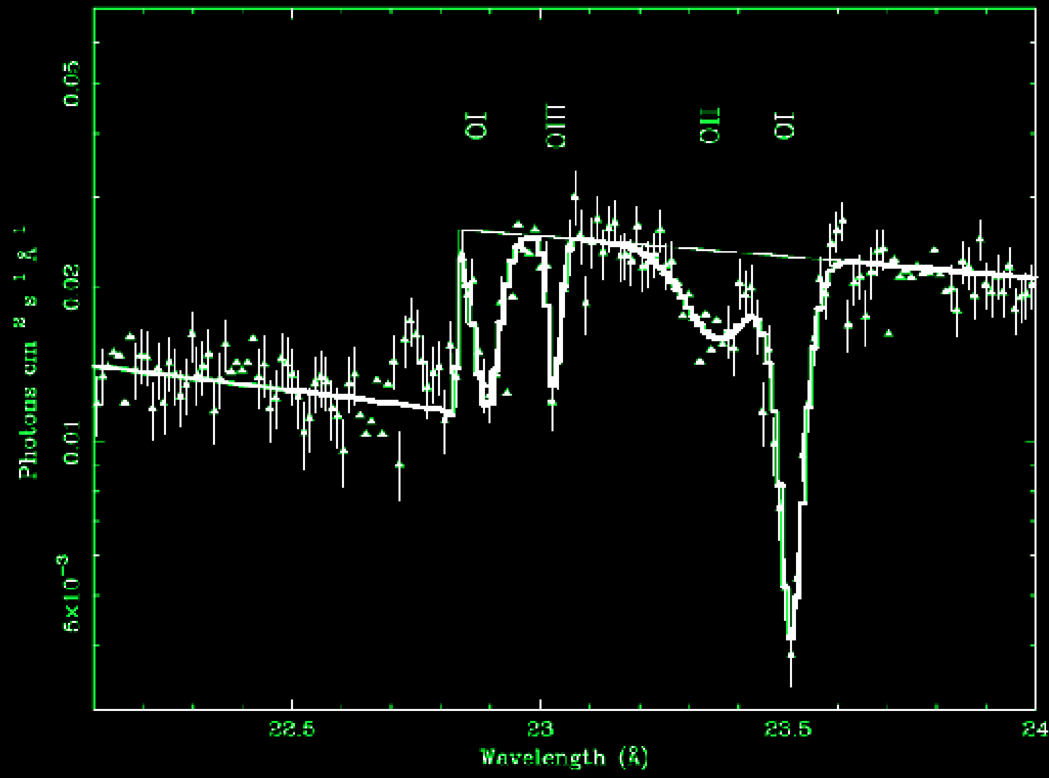

Spectrum can be interpreted by lines of O^+ and O^{++}
(Juett et al. 2004, ApJ, 612, 308)

Need observational data of better statistics
& laboratory data of compounds
(Costantini et al. 2005, A&A, 444, 187)

X-ray halo of Cyg X-2

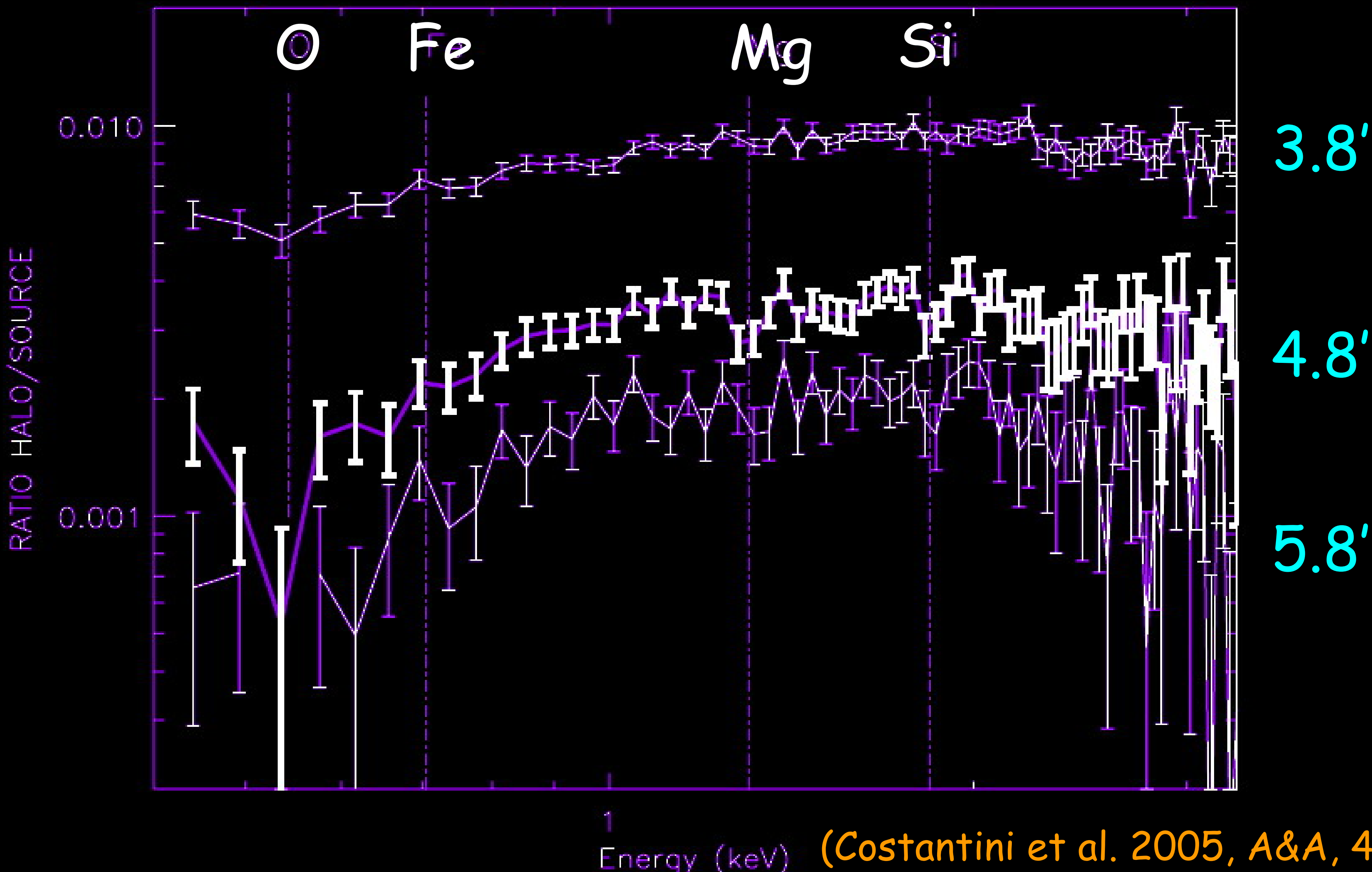

(Costantini et al. 2005, A&A, 444, 187)

Dips due to O, Mg, and Si edges are seen in the halo spectrum, indicating the presence of O-contained dust

X-ray absorption fine structure (XAFS)

Absorption edge in solids has fine structures depending on chemical bonds and compositions

Absorption edge energy of solid is different from gas

Distinguishable from gas absorption, providing a new method to estimate dust composition, chemical state, and abundance

X-ray Absorption Near-Edge Structures (XANES); $\Delta E \leq$ 10-20 eV

Extended X-ray Absorption Fine Structures (EXAFS); $\Delta E \geq$ 10-20 eV

Structures around edge

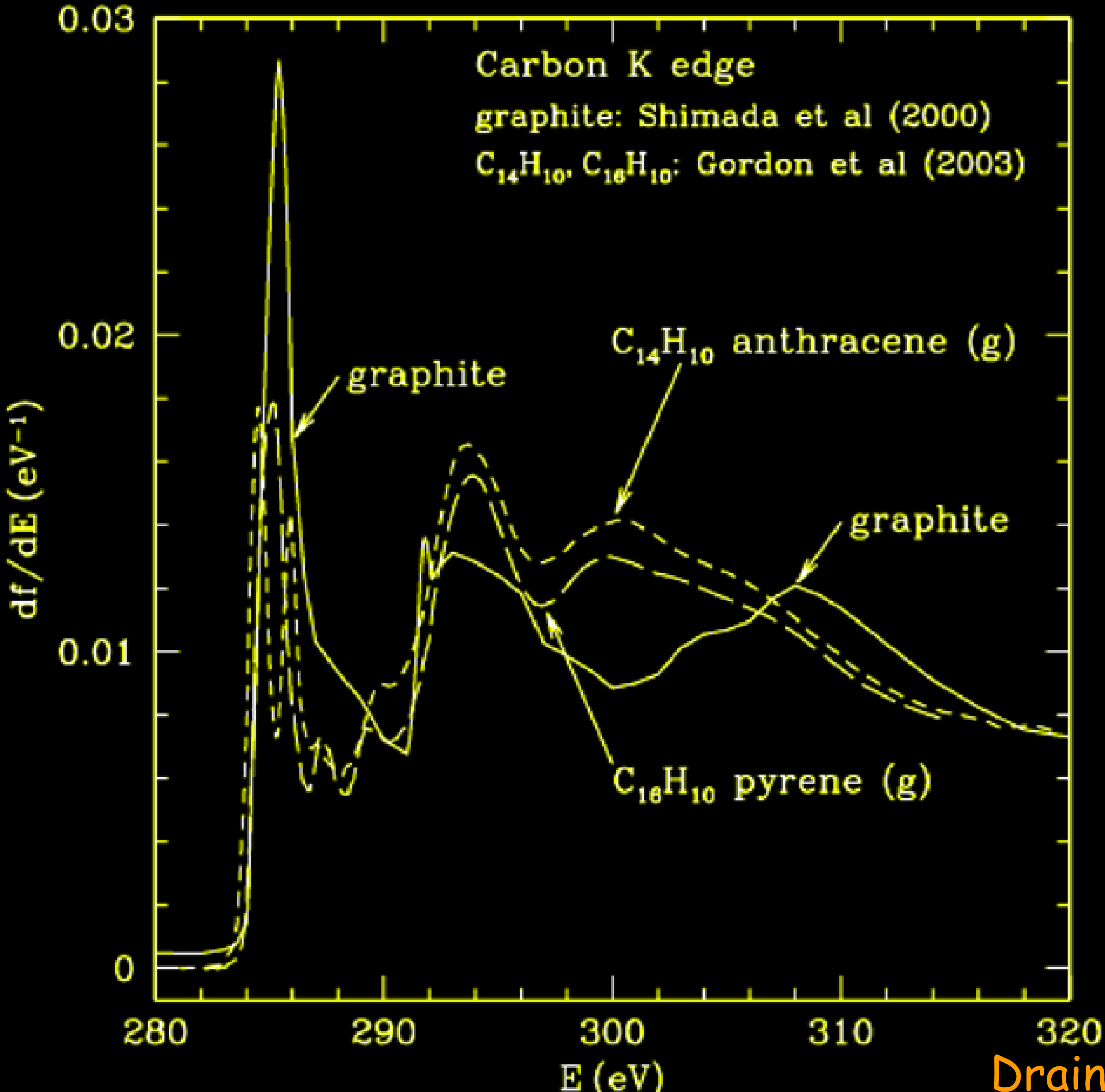

Draine (2003) ApJ, 598, 1026

Observations of XAFS

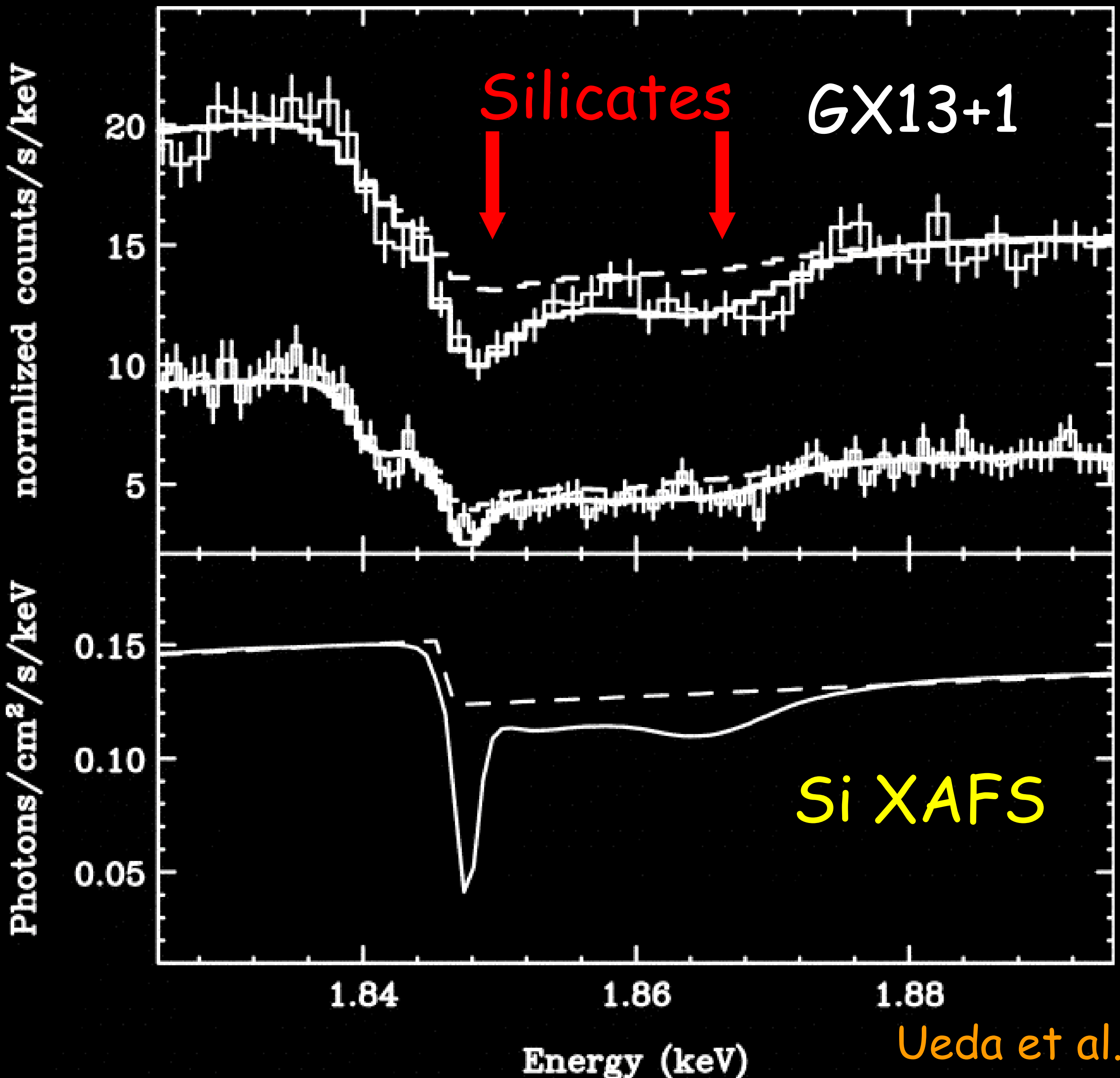

XAFS
Dust abundance
&
diagnostics
of chemical
state of element
in solid phase

Ueda et al. (2005) ApJ, 620, 274

What can we see in the infrared?

Infrared emission comes from warm objects

Dust grains are heated by stellar radiation and become warm in the ISM

Infrared observations of dust grains

Energy balance of dust grains

$$\int \sigma(\lambda, a)\, J_\lambda d\lambda = \int \sigma(\lambda, a)\, B_\lambda(T) d\lambda$$

absorption = radiation

$\sigma(\lambda, a)$: absorption cross-section of the grain

J_λ: incident radiation

For interstellar radiation field

$J_\lambda \sim \Sigma\, W_i\, F^* (T_i)$, $W_i \sim 10^{-13} \sim 10^{-14}$:dilution factor

F^*: stellar radiation, T_i = 7500, 4000, 3000K, +

(Mathis et al. (1983) A&A, 128, 212)

T ~ 20K

Orion@140μm by AKARI ®JAXA

http://www.ir.isas.jaxa.jp/ASTRO-F/Outreach/results/results.html#1119

Galaxy at optical

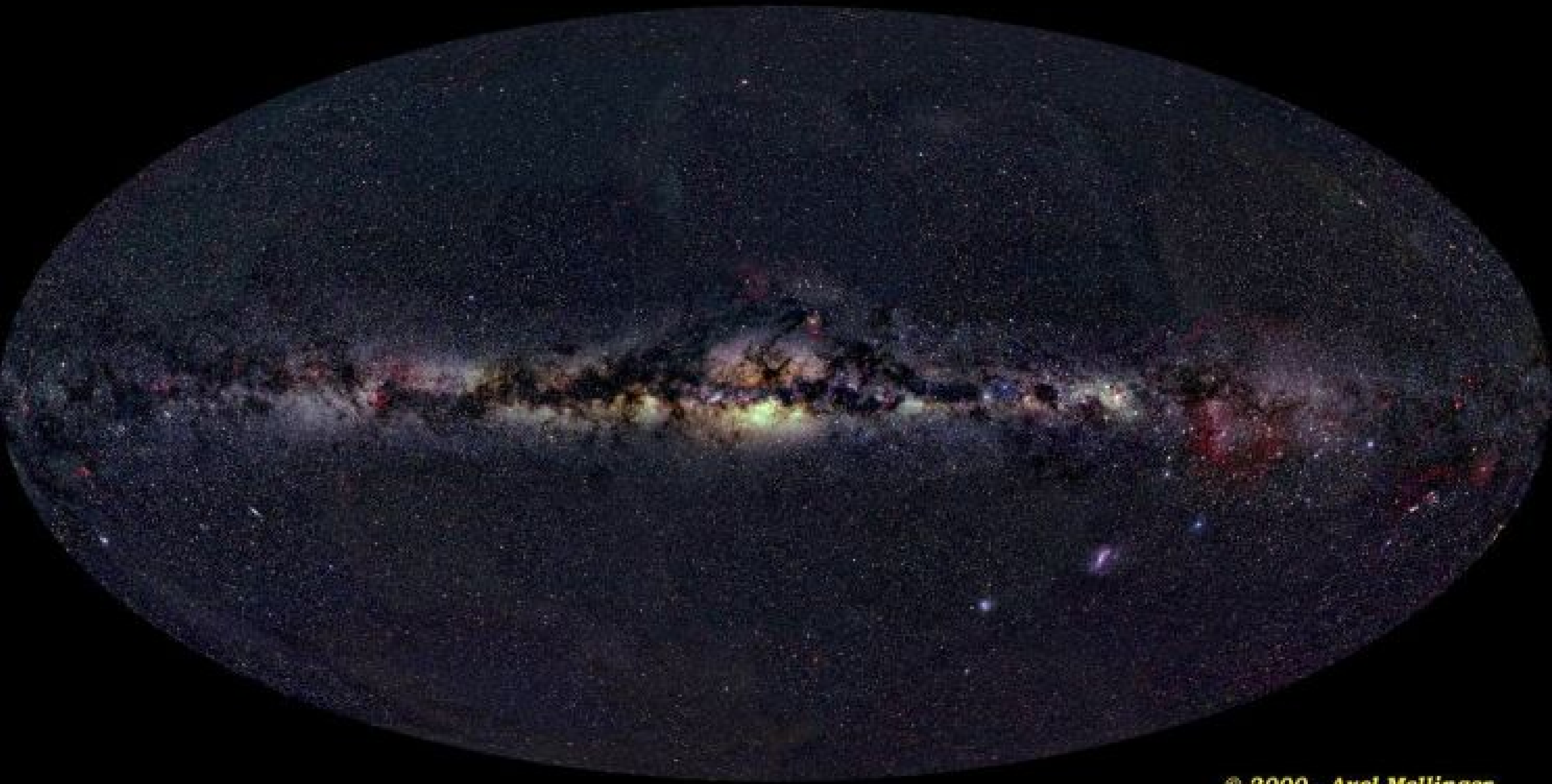

Credit & Copyright Axel Mellinger

Absorption by dust grains appears as dark lanes

Galaxy at 1.2μm

original schematics

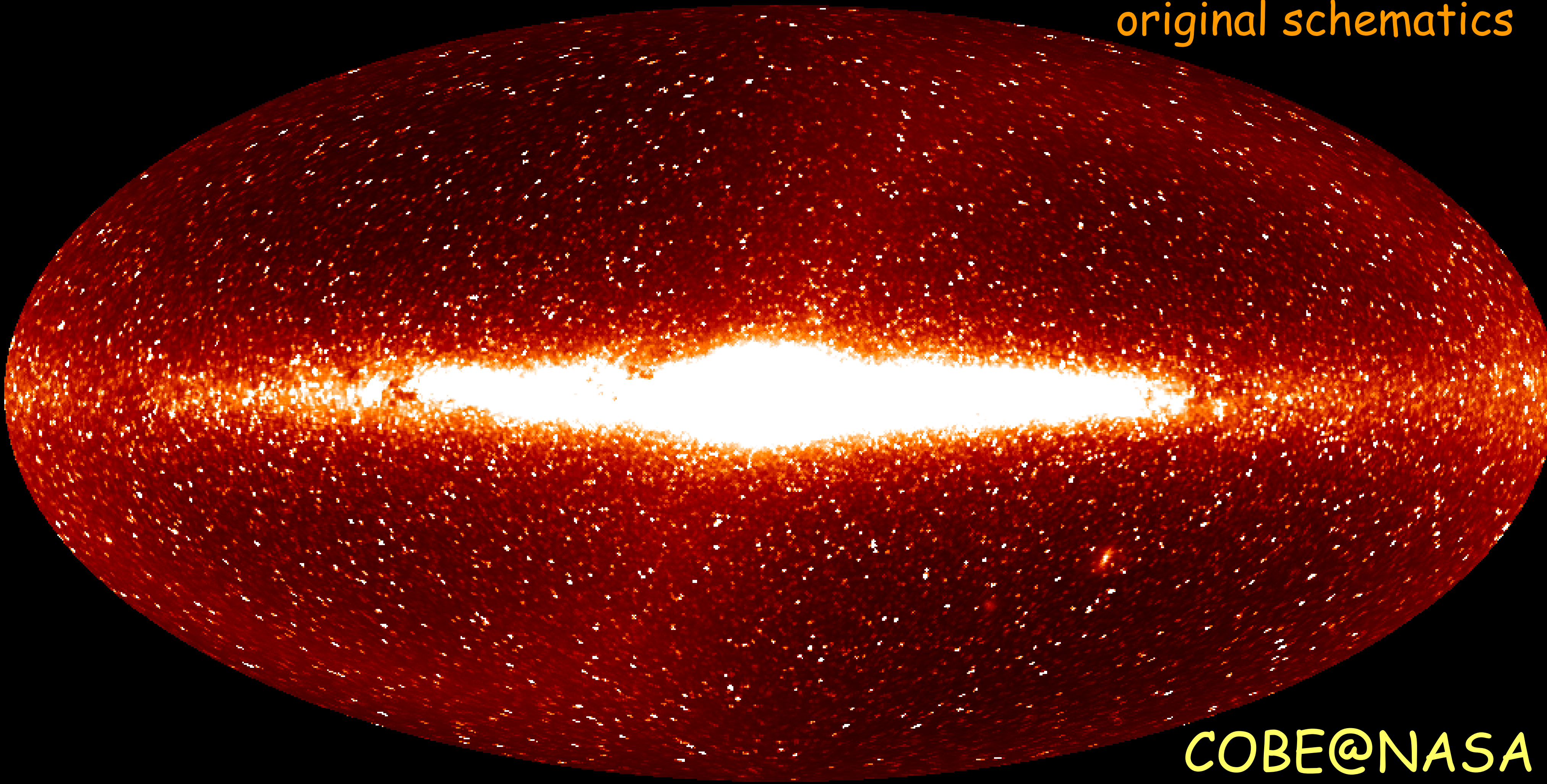

COBE@NASA

In near-infrared, most light comes from old stars (red giants) with less extinction

Galaxy at 12μm

original schematics

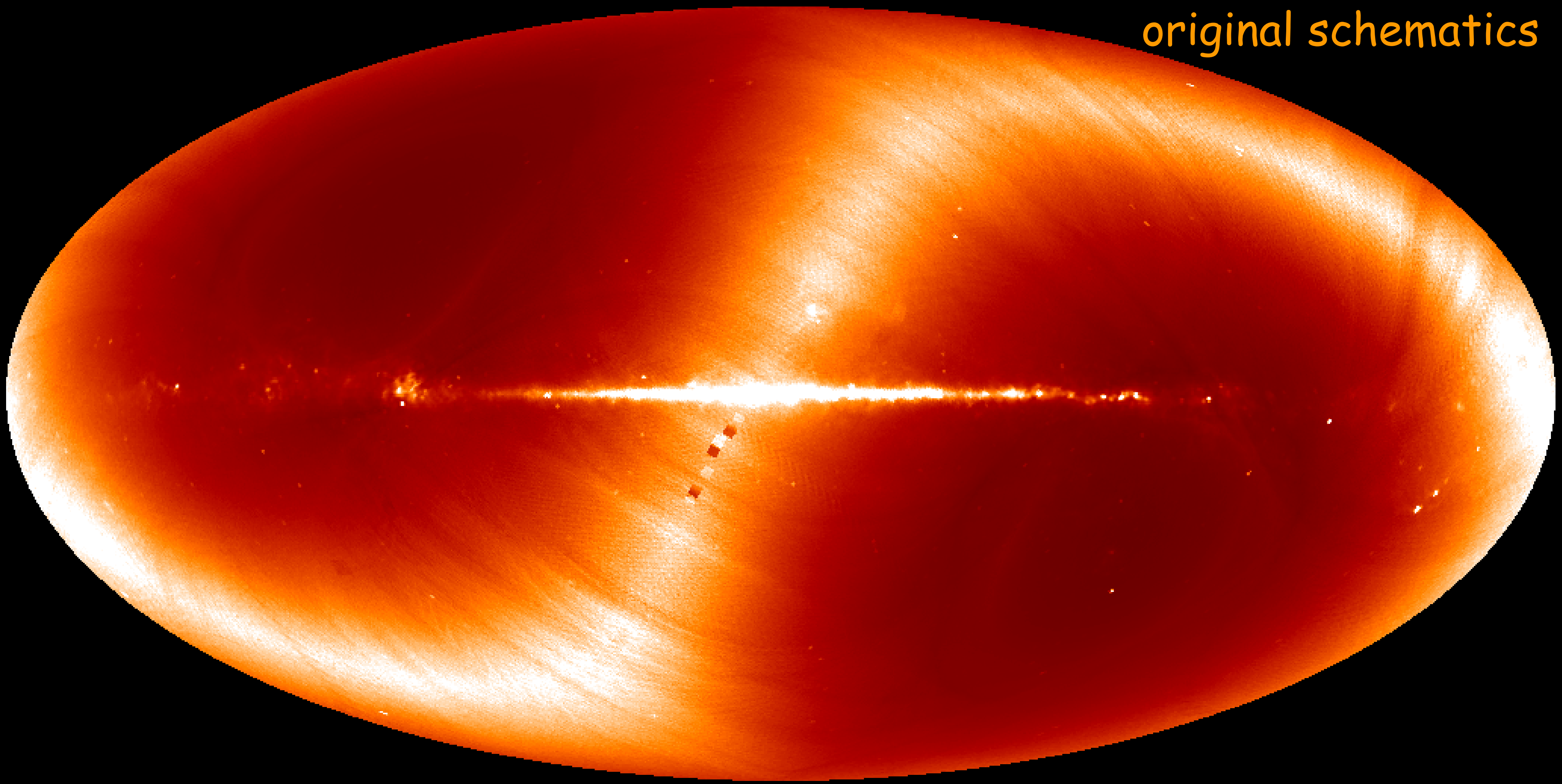

Diffuse emission from dust grains (~200-300K) in our solar system dominates in mid-IR

Galaxy at 140μm

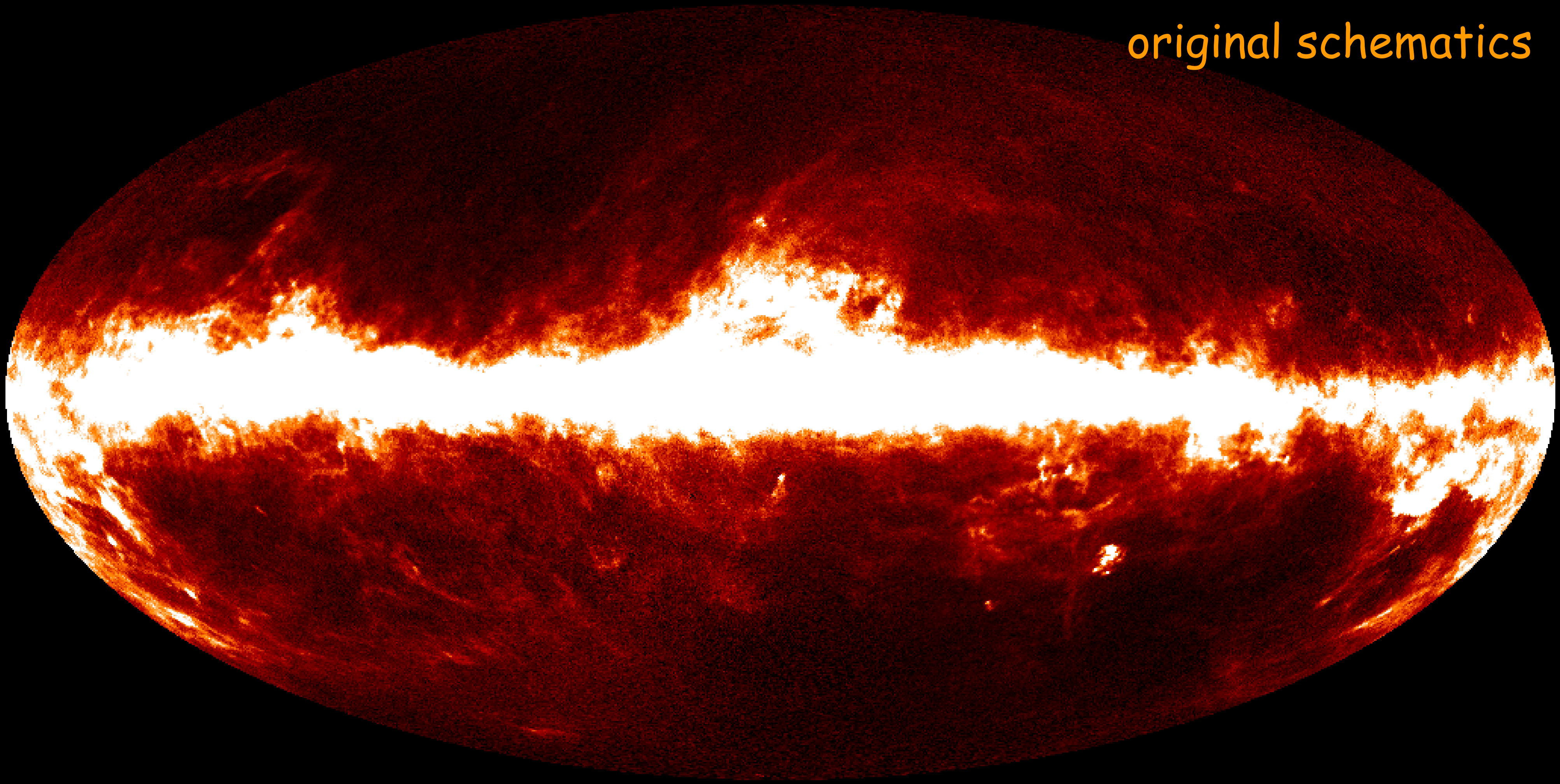

Diffuse emission from interstellar dust (~20K) dominates in FIR, well tracing ISM distribution

Mass estimate from FIR observations

FIR Emission: $I(\lambda) = \tau \, B_\lambda(T)$ (optically thin case)

$\tau = N \, C_{abs} = M \, k \, / \, D^2$,

(for $a \ll \lambda$, a: dust size, $C_{abs} \propto$ volume)

N: column density, M: total dust mass, D: distance

k: mass absorption coefficient of dust (cm^2/g)

(= C_{abs}/volume/ρ; ρ: specific weight of dust)

k is independent of a, for $a \ll \lambda$

From $I(\lambda)$ with k, T, & D, M can be estimated

(typical k ~ 0.1 cm^2/g @250μm)

Hildebrand (1983) QJRAS, 24, 267

Be aware of the assumptions behind the formula:

optically thin, single temperature, k, …

Why do we observe in IR?

Origin of our Universe
Remote galaxies are red-shifted into IR

Search for extraterrestrial life
Planets are bright and
a better contract against the Sun in IR

Less extinction in the IR and the emission from star-forming regions peaks in the FIR (~100μm)
ISM can be studied most efficiently in MIR to FIR, including star-forming regions in our Galaxy & galaxies

IC1396@9+18μm by AKARI
http://www.ir.isas.jaxa.jp/ASTRO-F/Outreach/results/results.html#1101

Material evolution in the ISM

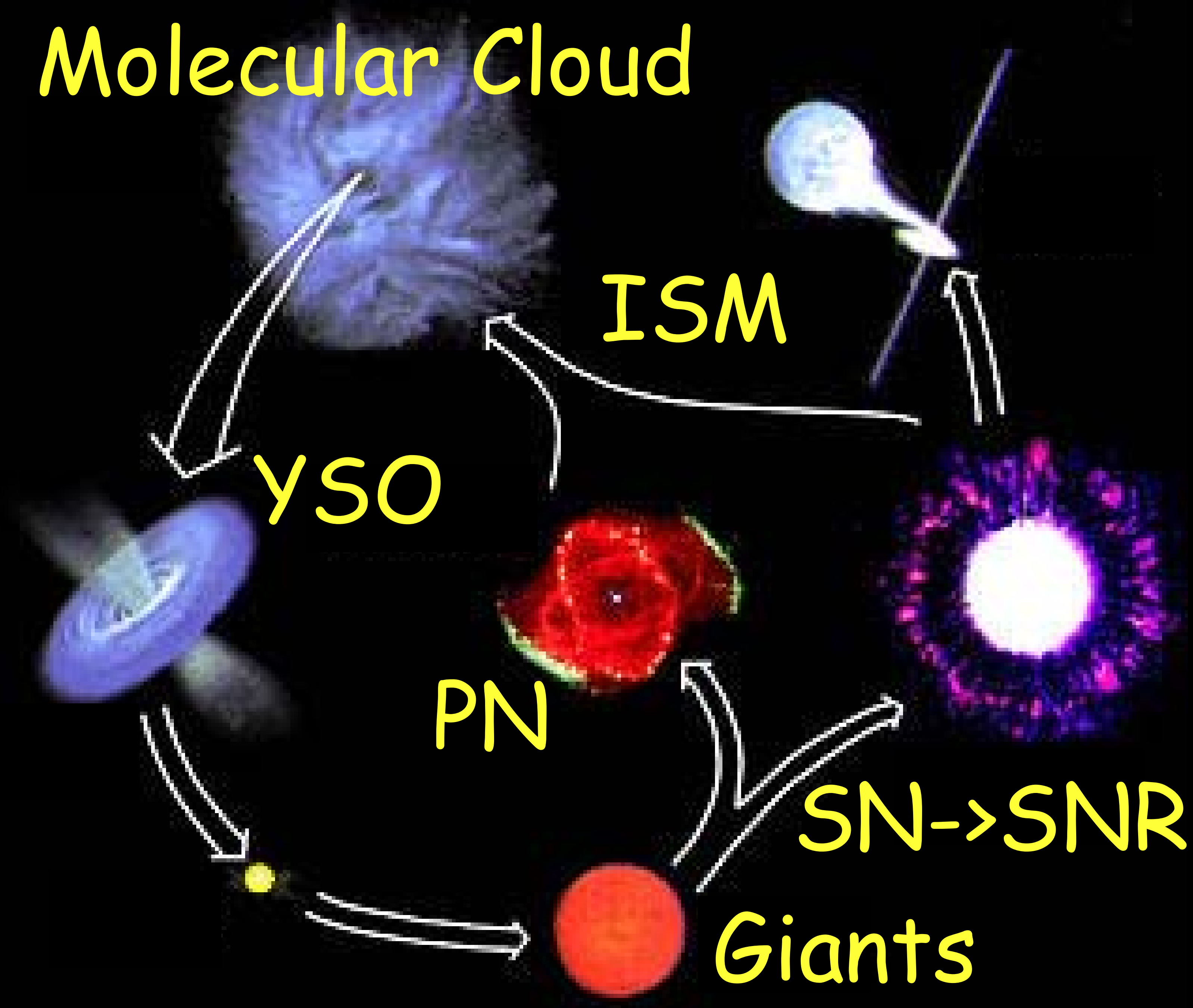

Infrared Observations from Space

Only a limited range of IR can be observed from ground

Emission from terrestrial atmosphere disturbs sensitive IR observations

Cooled telescopes in space provide ideal facilities for IR observations

from Astro-F booklet

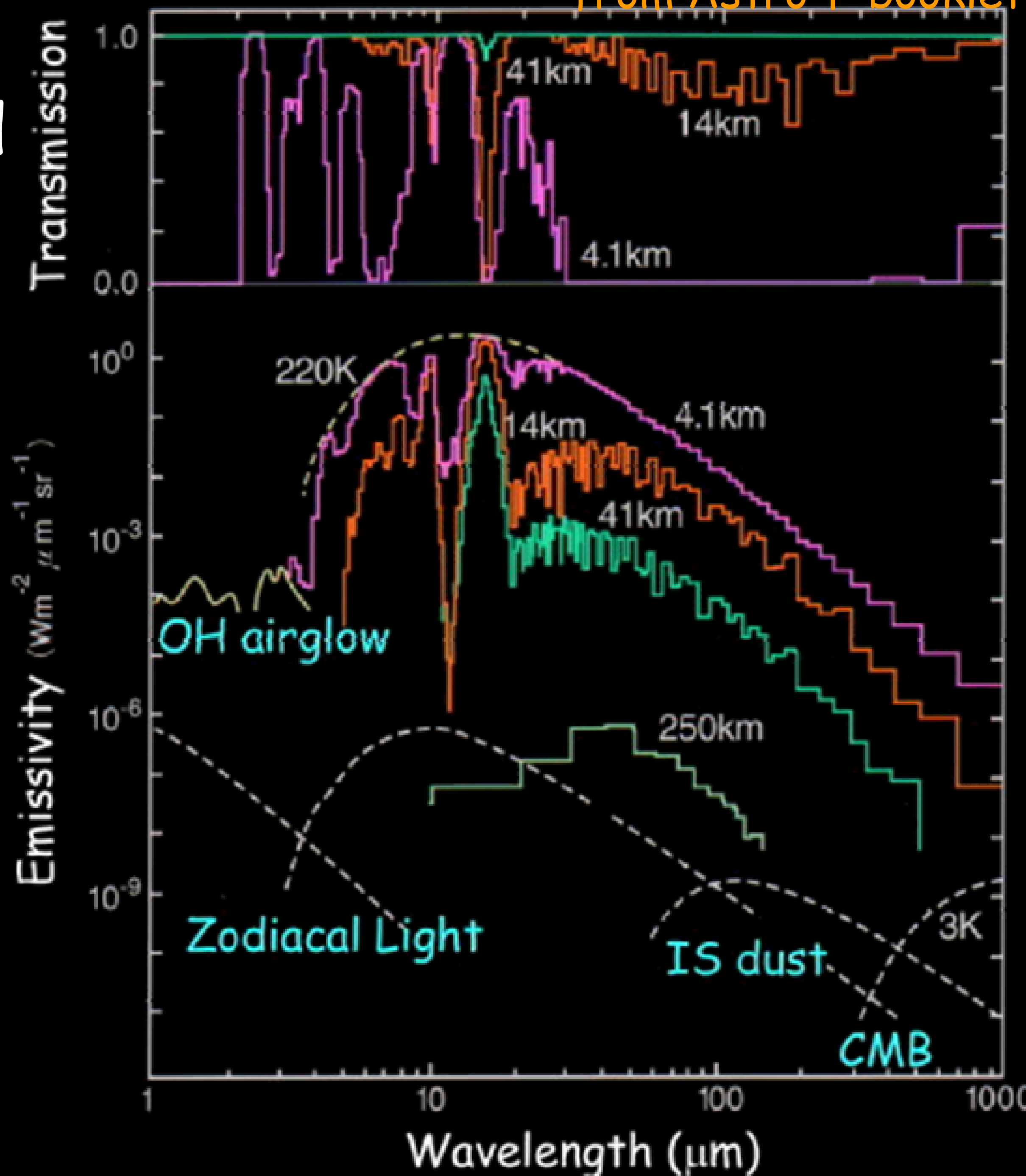

Cooled Infrared Telescope in Space

Space mission has a stringent constraint on the weight

Launching conditions are not friendly for telescopes

Cryogenic distortion has to be carefully taken care of

Light-weight, strong, and small thermal distortion mirrors are required for cooled telescope systems

Keeping a telescope cold on the orbit requires new technology development (space cryogenics)

IC4954/4955@9+18μm by AKARI

Infrared Astronomical Satellite (IRAS)

First IR satellite mission by USA, UK, & NL

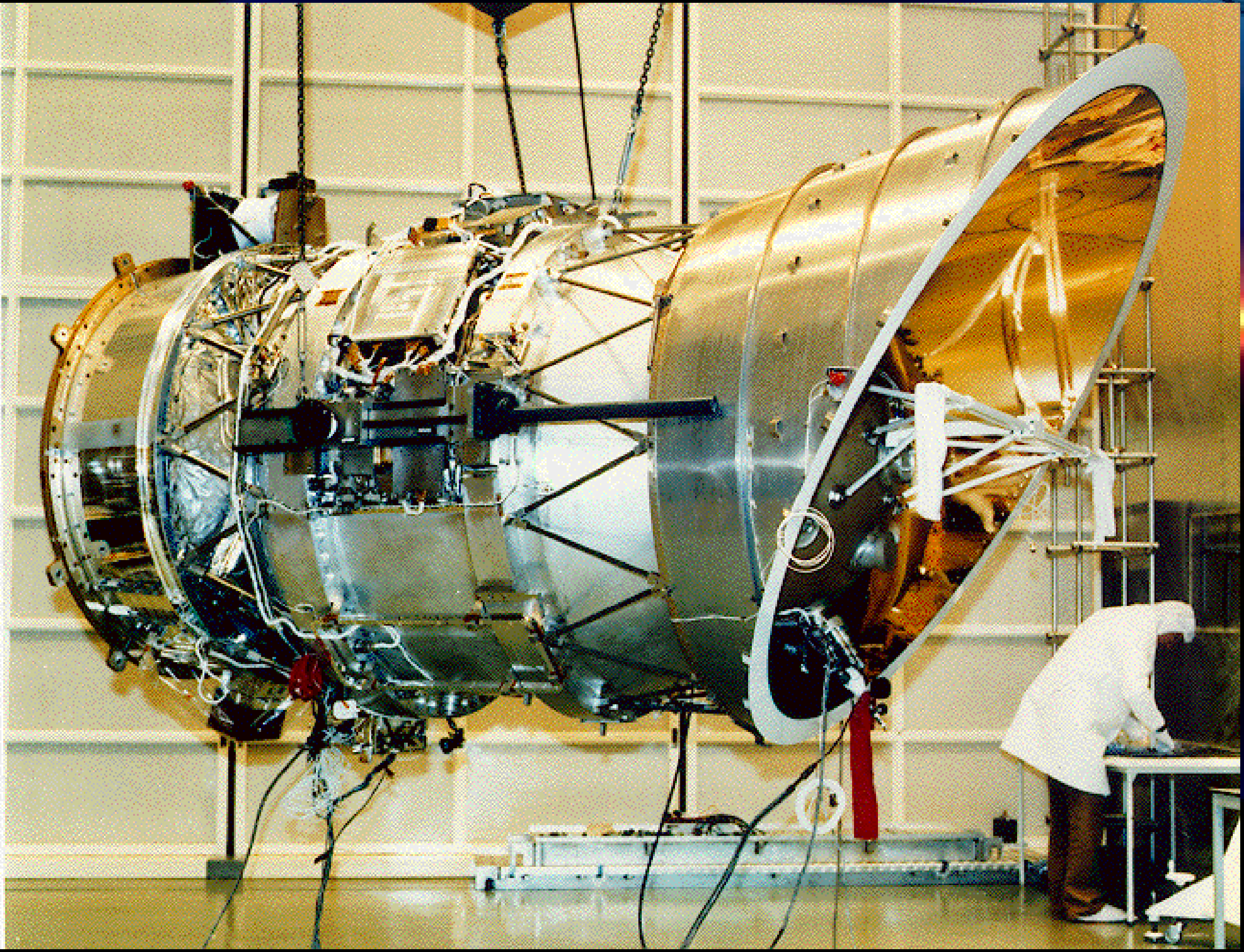

60cm Be mirrors
Sun-synchronous polar orbit
All-sky survey at 12, 25, 60, & 100μm
+ spectroscopy
+ CPC
10 mo observation with 500l LHe

@NASA

http://coolcosmos.ipac.caltech.edu/image_galleries/IRAS/iras2.html

All-sky observations of IRAS

Observing the sky in the direction opposite to earth center; In 6 months, all-sky can be observed

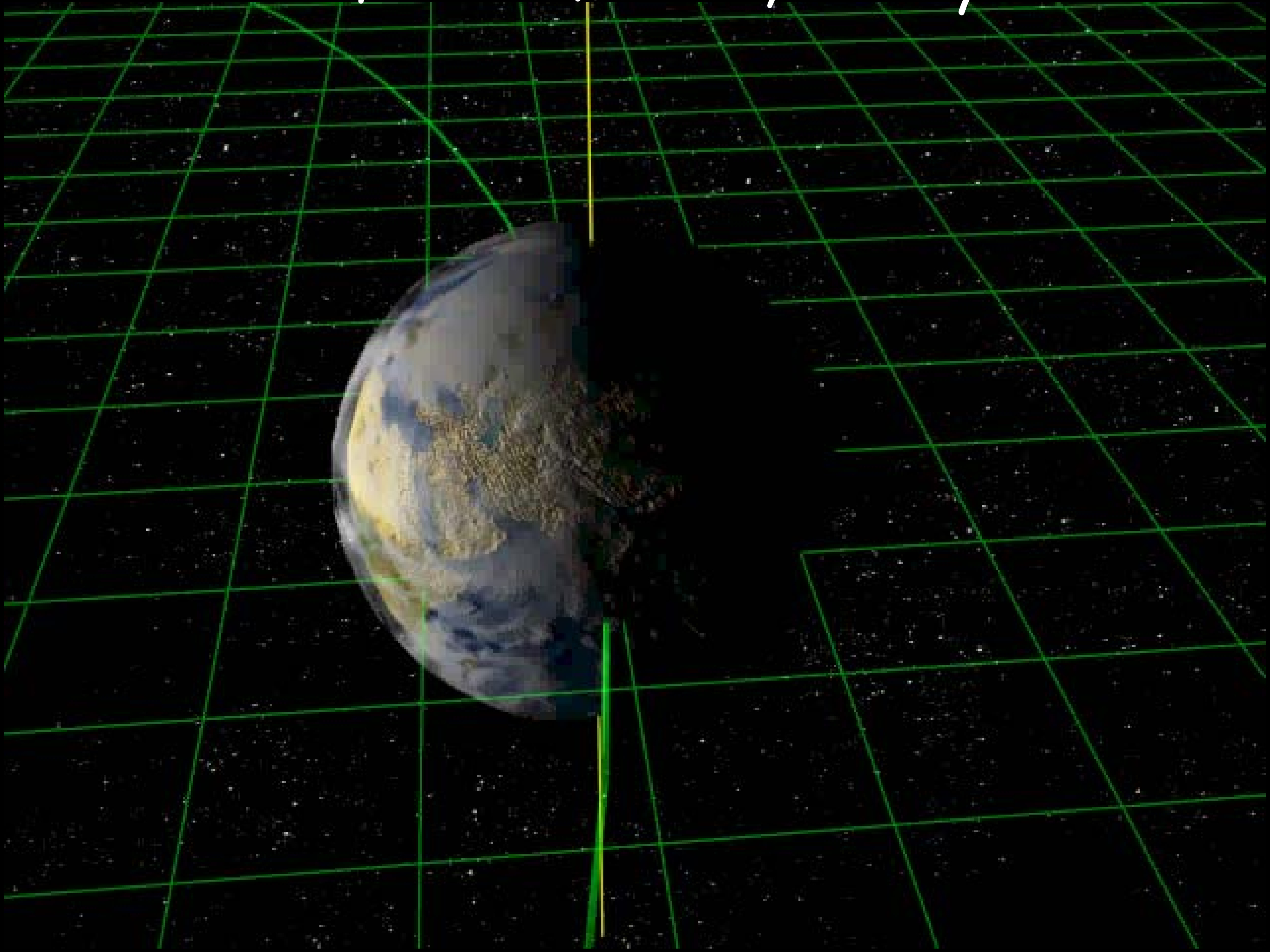

IR satellites after IRAS

COBE/
DIRBE 1989
(NASA)
18cm Al

MSX 1996
(USA)
35cm Al

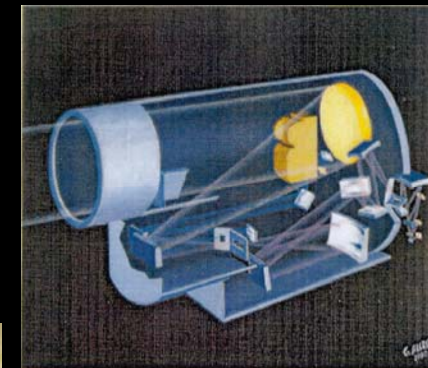

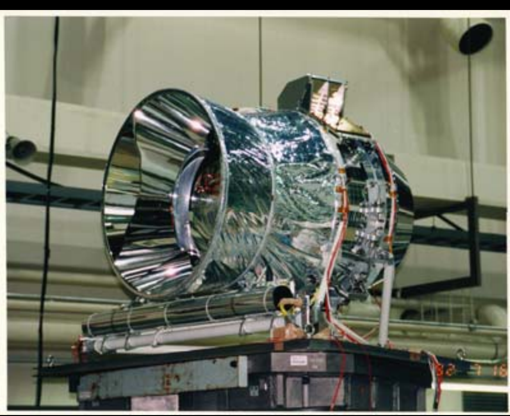

IRTS 1995
(ISAS
+ NASA)
15cm Al

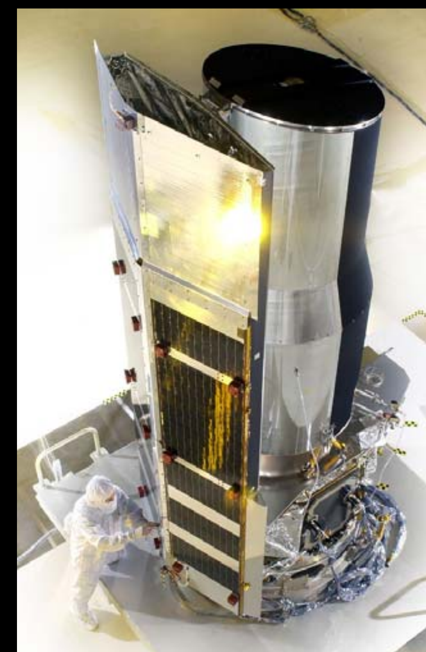

Spitzer
2003
(NASA)
85cm Be

ISO 1995
(ESA+
ISAS+NASA)
60cm fused
quartz

AKARI 2006
(ISAS + ESA)
70cm SiC

Survey; Observatory;
Survey + observatory

AKARI satellite

70cm SiC mirror
180L LHe + cryocoolers enabled
18 month cold mission (2006.2-2007.8)
JAXA mission with participation of ESA, collaboration with UK, NL, & Korea

All-sky survey surpasses IRAS database
+
Pointing observations of imaging and spectroscopy in 2-180μm

AKARI SiC light-weight mirror

Porous SiC core

CVD (Chemical Vapor Deposition) SiC coat

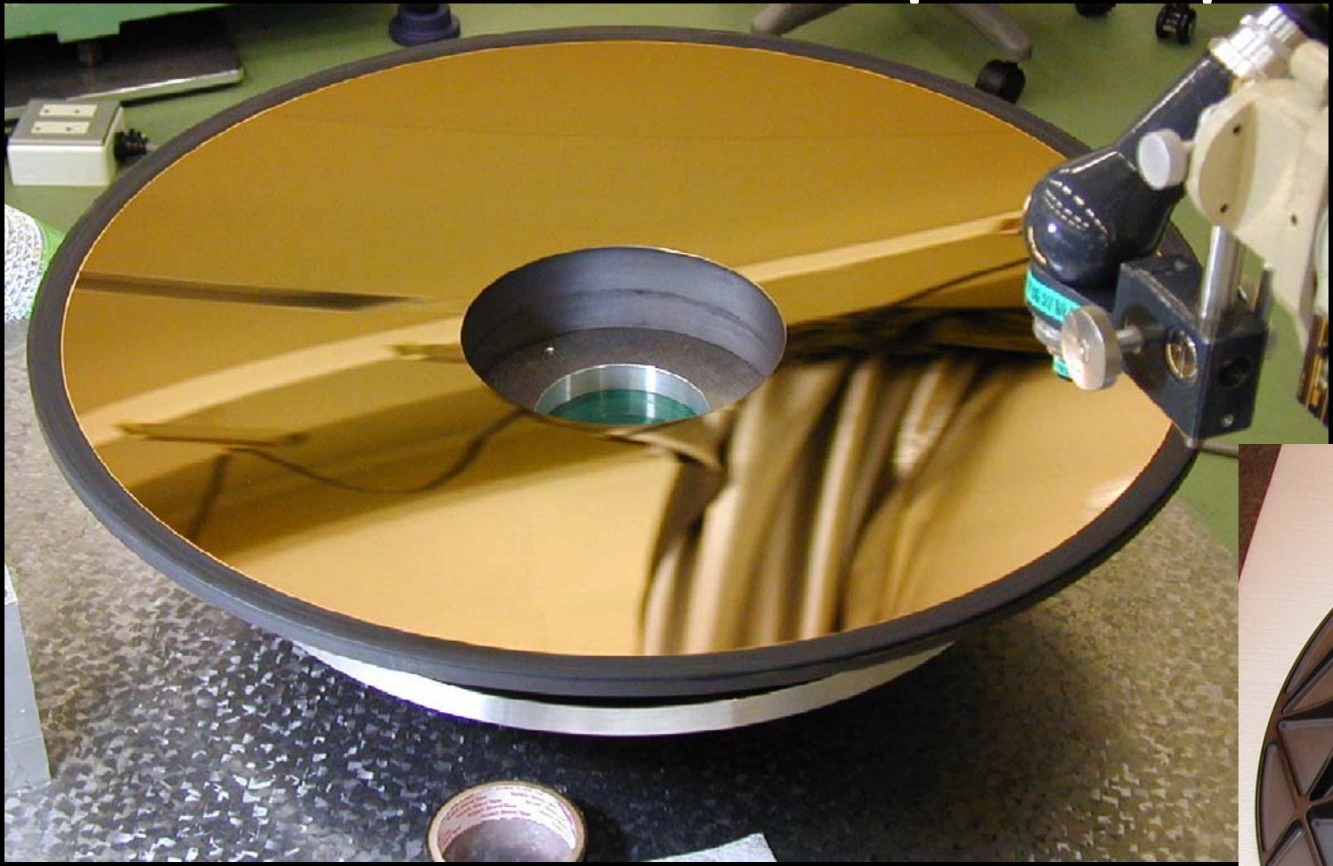

weight~11kg

Vibration test

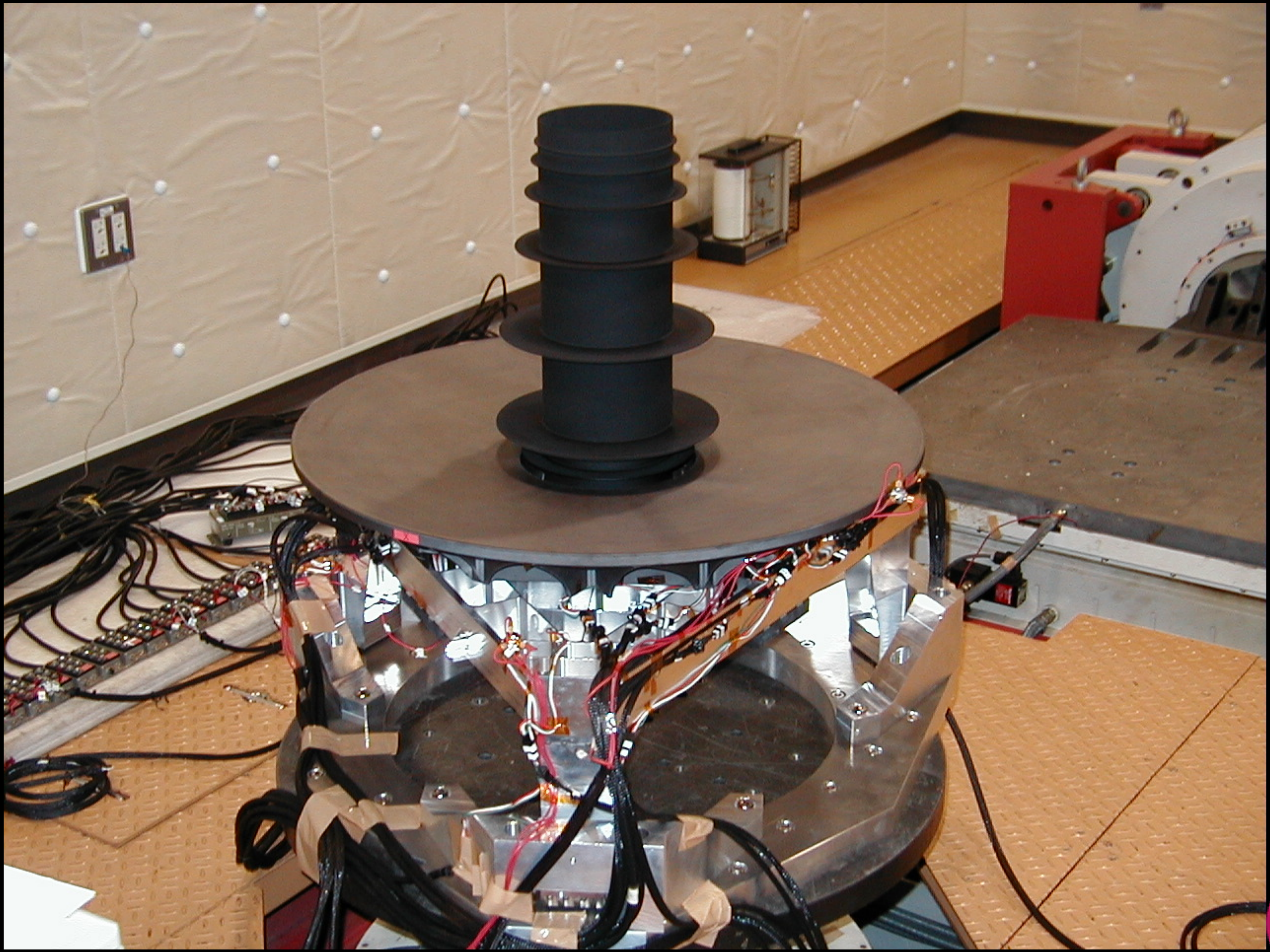

Ahhh

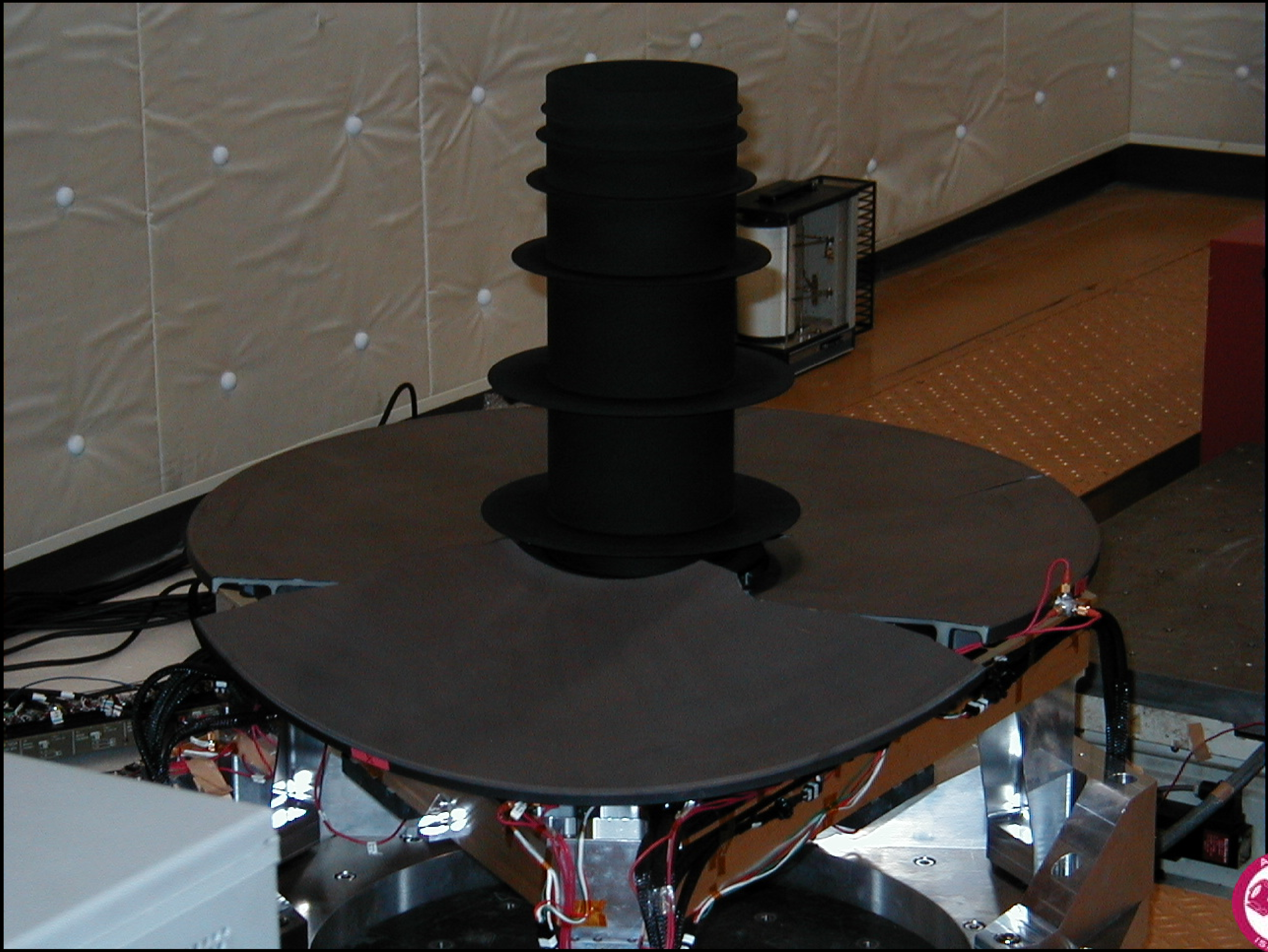

Cryo telescope test chamber

Cooling with LHe

Interferometer measures distortion with cooling

Telescope cryo-test

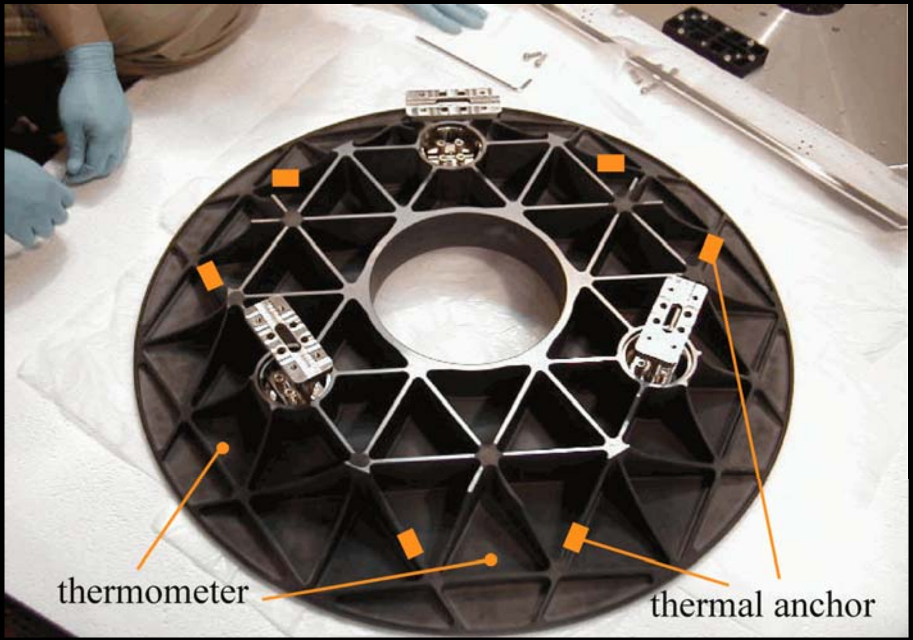

Kaneda et al. (2005) Appl. Opt. 44, 6823

Focal-plane instruments (FPIs)

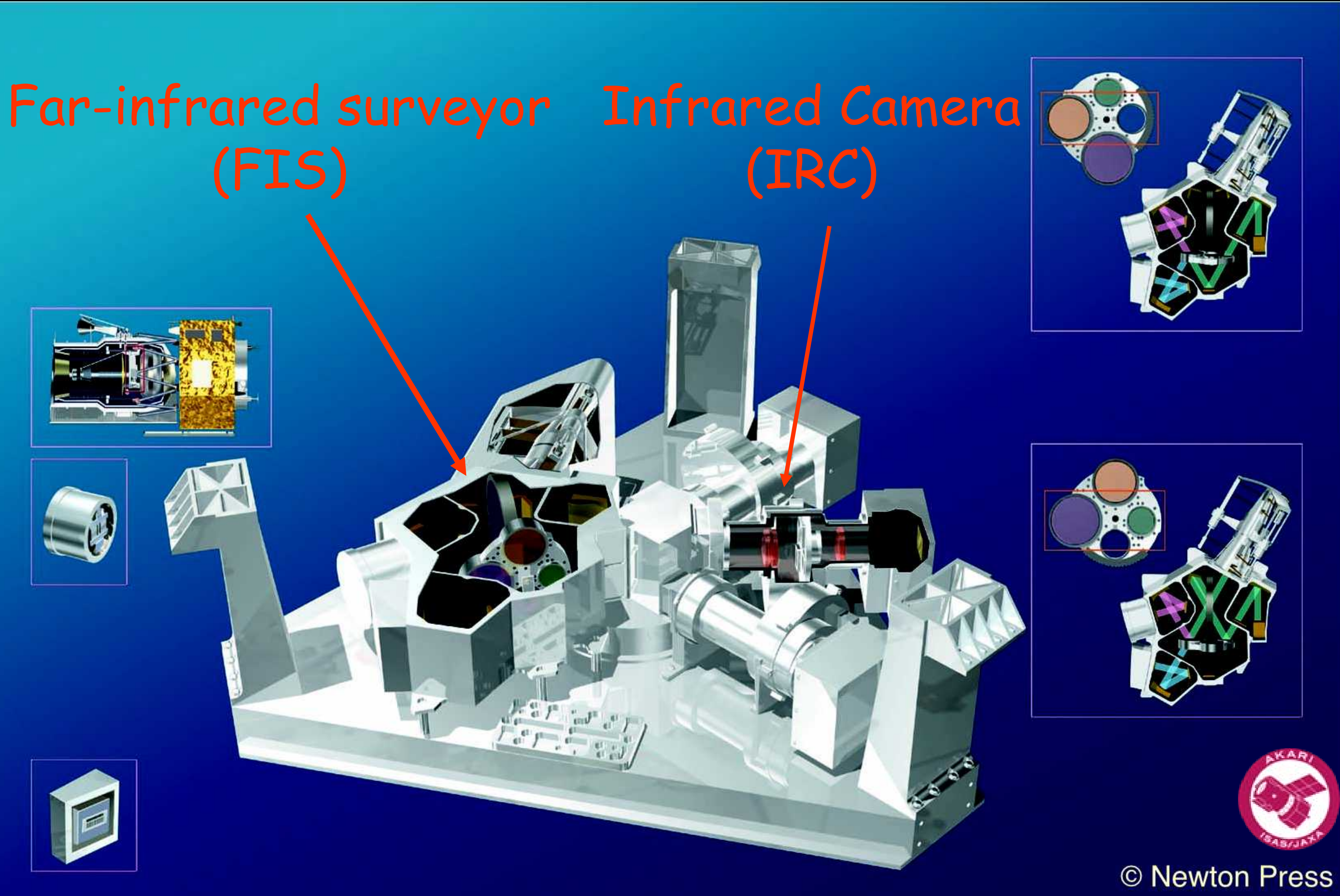

FPIs

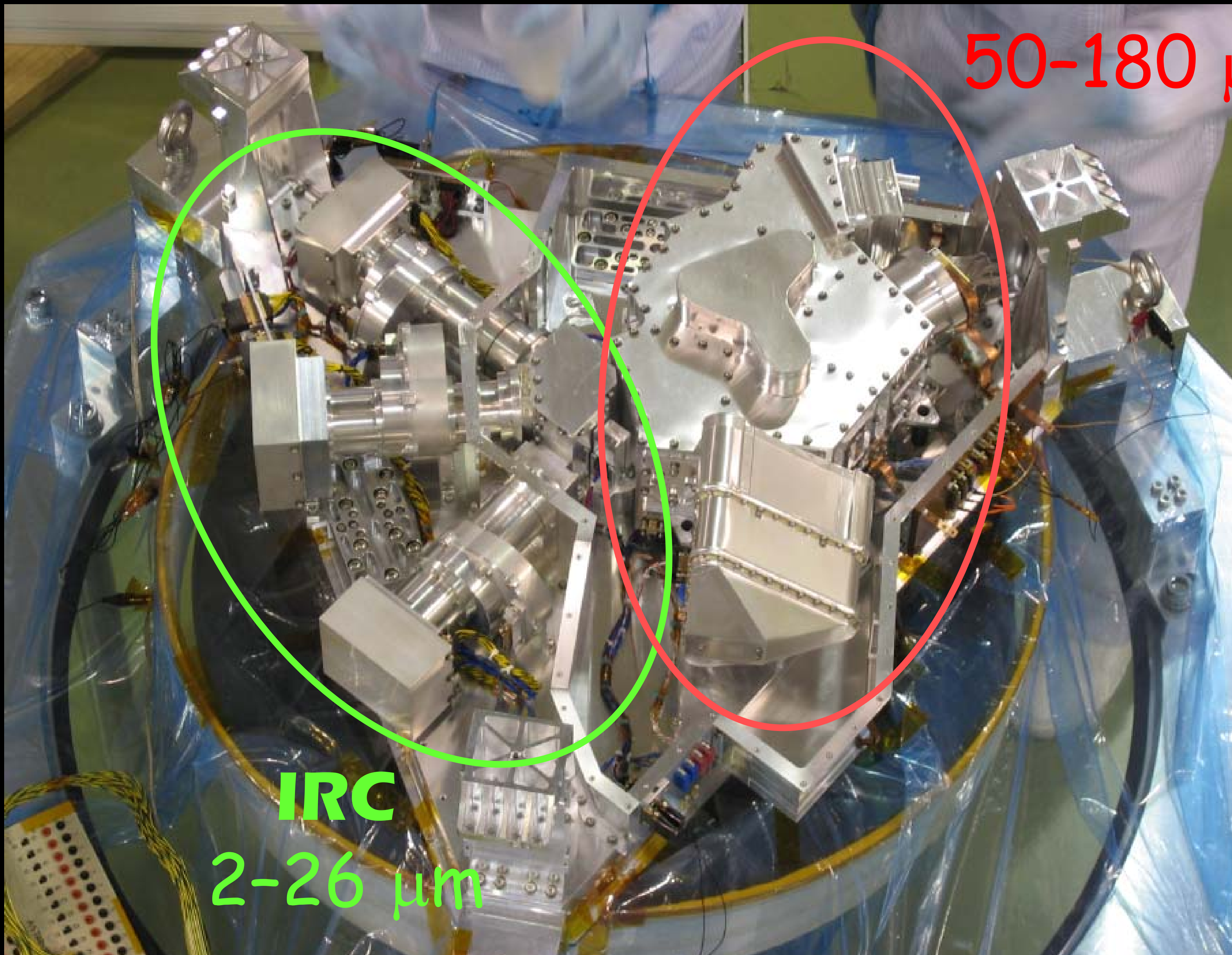

FIS

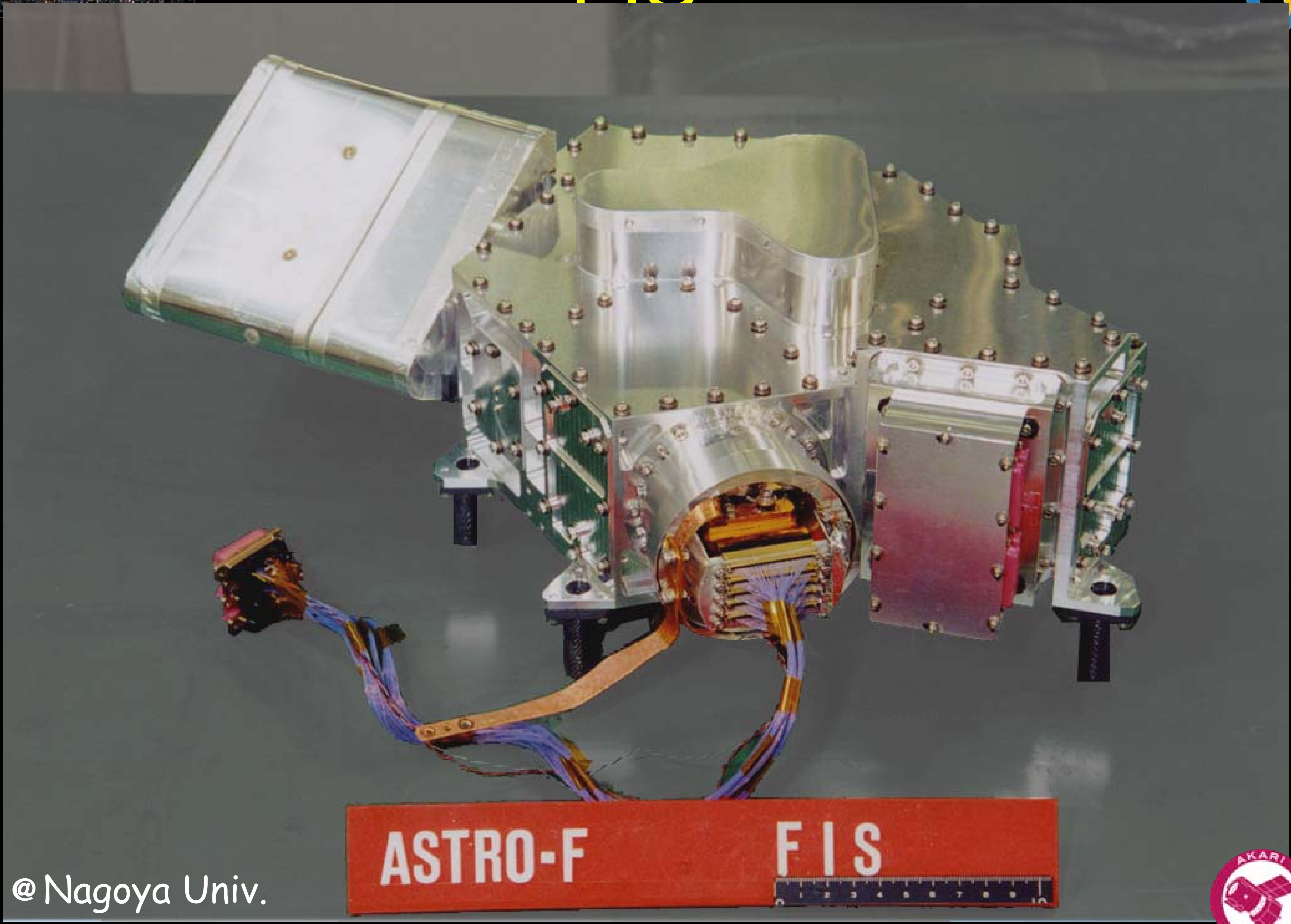

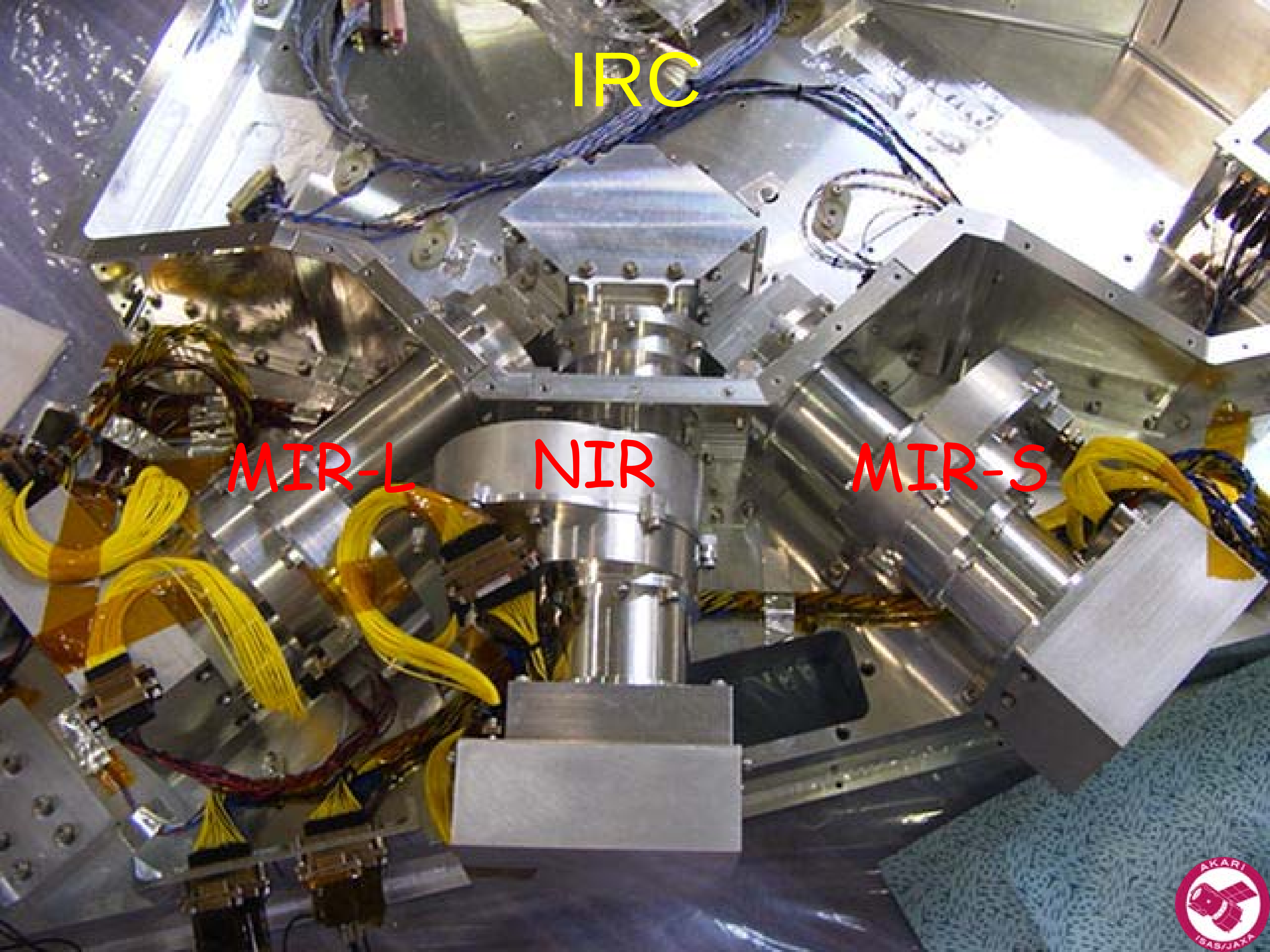
IRC
MIR-L
NIR
MIR-S

FIS

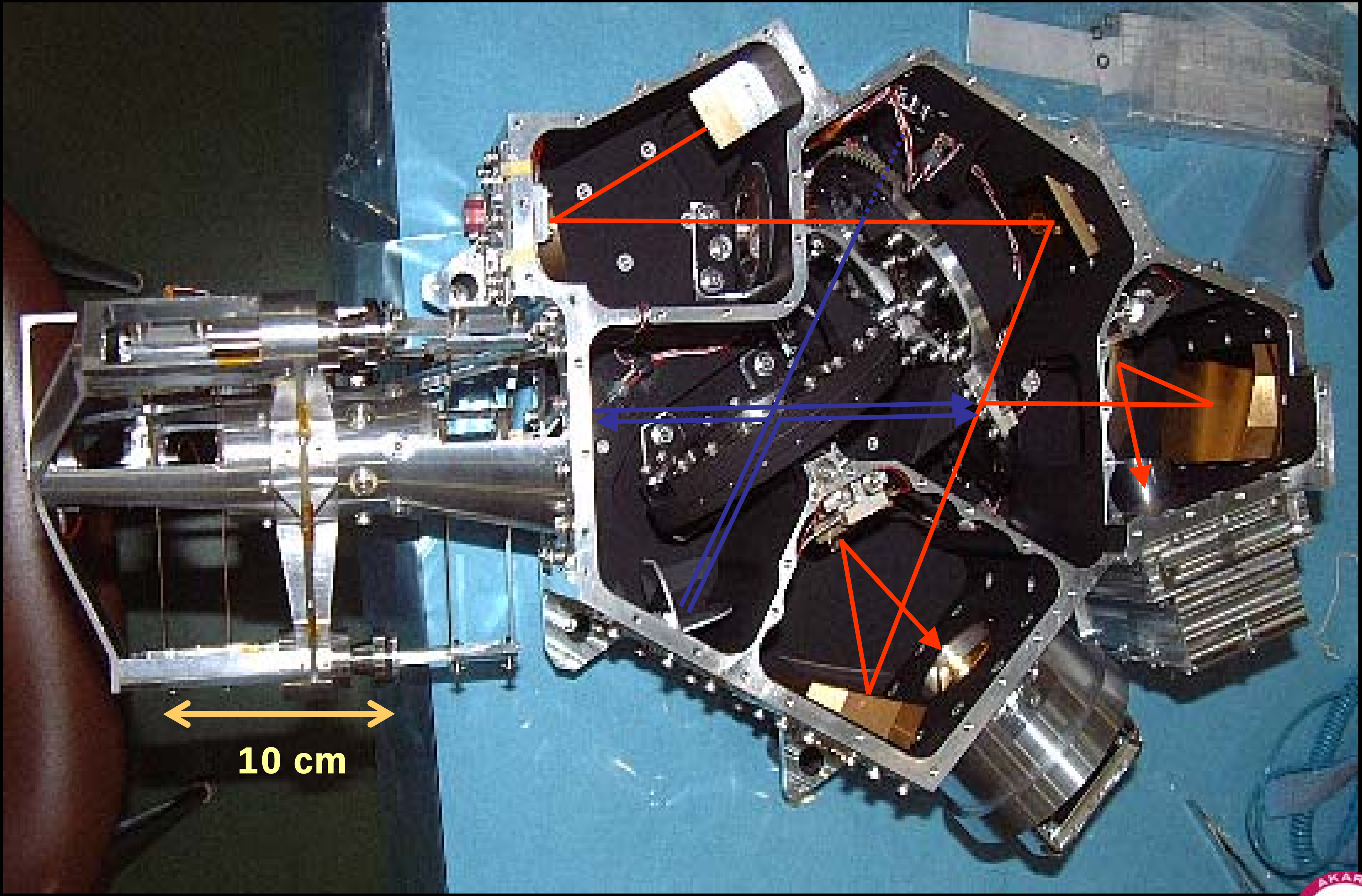

Infrared Observations of interstellar dust grains

尾中 & 石原 2009,
天文月報, 102, 103

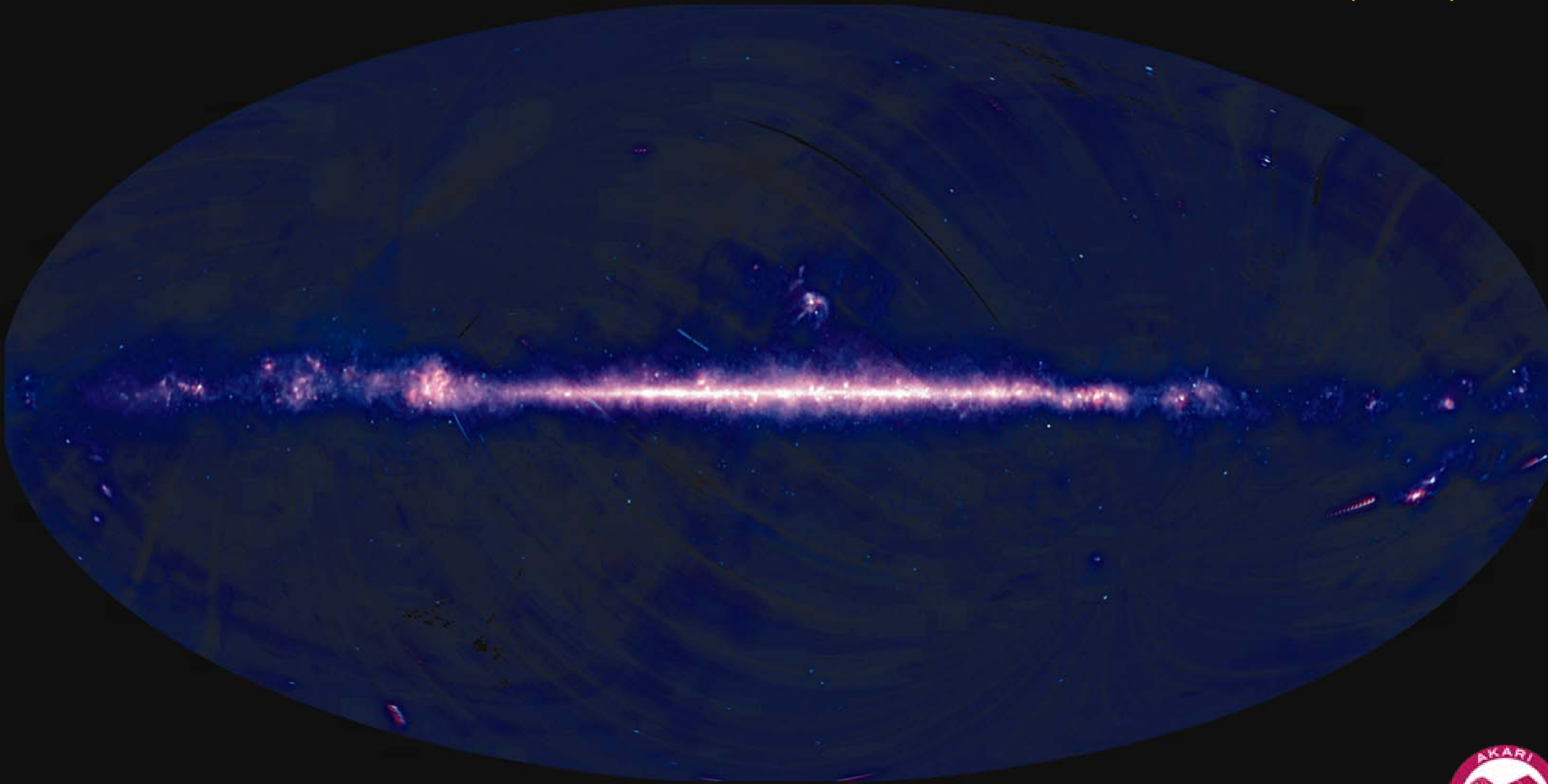

AKARI 9/18μm all-sky map

Diffuse Galactic Infrared Emission

λ>100μm
thermal emission

25-60μm
excess

6-12μm
UIR bands
(polycyclic aromatic hydrocarbons: PAH)

⬇

Stochastic heating or IR fluorescence model

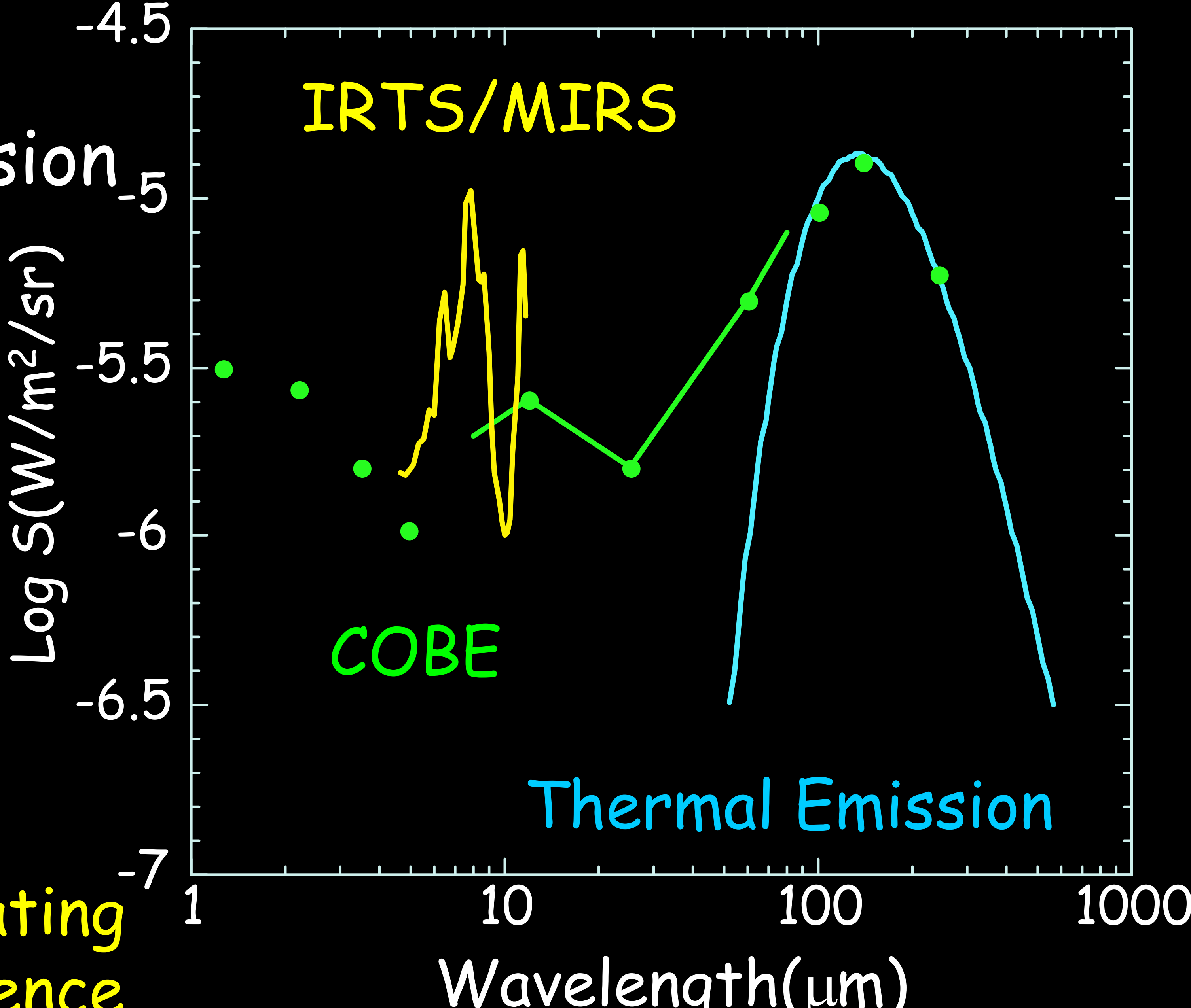

original schematics

Emission bands in MIR

Diffuse IR emission spectra of the Galactic Plane

"Unidentified Emission Bands" at (3.3), 6.2, 7.7, 8.6, & 11.3μm (+ more)

Onaka et al. 1996
PASJ, 48, L59

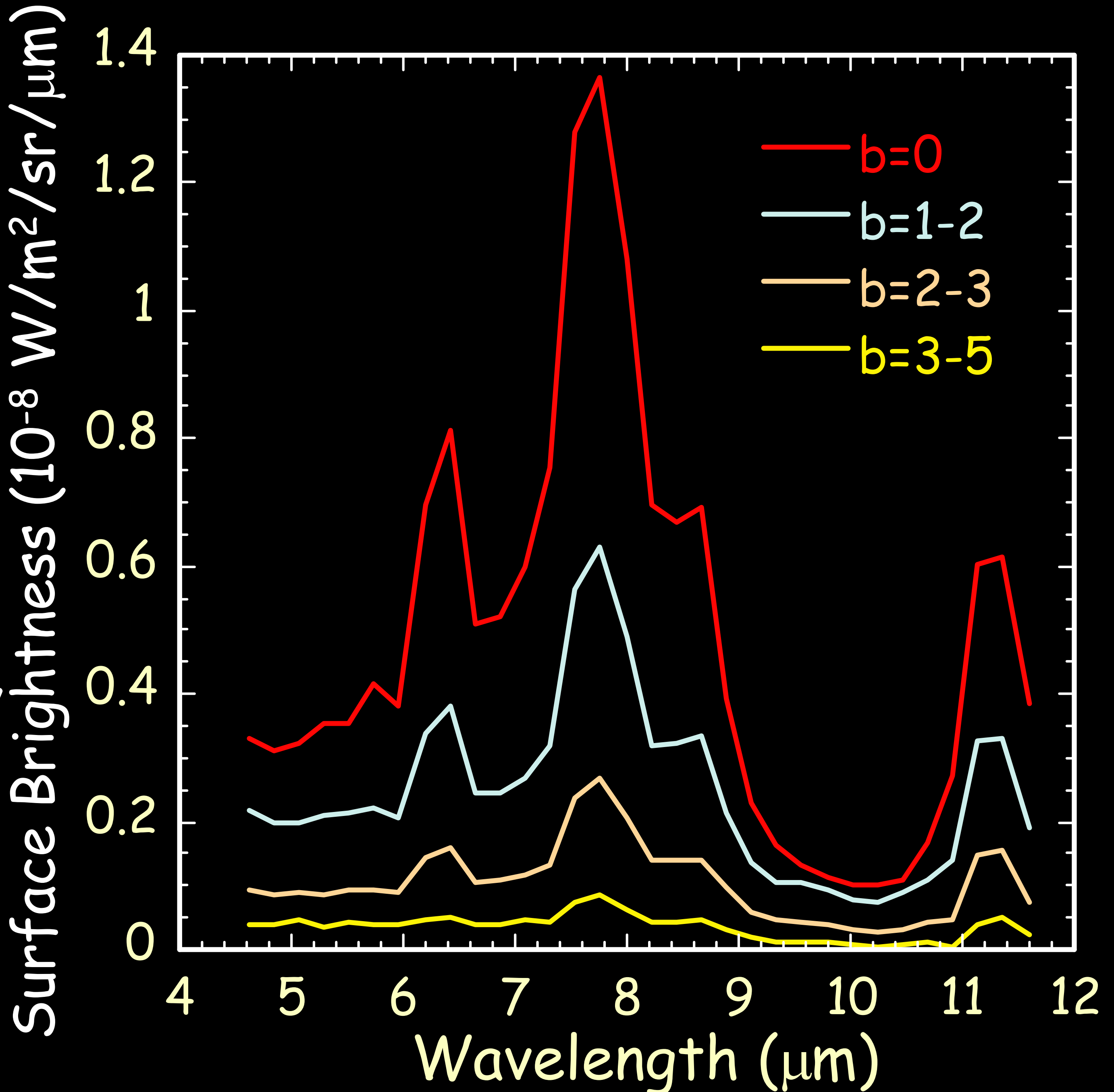

UIR band carriers (organic compounds in the ISM)

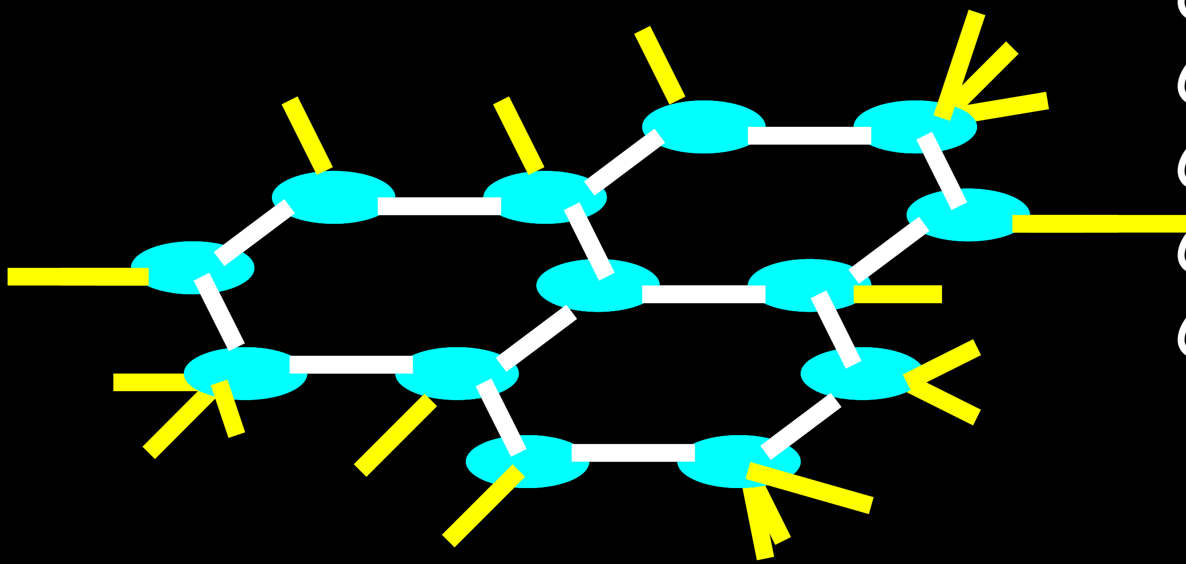

C-H stretch 3.3 μm
C-C bend 6.2 μm
C-C 7.7 μm
C-H bend (in plane) 8.6 μm
C-H bend (out of plane) 11.2 μm
enhanced by ionization

Observed bands can be attributed to vibrations of Polycyclic aromatic hydrocarbon (PAHs)
But exact nature of the carriers remains unclear

Relative band ratios should depend on physical conditions (e.g., ionization) of the band carriers

Correlation of UIR bands with total FIR intensity

Total FIR intensity is a product of the dust column density and the incident radiation intensity

$$\mathrm{FIR} = \tau_0 \int (\lambda_0/\lambda)^{\beta} B_{\lambda}(T)\, d\lambda$$

$$= \langle\tau_{abs}\rangle\, G_{\odot} \mathrm{x} G_o \; / 4\pi$$

Go: radiation intensity in units of solar neighborhood value $G_{\odot}$ (= 1.6×10^{-6} Wm^{-2})

Stochastic heating or IR fluorescence model predicts UIR band intensity is also a product of the column density and the radiation intensity

UIR band strength $\propto \tau$ Go $\propto$ FIR

[Go $\propto T^{4+\beta}$, $\langle\tau_{abs}\rangle/\tau_{100\mu m}$ = 700 -> Go]

UIR7.7μm/FIR in W51 by IRTS

Good correlation with total FIR

Supporting stochastic heating or fluorescence model

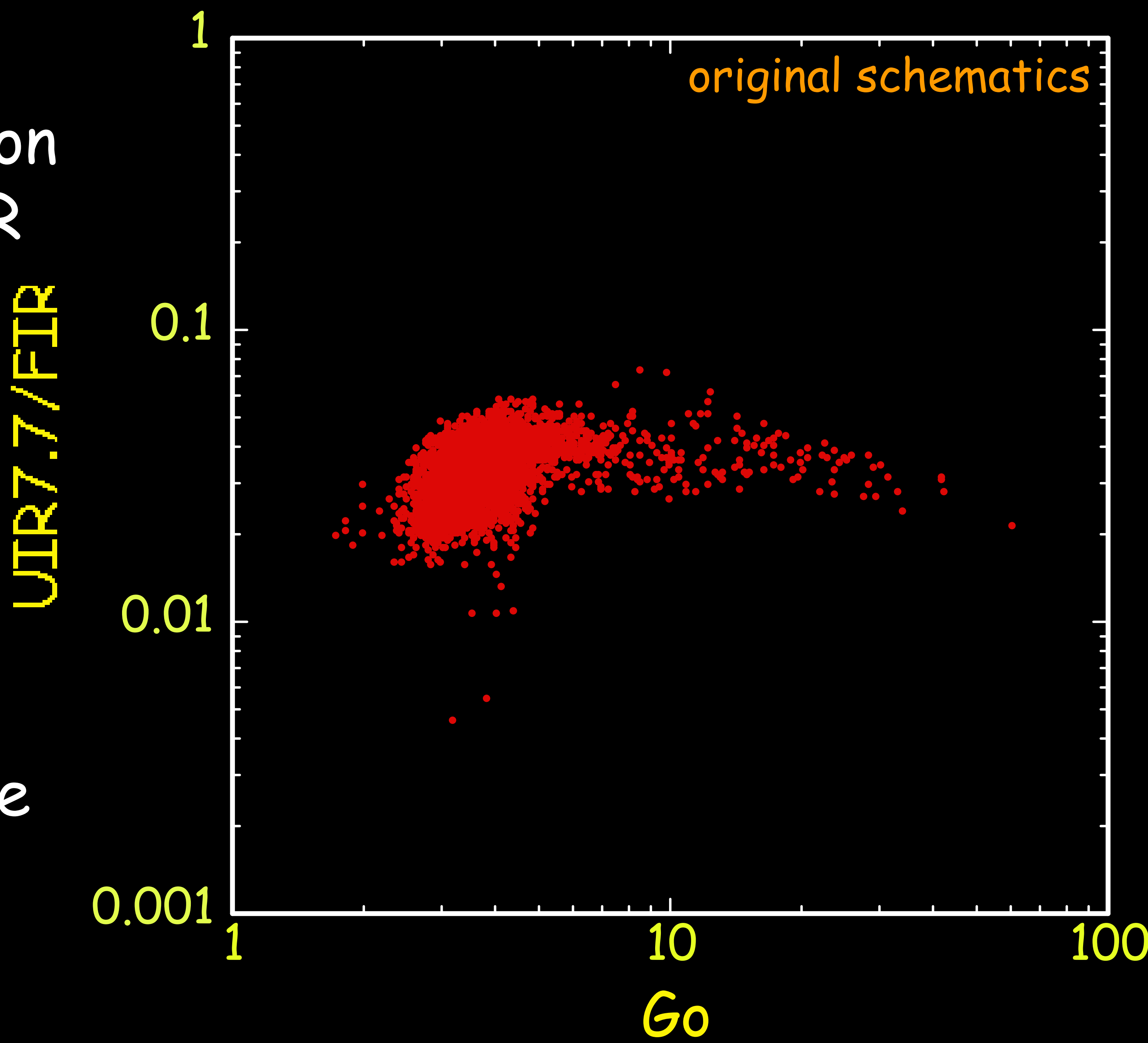

UIR bands in ionized regions

ISO observations of Carina & S171 regions

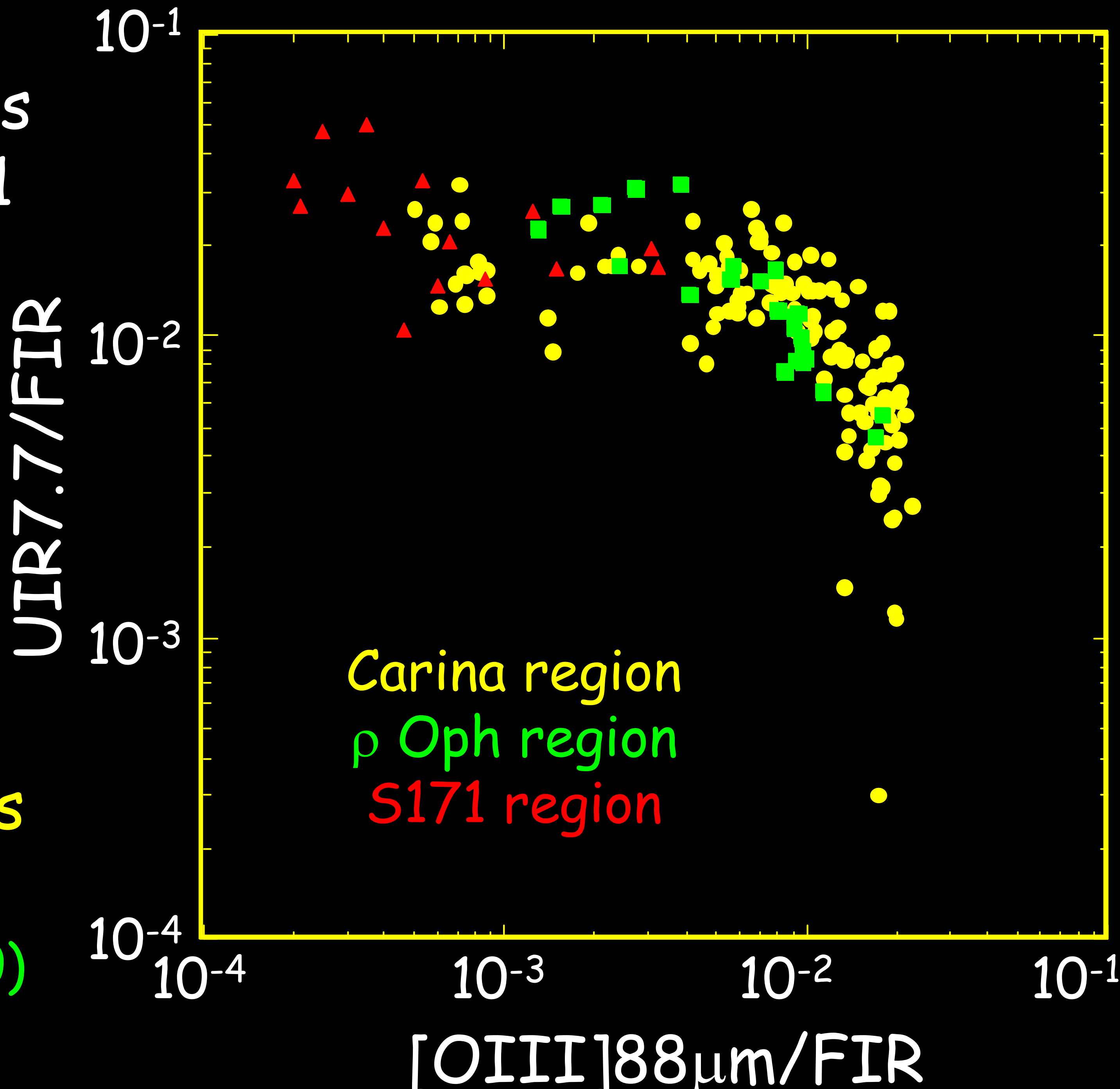

UIRs weaken in ionized regions

Onaka et al. (2000) ESA SP-456, 55

PHT-S Results of Galactic Plane

No systematic variations in the UIR bands on GP

l = ±5, ±15, ±30, ±60 & b = 0, ±1 (49 quiet regions)

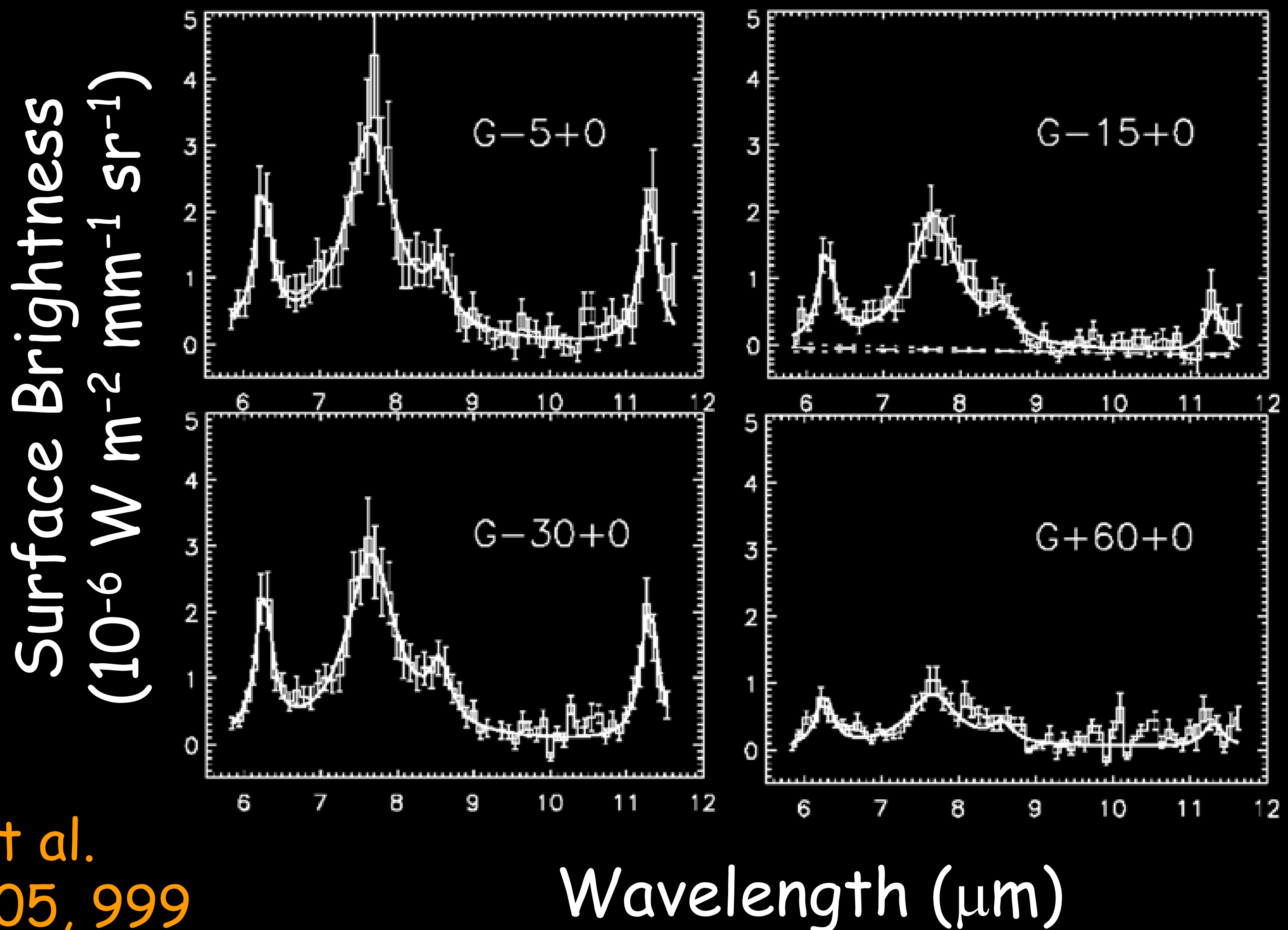

Kahanpää et al. (2003) A&A 405, 999

IRAS100μm & UIR7.7μm

Area I	Area II	Area III	Area IV
l ~ -10	l ~ +50	l ~ -130	l ~ +170

IRAS100μm Good correlation between UIR & 100μm

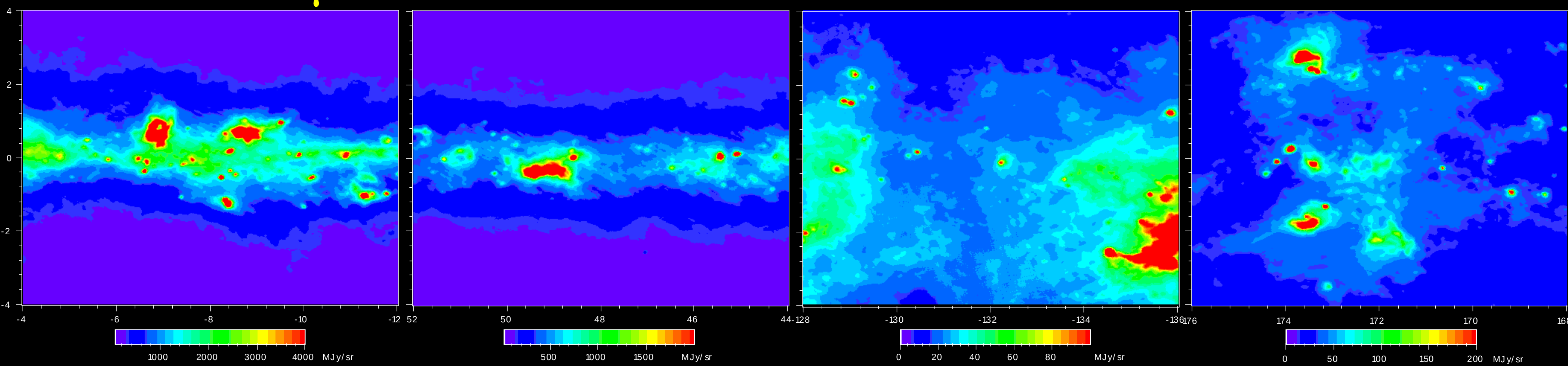

UIR7.7μm

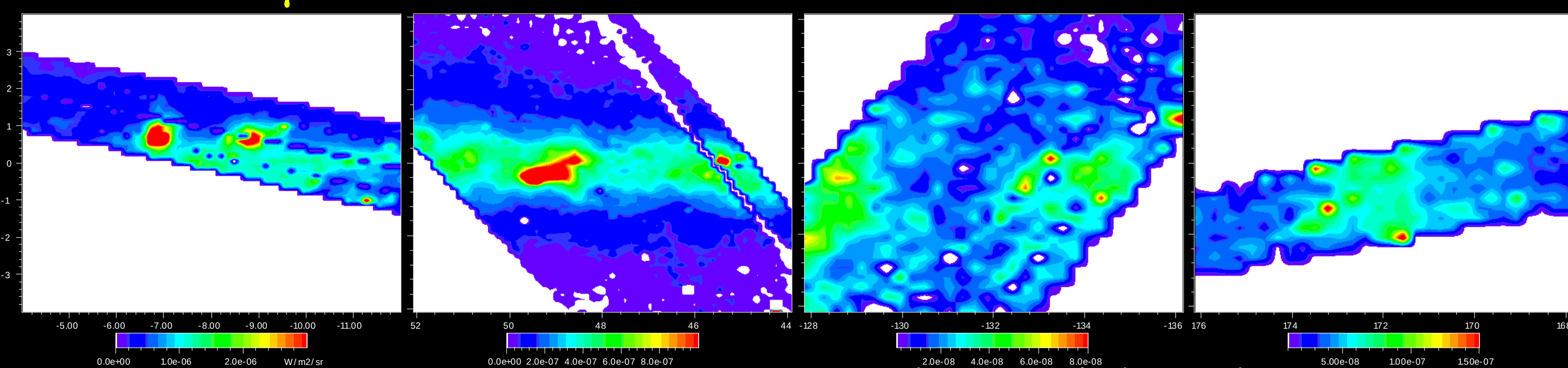

Sakon et al. (2004) ApJ, 609, 203

Typical Spectra

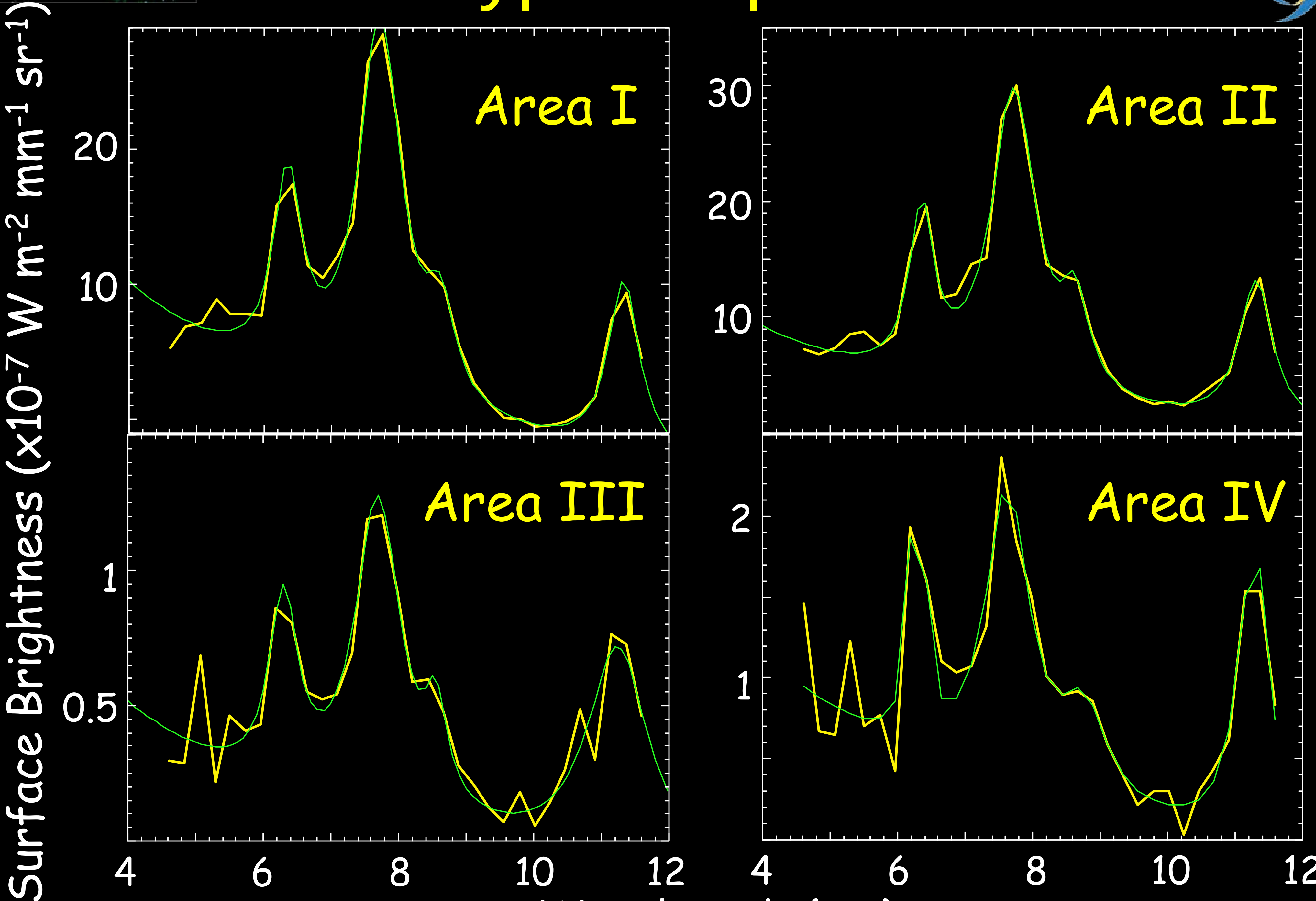

Sakon et al. (2004) ApJ, 609, 203

Variations in the UIR bands

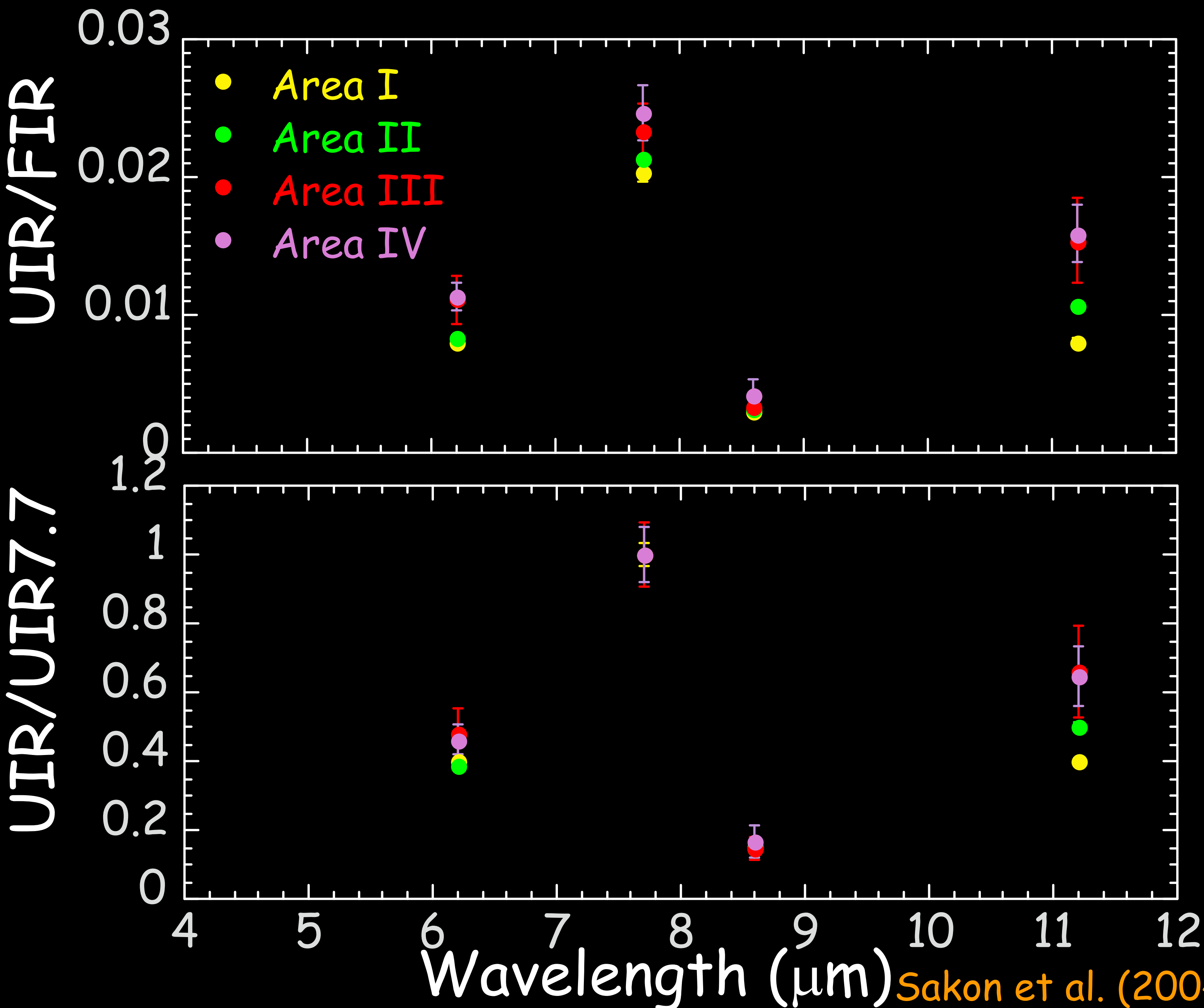

UIR/FIR larger in outer region

11.3/7.7 larger in outer region

Sakon et al. (2004) ApJ, 609, 203

UIR bands in galaxies

Emission from the Galactic plane shows tiny variations
External galaxies provide extreme conditions

Major UIR bands are at 3.3, 6.2, 7,7, 8.6, 11.2μm ubiquitously seen in spiral & starburst galaxies
The variations seen among normal galaxies are small based on ISO observations

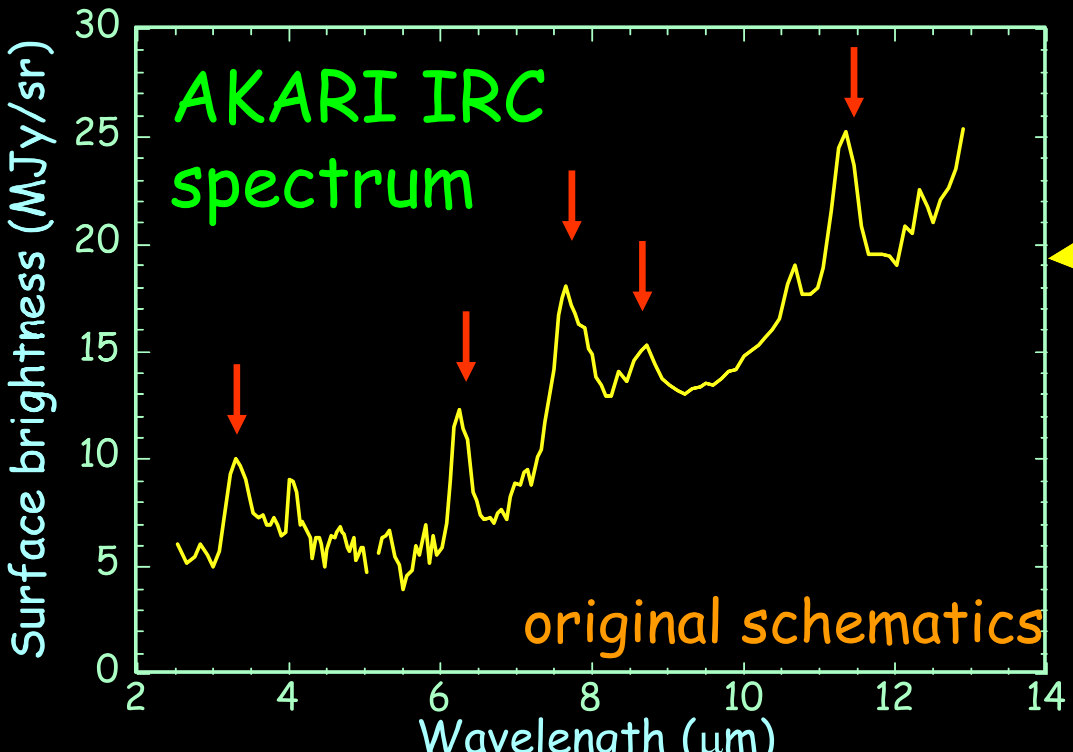

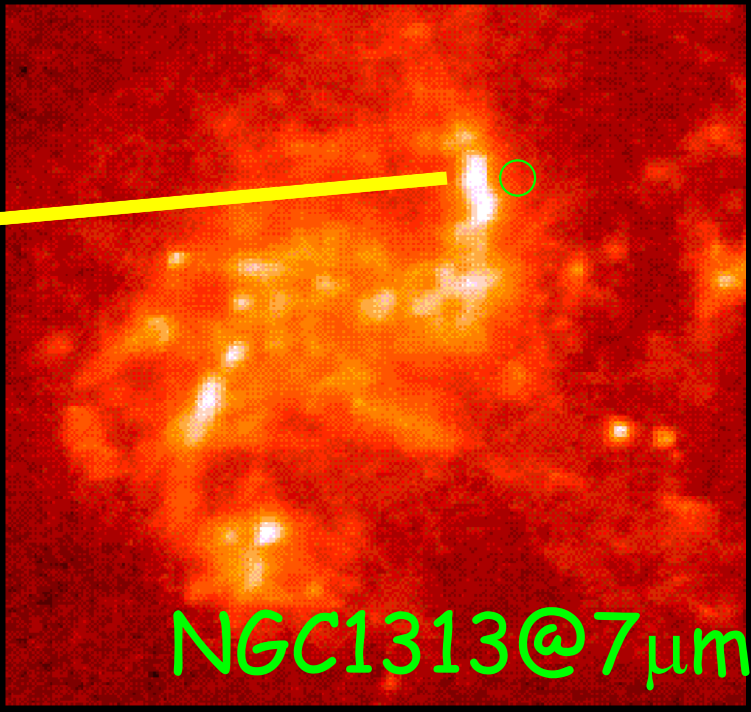

UIR bands in elliptical galaxies

Elliptical galaxies are a matured, processed system

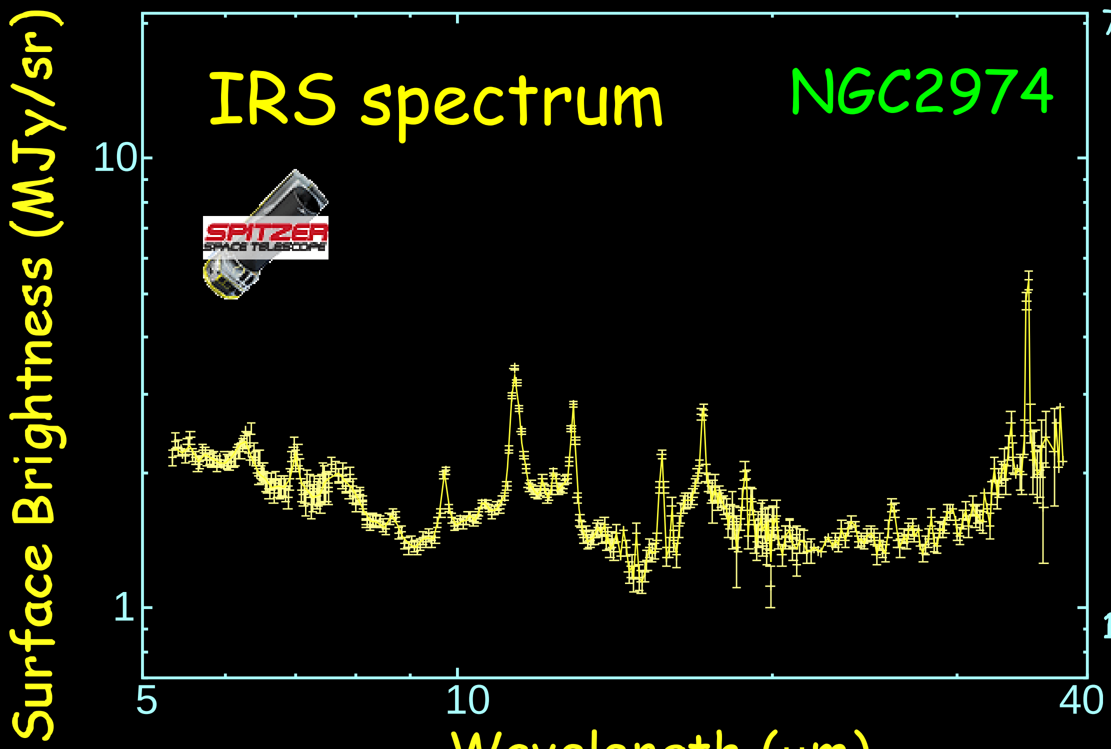

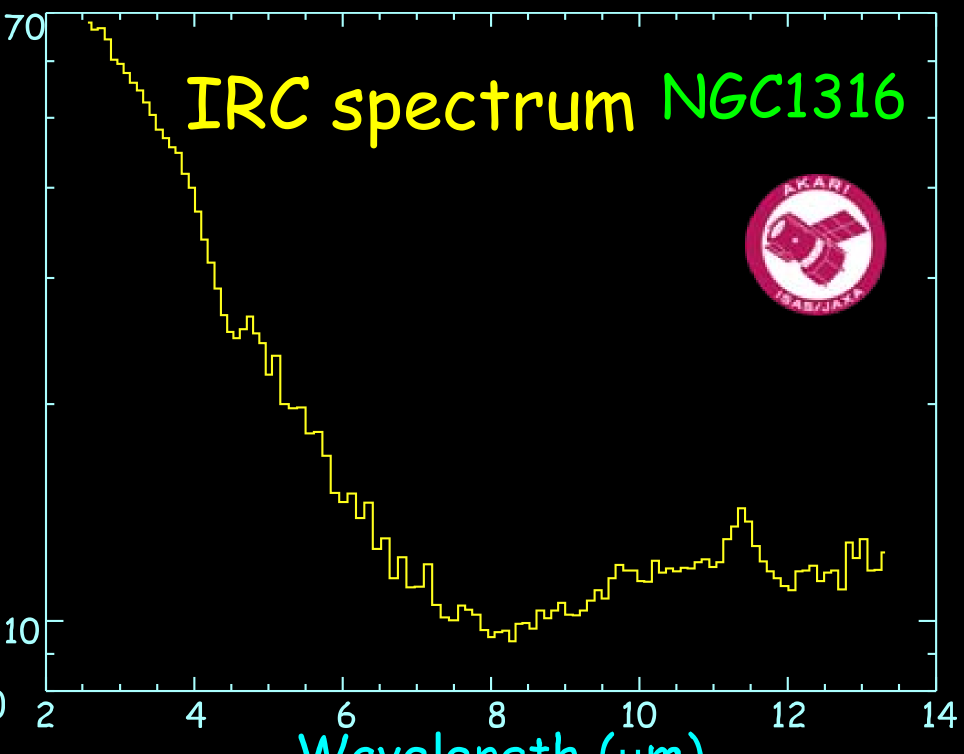

Kaneda et al. (2005) ApJL 632, L83 Kaneda (2007) ApJL, 666, L21

11.3 and 17μm complex are clearly detected
6.2, 7.7, & 8.6μm are very weak

No detection of 3.3μm in NGC 1316 suggests dominance of large & neutral PAHs

7.7μm/11.3μm band ratio variation in star-forming galaxies

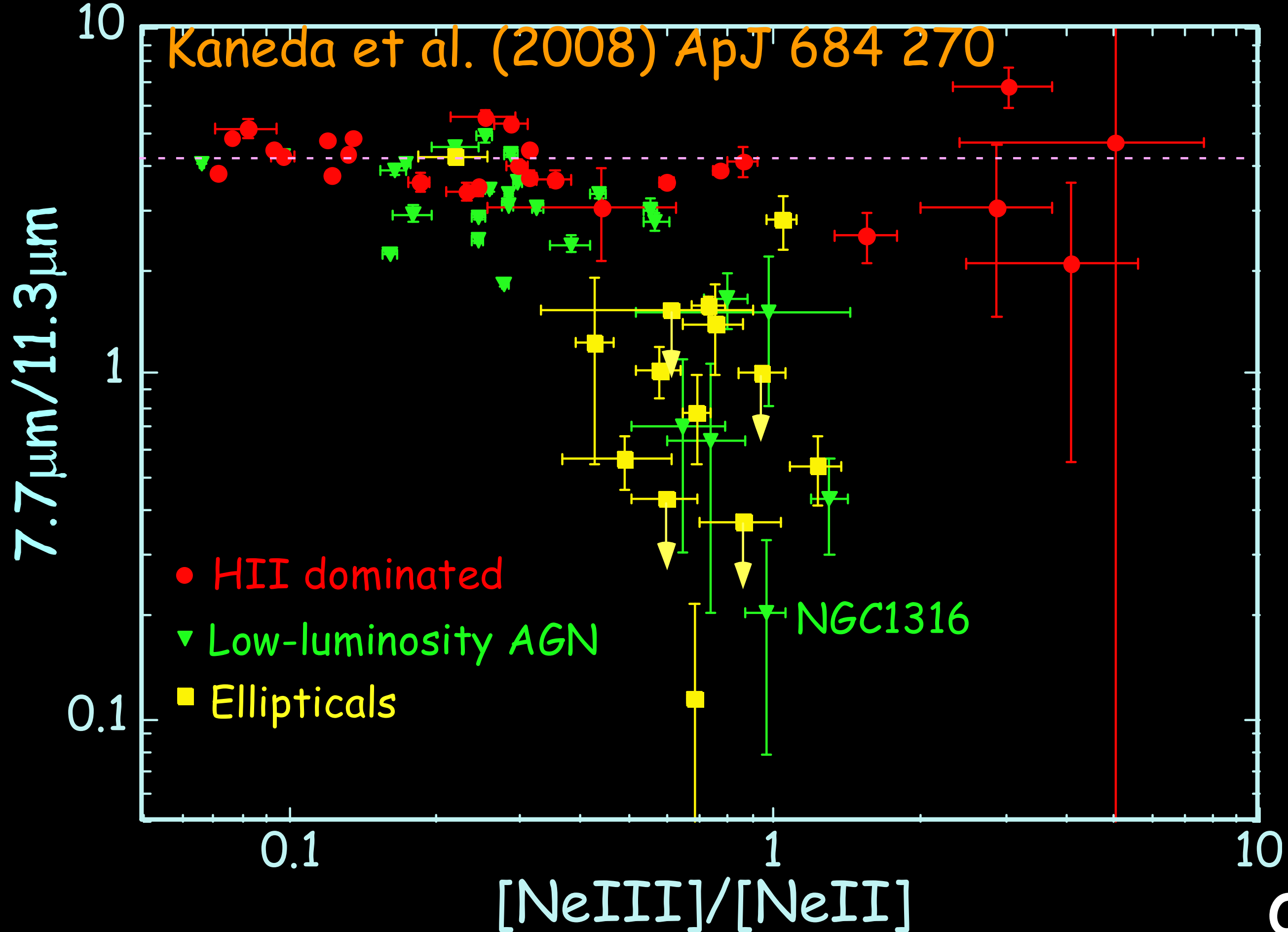

Smith et al. (2007) ApJ 656, 770
Kaneda et al. (2008) ApJ 684 270

Ellipticals (■) or galaxies with AGN (▼) show lower 7.7/11.3μm ratios

cf. AGN activity in NGC1316 ceased 100Myr ago, suggesting effects other than AGN also play a role

Dwarf (young) galaxies (high [NeIII]/[NeII]) do not show any systematic difference in the band ratio

AKARI observations of NGC6946

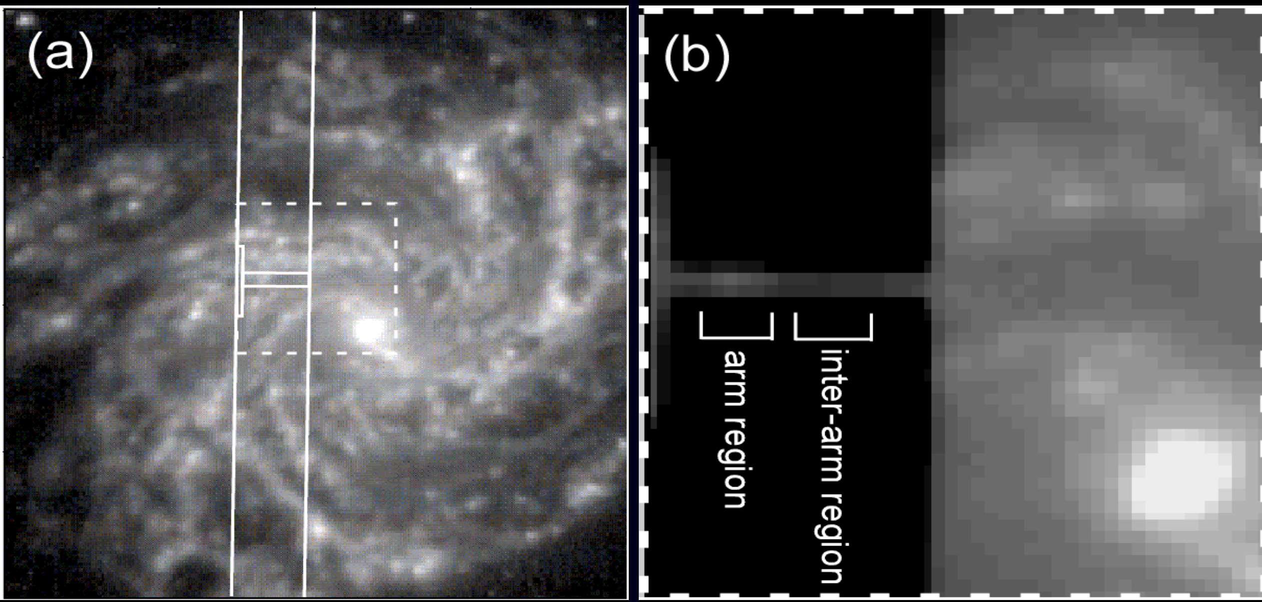

Interarm region has a lower 7.7/11.3 ratio than arm region

Sakon et al. (2007)
PASJ, 59, S483

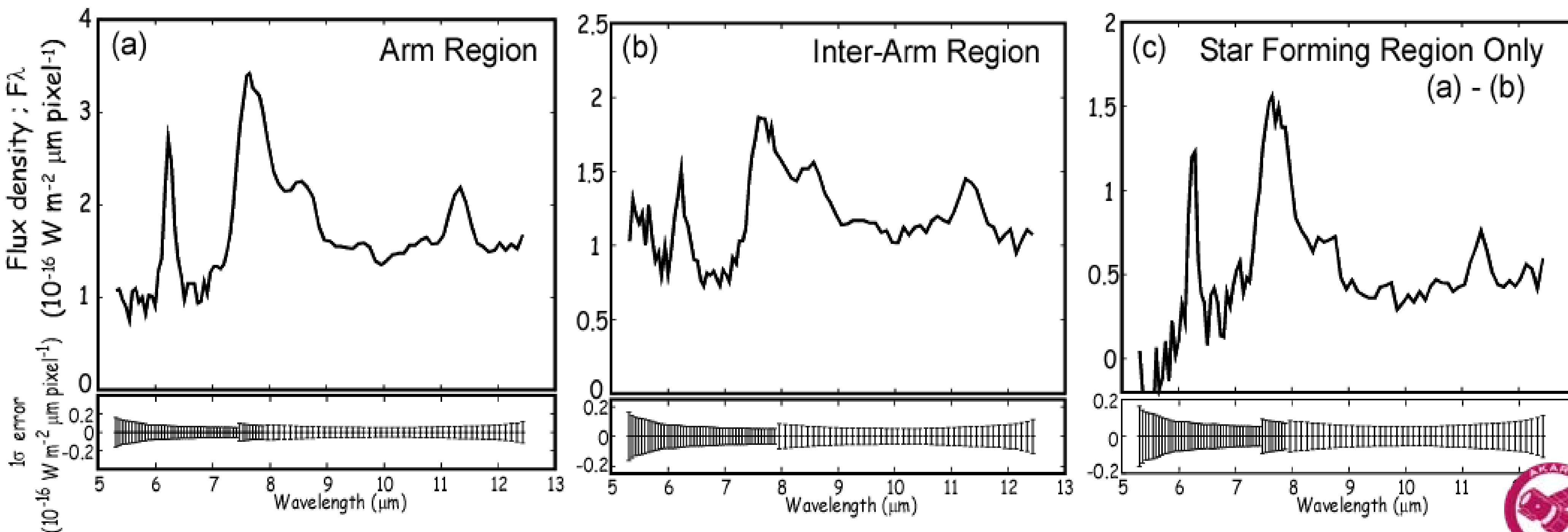

UIR band variations seen in galaxies

(6.2, 7.7)/11.3μm band ratio decreases
in inter arm regions
Elliptical galaxies associated with hot plasma
(indicated by X-ray emission)
have extremely weak 6.2 & 7.7μm bands

Ionization effects* or band carrier processing
in plasma environments?

- 6.2 and 7.7μm bands are enhanced
- by ionization of PAHs

UIR bands in extended structures of galaxies
(halo, jets, …) associated with ionized gas ?

M82 seen by AKARI

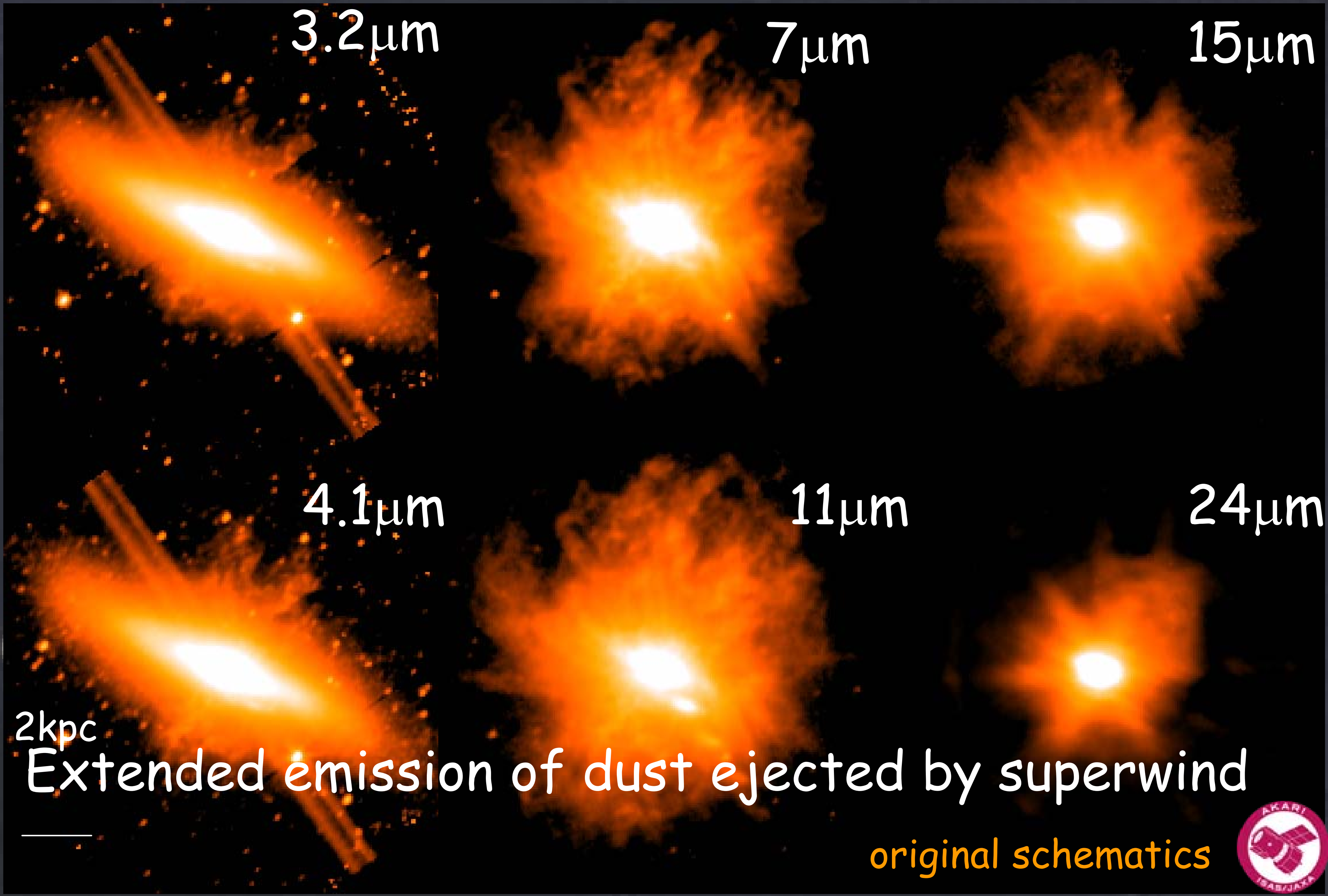

UIR bands in M82 filaments

Red: Hα, Green: 7μm　　　　3.2μm (B)+ 7μm(G) + 15μm (R)

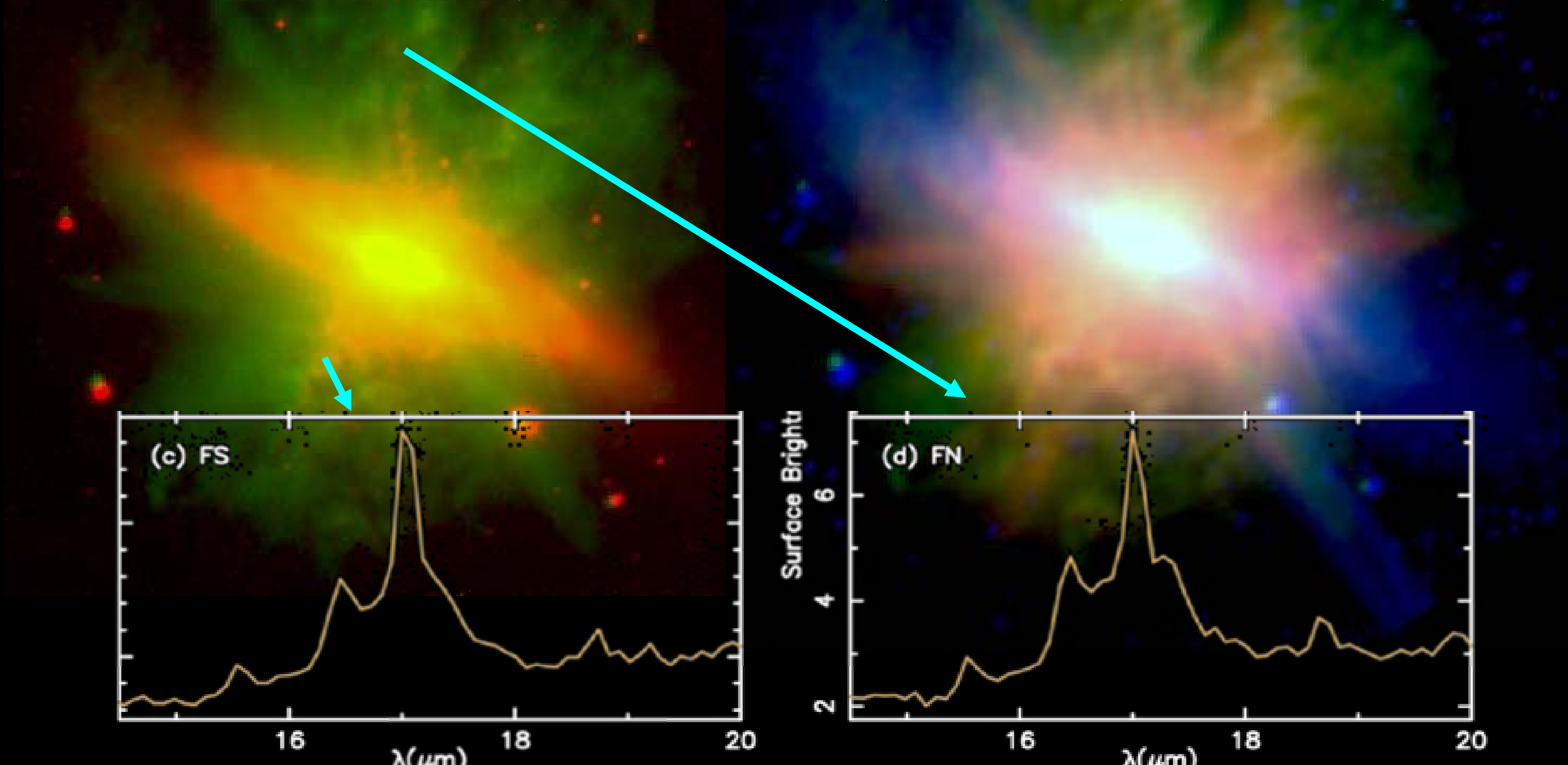

Engelbracht et al. (2006) ApJL, 642, L127

UIR band detected in filamentary structures seen in 7-15μm extended over Hα features

PAHs survive in superwind?

UIR band ratio variation in M82

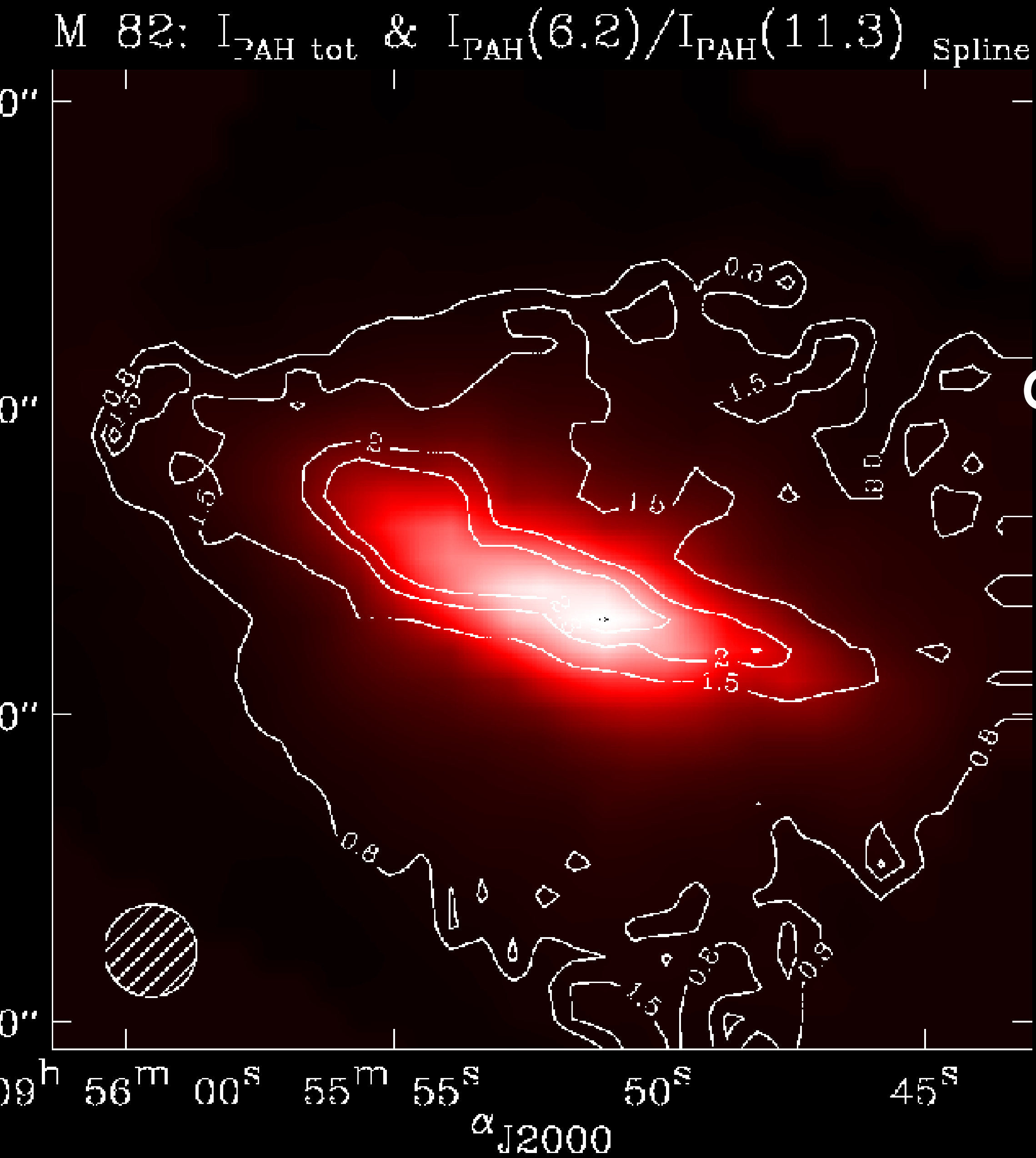

6.2, 7.7, & 8.6μm are well correlated

6.2 (7.7)/11.3μm is low outside the galactic plane

A similar trend seen in the interarm regions of NGC6946 and the outer region of our Galaxy

Galliano et al. (2008) ApJ 679, 310

NGC1569 seen by AKARI

Nearby starburst dwarf (12+log(O/H)=8.13)

Several filaments produced by galactic winds

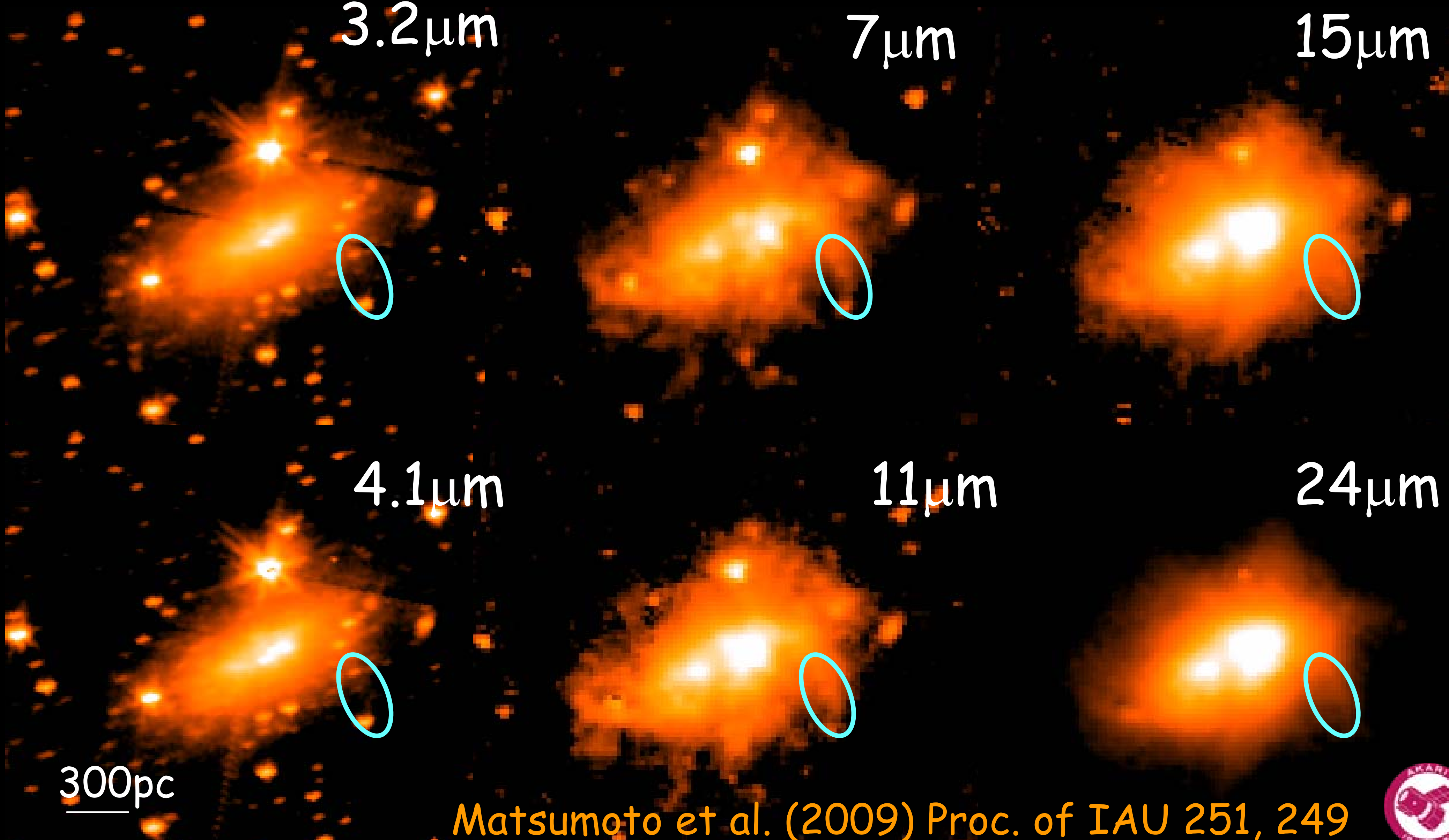

Matsumoto et al. (2009) Proc. of IAU 251, 249

UIR band associated with filaments

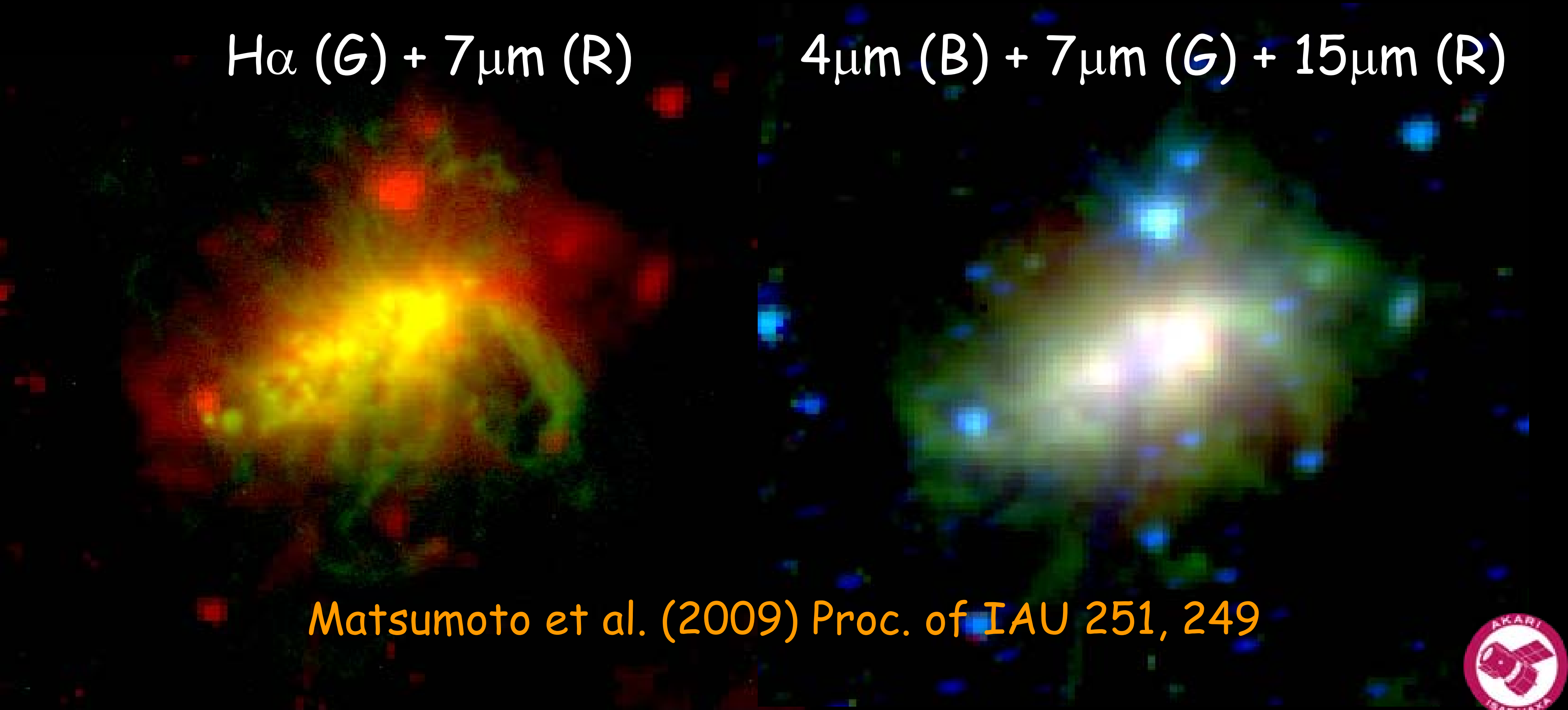

7μm emission well correlated with Hα filaments
Band carriers present in filaments of ~10^6yr old, where destruction should be very fast (~1000yr)
Produced from fragmentation in the shocked region?

AKARI Spectroscopy of a filament of NGC1569

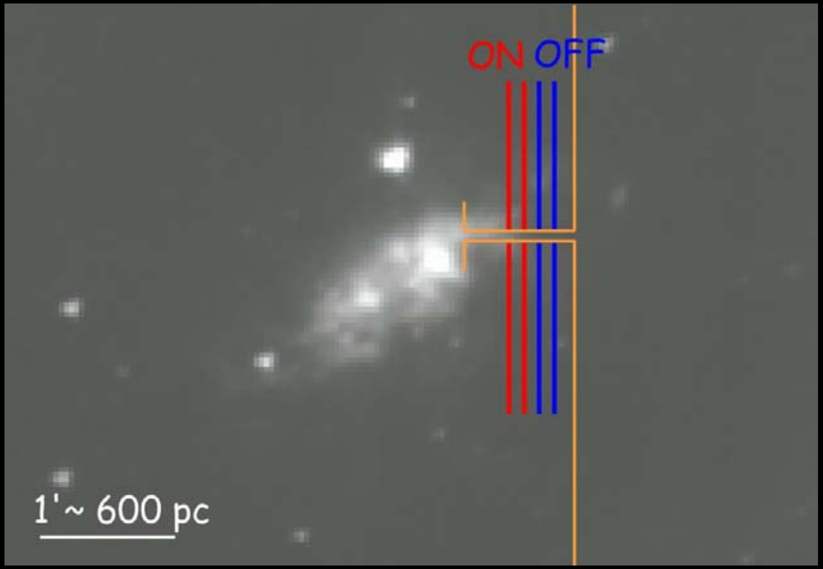

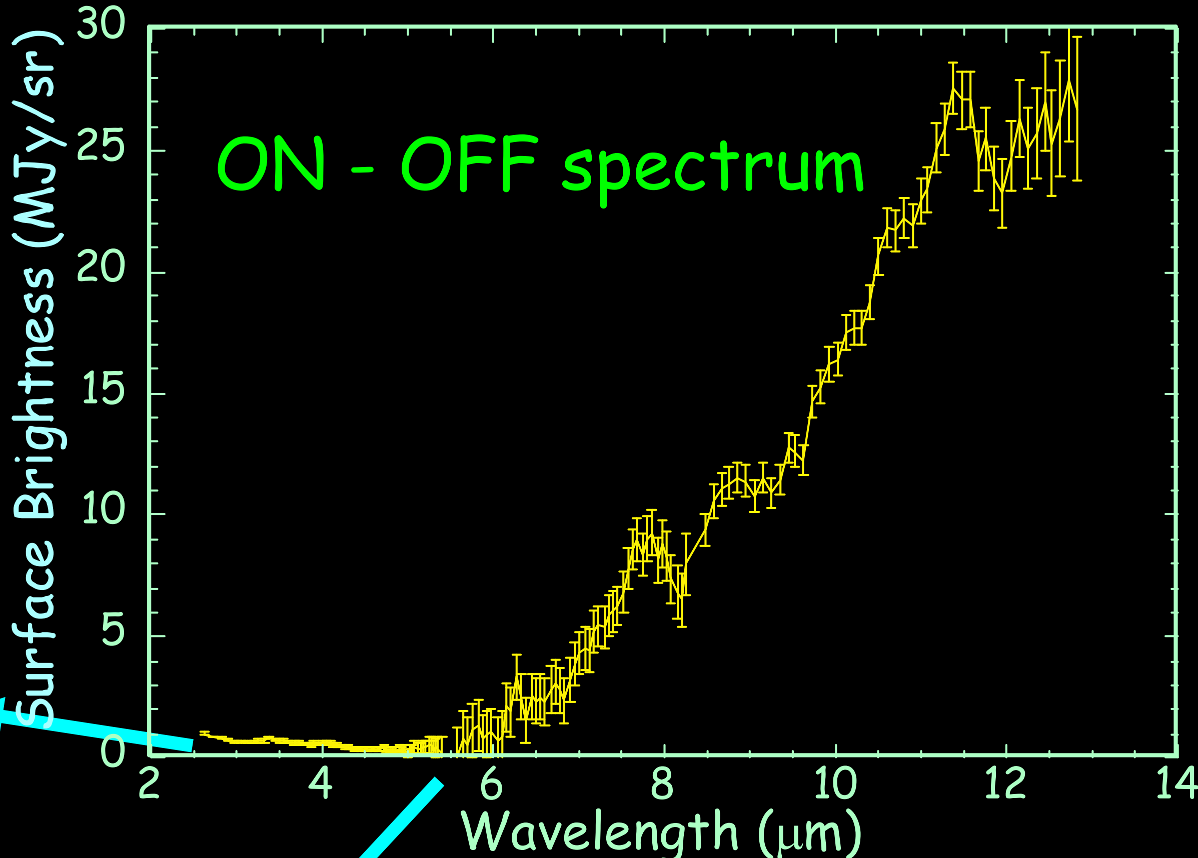

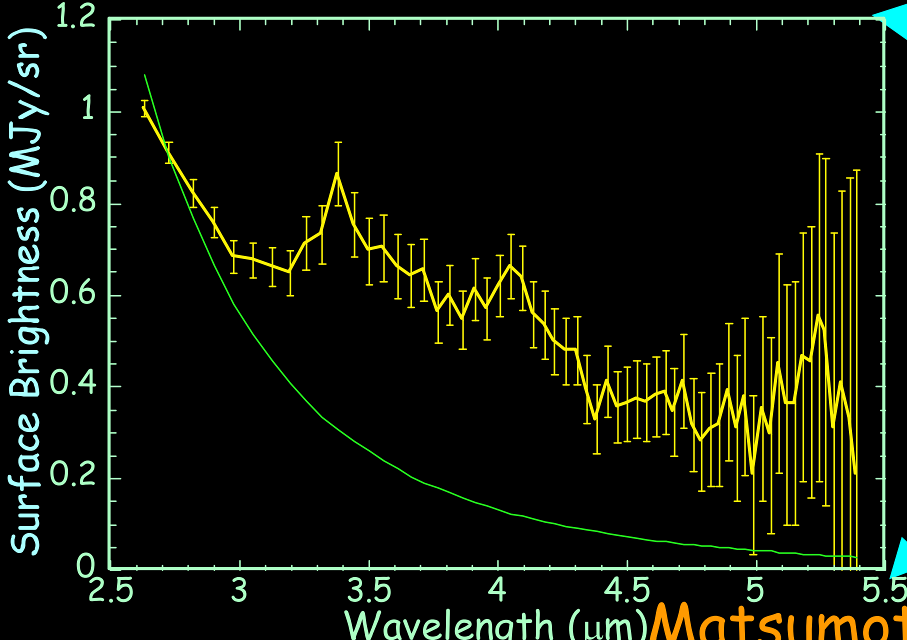

3.3, 6.2, 7.7, (8.6), & 11.3μm bands + NIR excess are detected in the Hα filament

Matsumoto et al. (2009) Proc. of IAU 251, 249

Spectra of Filament & Disk

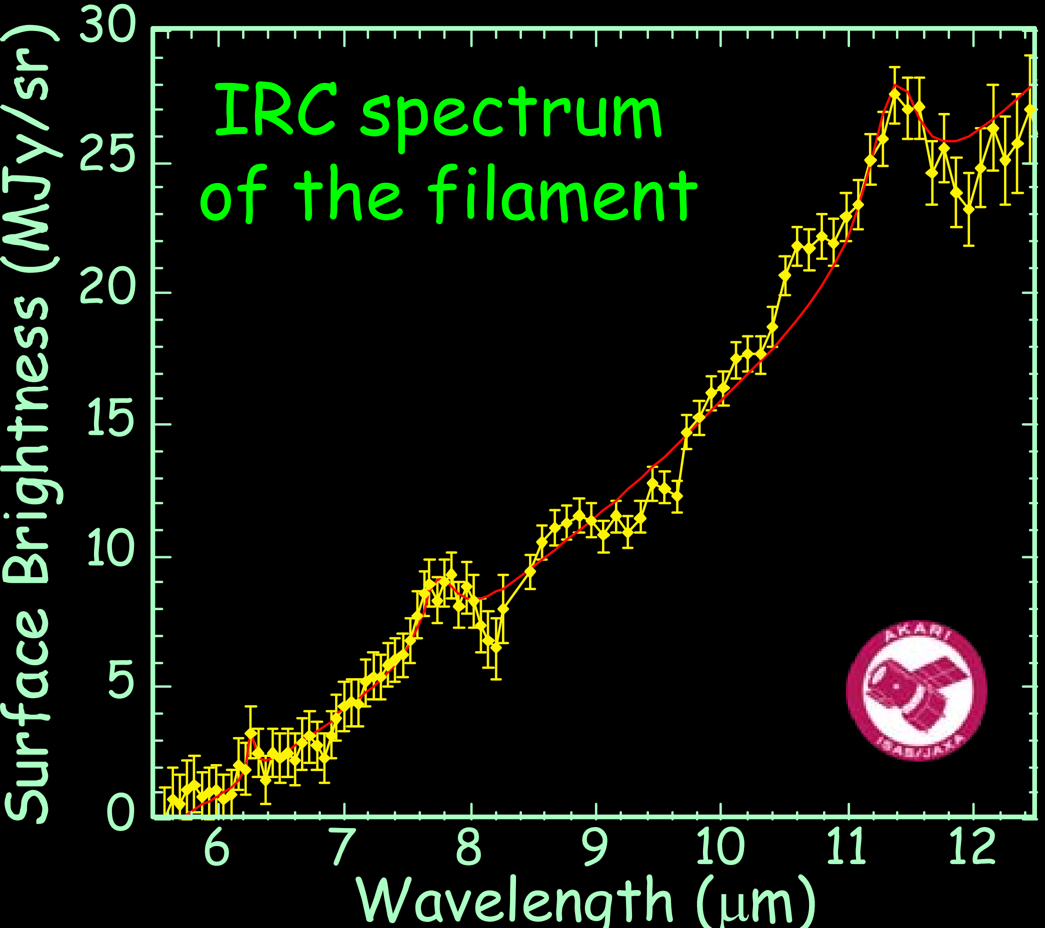

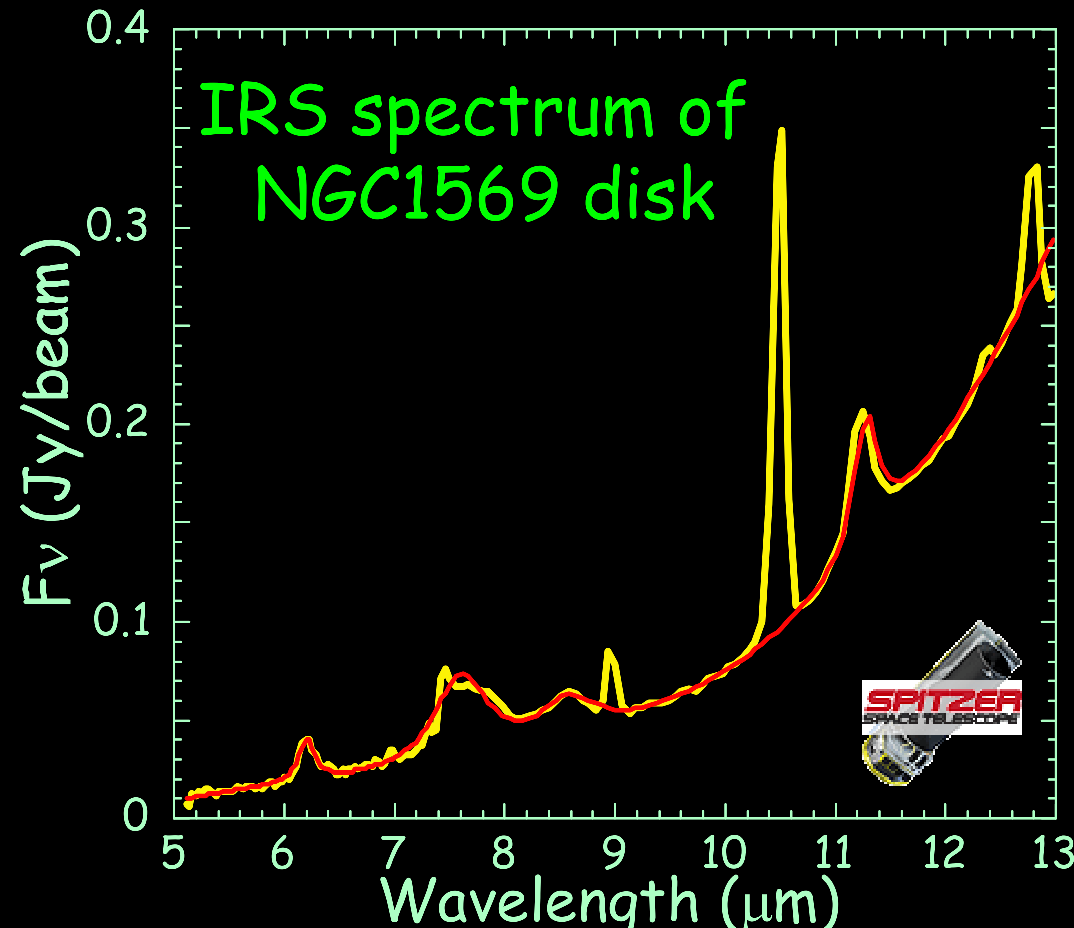

Matsumoto et al. (2009) Proc. of IAU 251, 249

7.7/11.3μm ratio is smaller in the filament than in disk

7.7μm band seems to be narrower

Comparison of band ratio

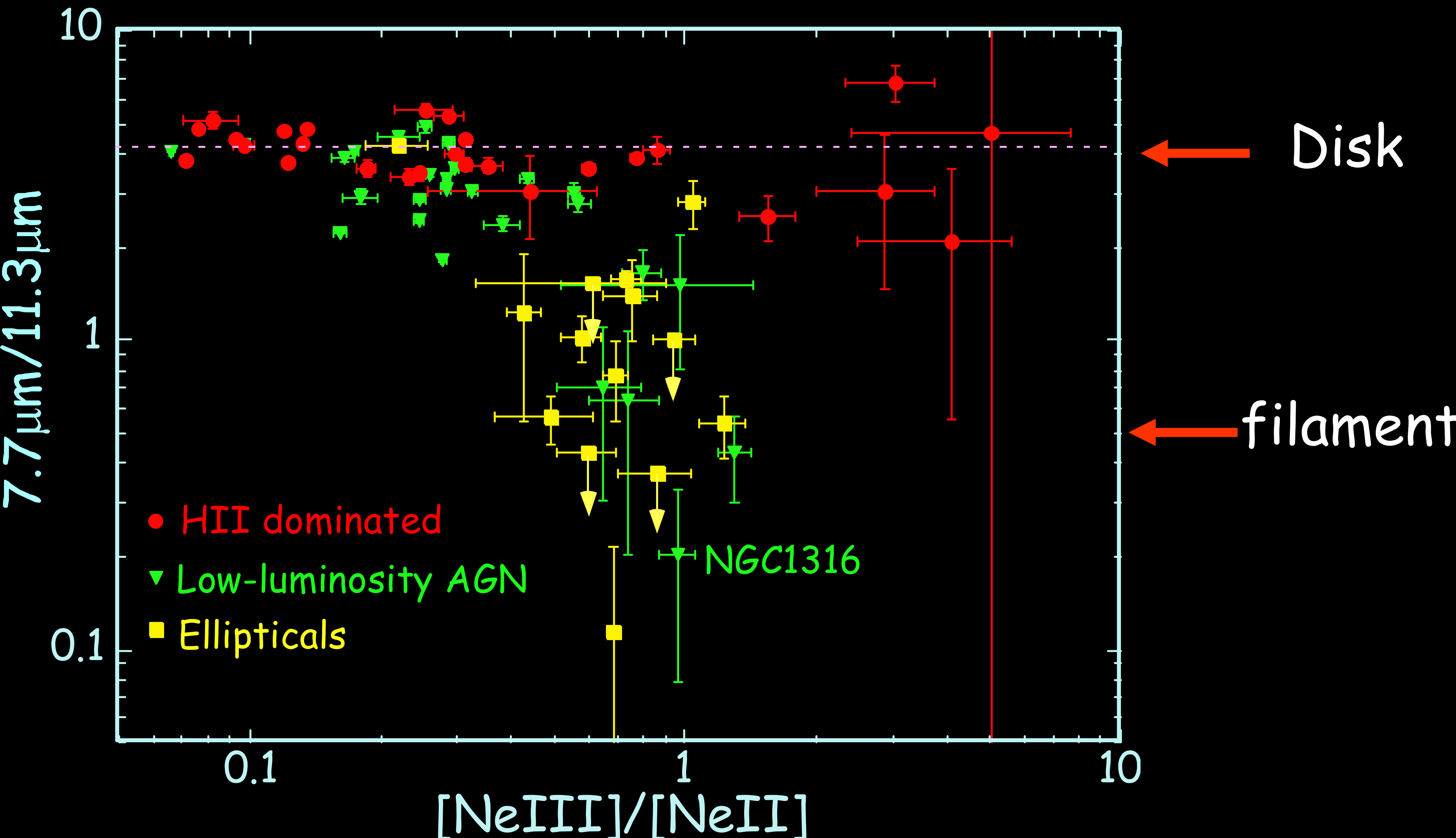

Kaneda et al. (2008) ApJ 684 270

HII regions in M101

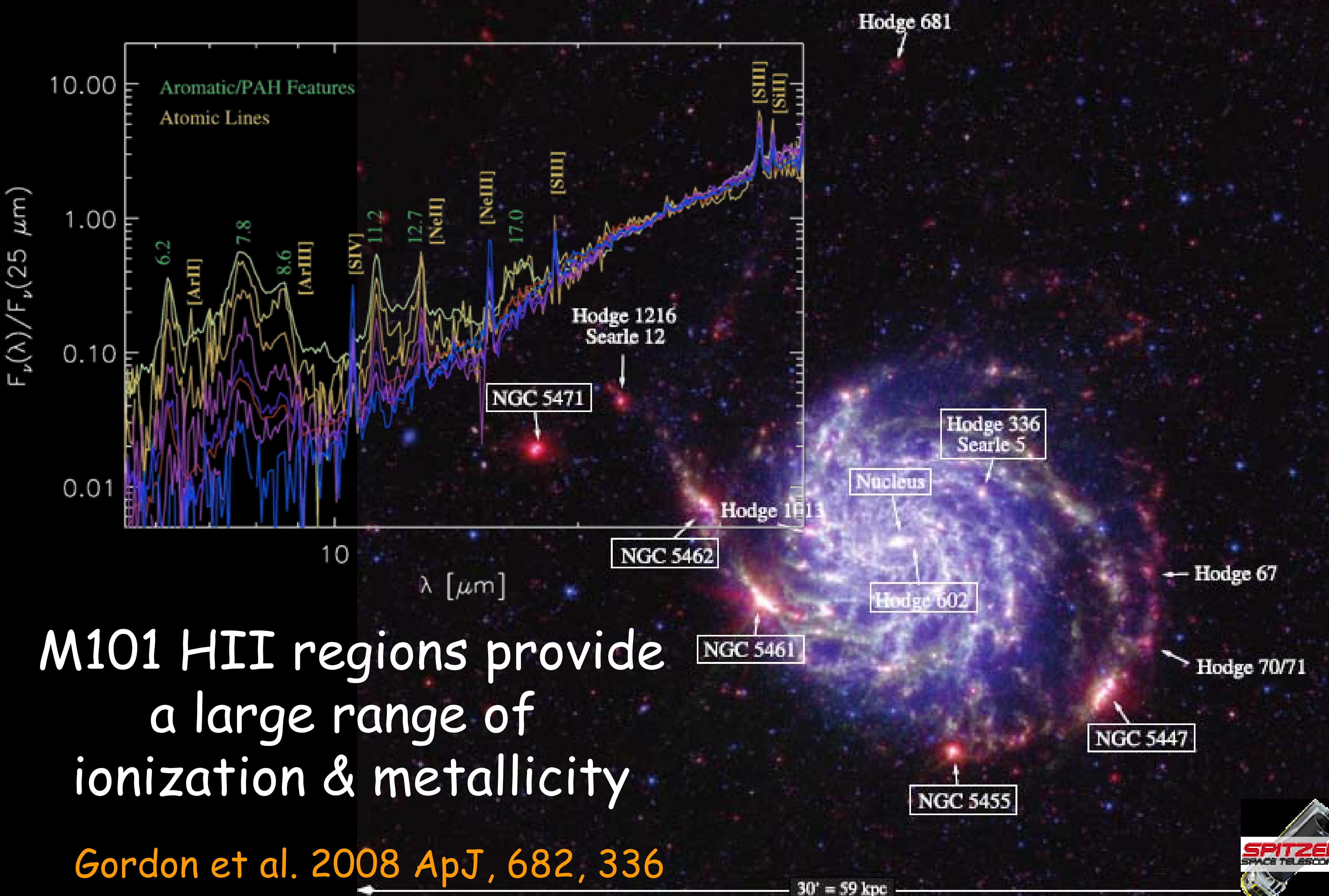

M101 HII regions provide
a large range of
ionization & metallicity

Gordon et al. 2008 ApJ, 682, 336

UIR band equivalent width vs metallicity & ionization

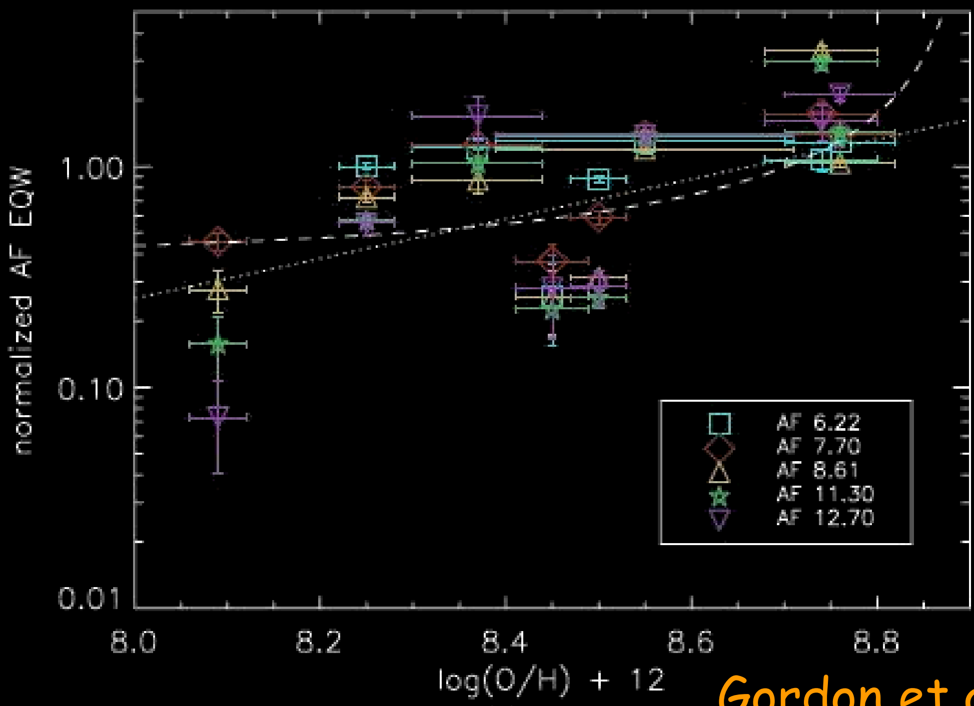

Metallicity

Gordon et al. 2008 ApJ, 682, 336

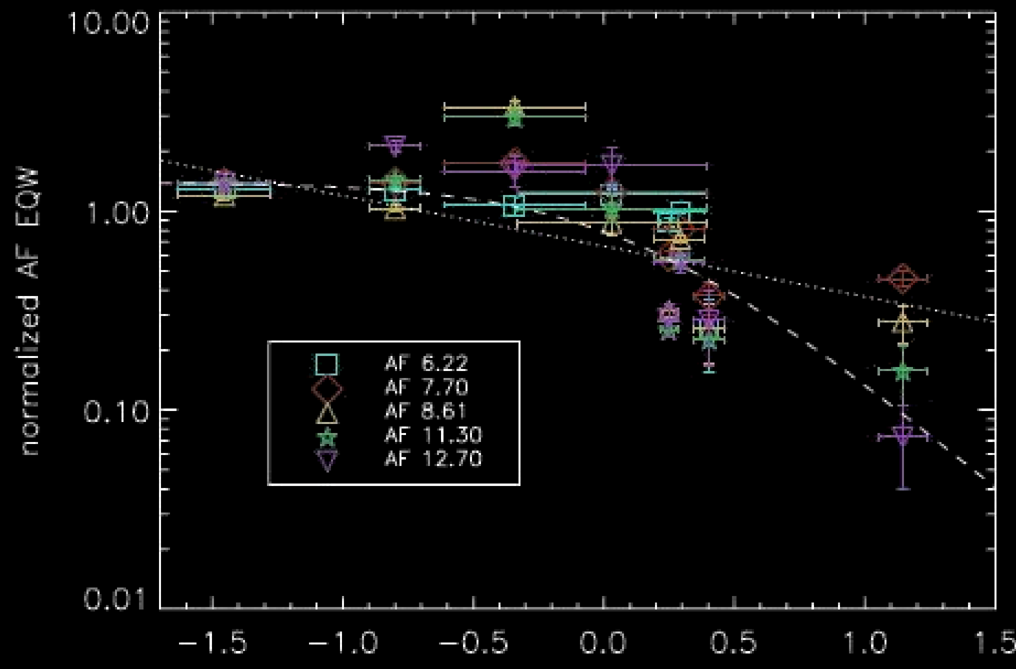

Ionization

No clear correlation with metallicity

UIR band decreases in highly ionized regions, indicating the decrease of the band carriers

No correlation of band ratios

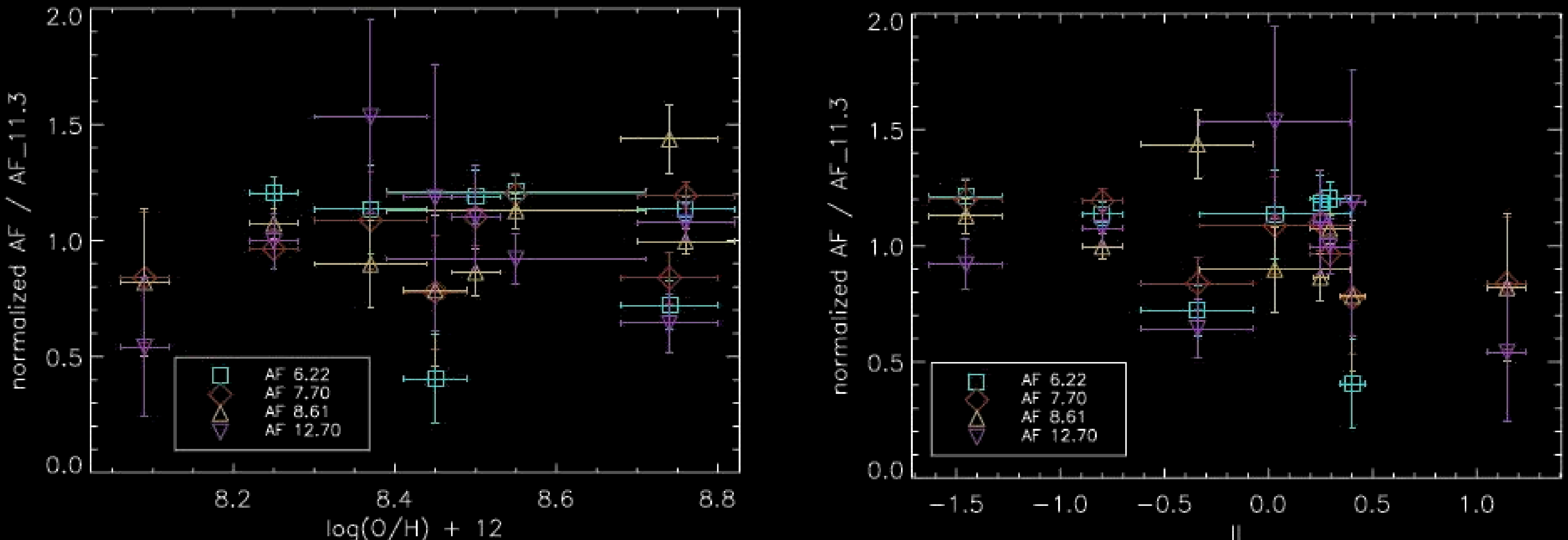

Gordon et al. 2008 ApJ, 682, 336

6.2/11.3 & 7.7/11.3 are expected to increase with the ionization parameter,

but no systematic trend is seen in M101 HII regions

A trend of band carrier processing seen so far is only the 6.2/11.3 & 7.7/11.3 decrease in hot plasma environments (halo, jet, elliptical galaxies)

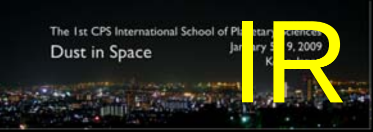

IR spectroscopy for the study of gas abundance

Forbidden lines have negligible coupling with radiation and are excited exclusively by collisions
Intensity is a function of local temperature and density of the collision partner

Forbidden lines in IR
Less affected by extinction
ΔE < kTe; insensitive to Te
Intensity is a function of density only

IR spectroscopy provides a unique opportunity to study elemental abundance in dense star-forming regions

All Sky Map@9μm by AKARI

Large Si abundance in active regions

[SiII]35μm
ISO observations of Carina region
(Mizutani et al. 2004, A&A, 423, 579)
S171 & ρOph regions
(Okada et al. 2003, A&A, 412, 199; Onaka et al. 2006, A&A, 640, 383)

>10-25% Si in gas phase even in high-density regions
(≲ ~5% in ISM)
Large amount of Si in volatile grains other than silicates?
Then how is Fe?

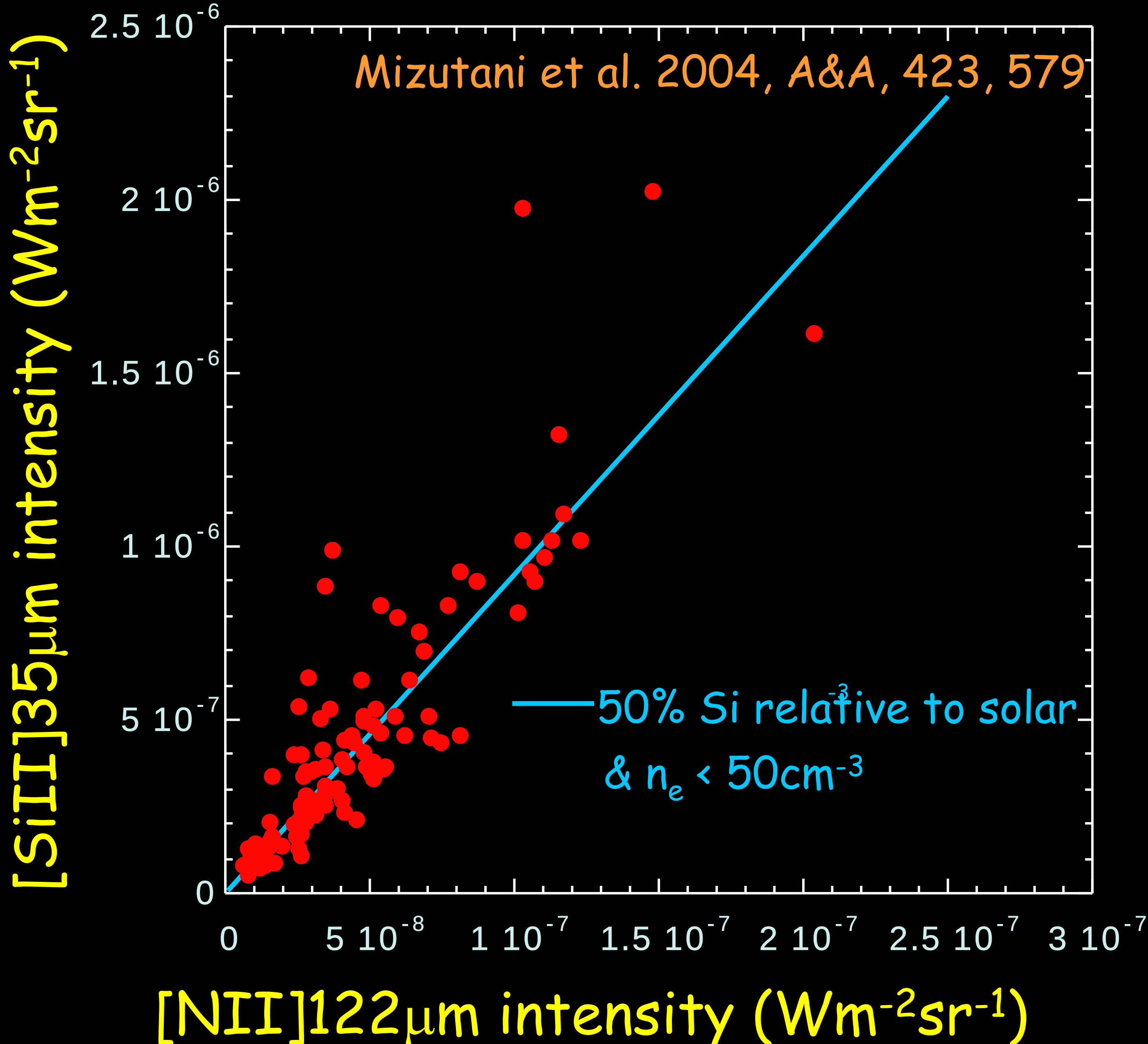

Si & Fe gas abundance in HII regions

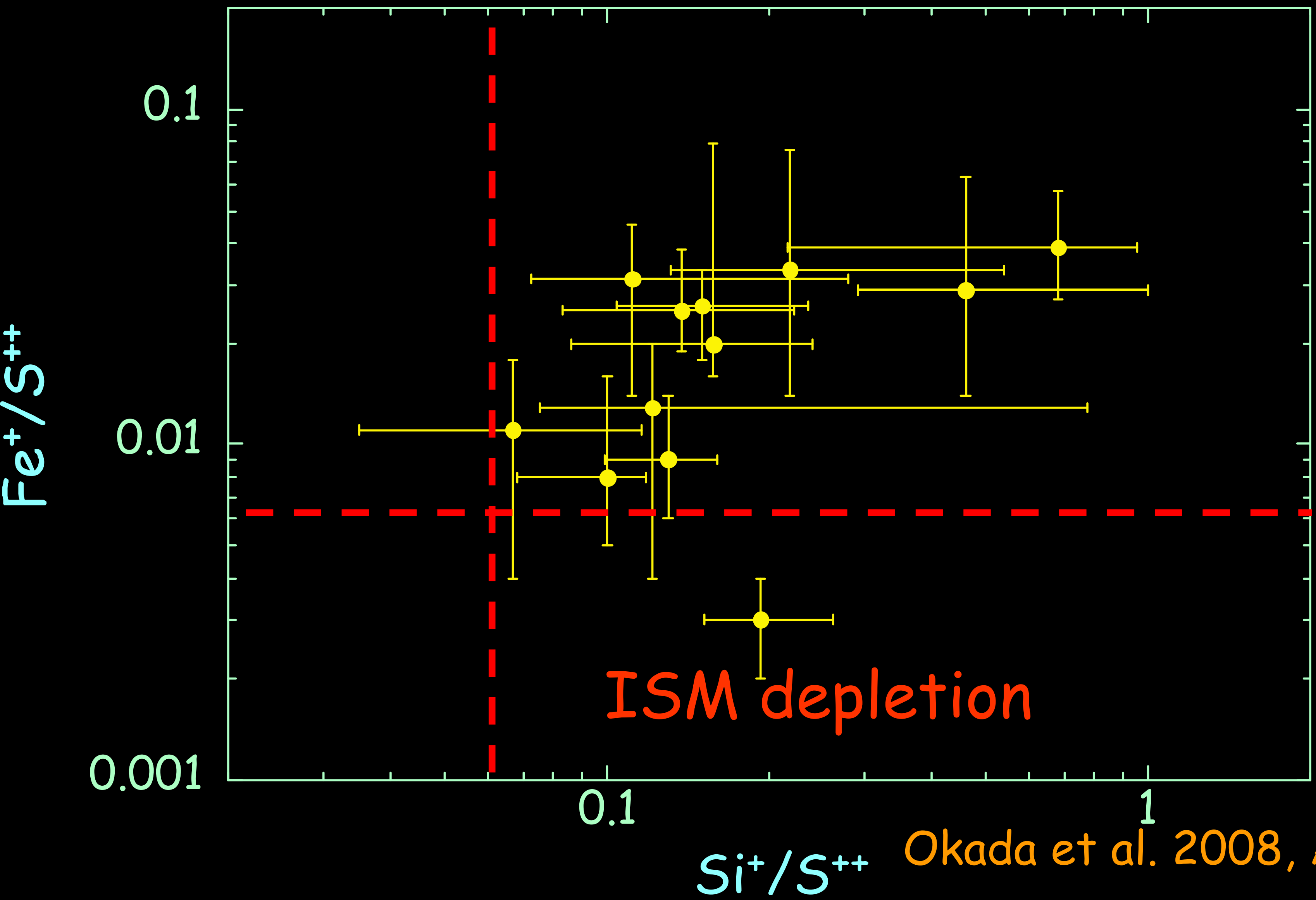

Large gas Si is common in HII regions
Fe is in a different component from volatile Si

Okada et al. 2008, ApJ, 682, 416

IR spectroscopy is efficient for the study of gas abundance in dense active regions

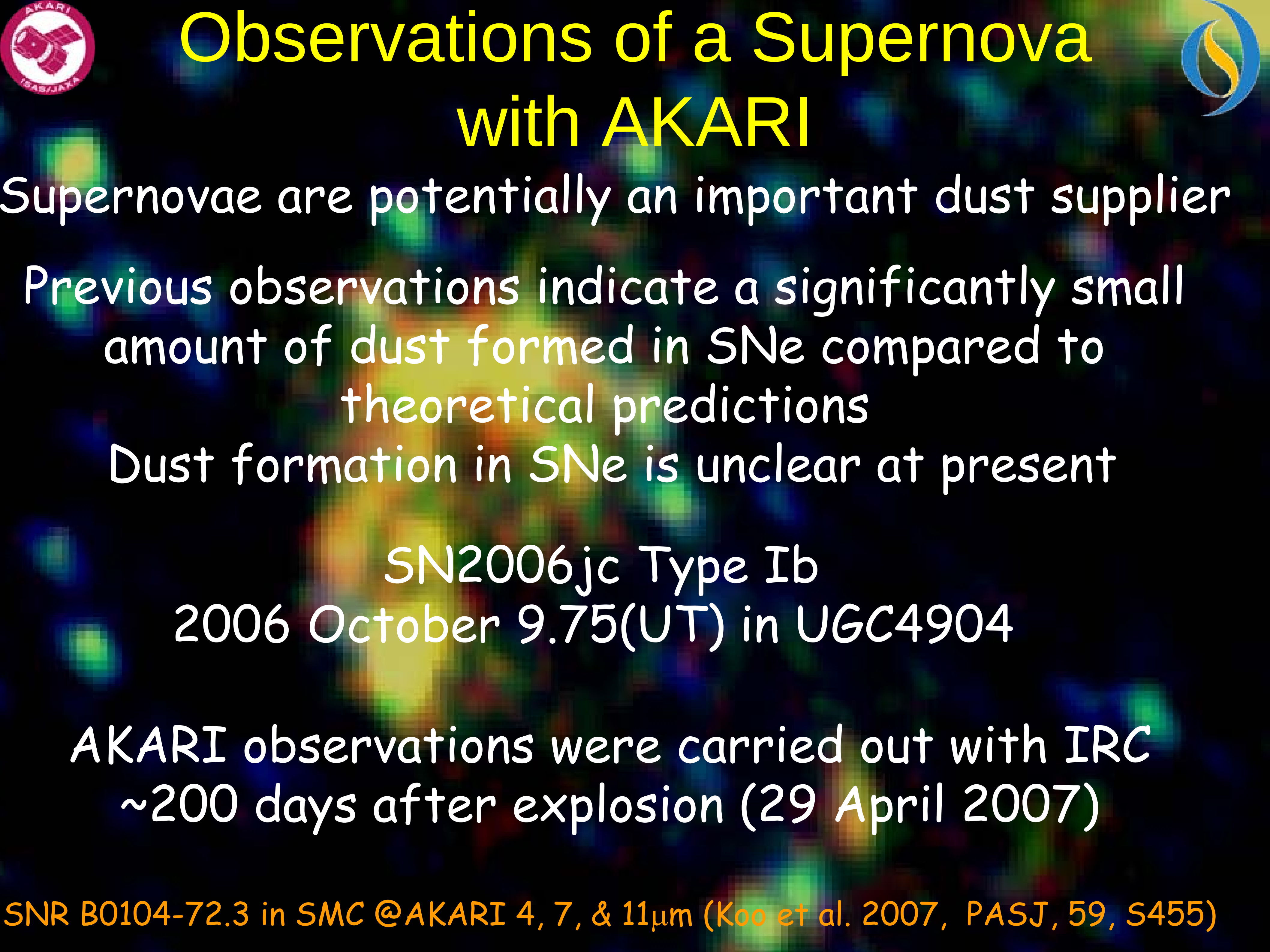
Observations of a Supernova with AKARI
Supernovae are potentially an important dust supplier
Previous observations indicate a significantly small amount of dust formed in SNe compared to theoretical predictions
Dust formation in SNe is unclear at present
SN2006jc Type Ib
2006 October 9.75(UT) in UGC4904
AKARI observations were carried out with IRC
~200 days after explosion (29 April 2007)
SNR B0104-72.3 in SMC @AKARI 4, 7, & 11μm (Koo et al. 2007, PASJ, 59, S455)

AKARI observations of SN2006jc

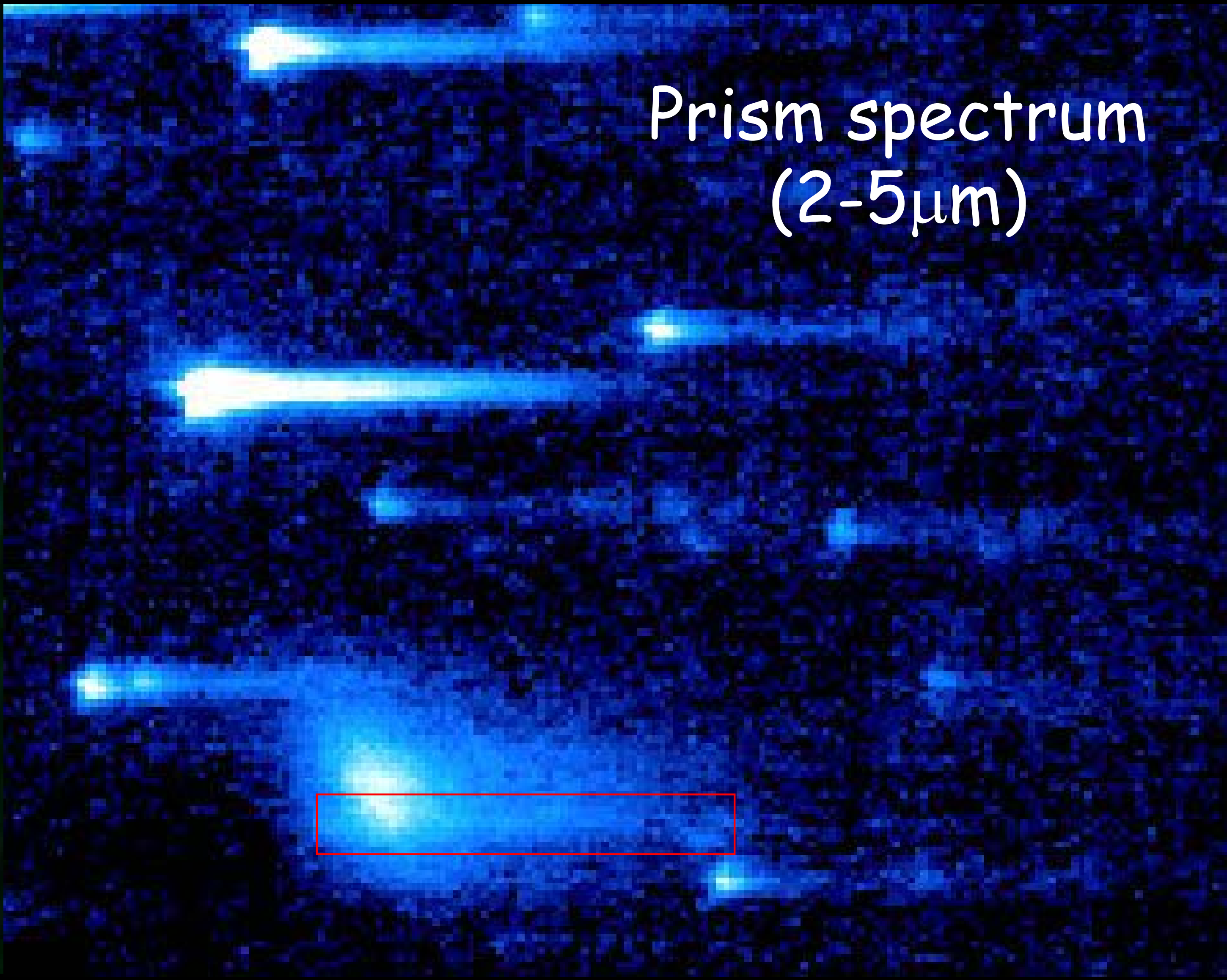

Strong emission in MIR detected

I. Sakon et al. (2009) ApJ in press

Strong MIR emission from circumstellar dust

Best fit: Hot (~800K: SN dust) and warm (~300K: circumstellar) carbon dust

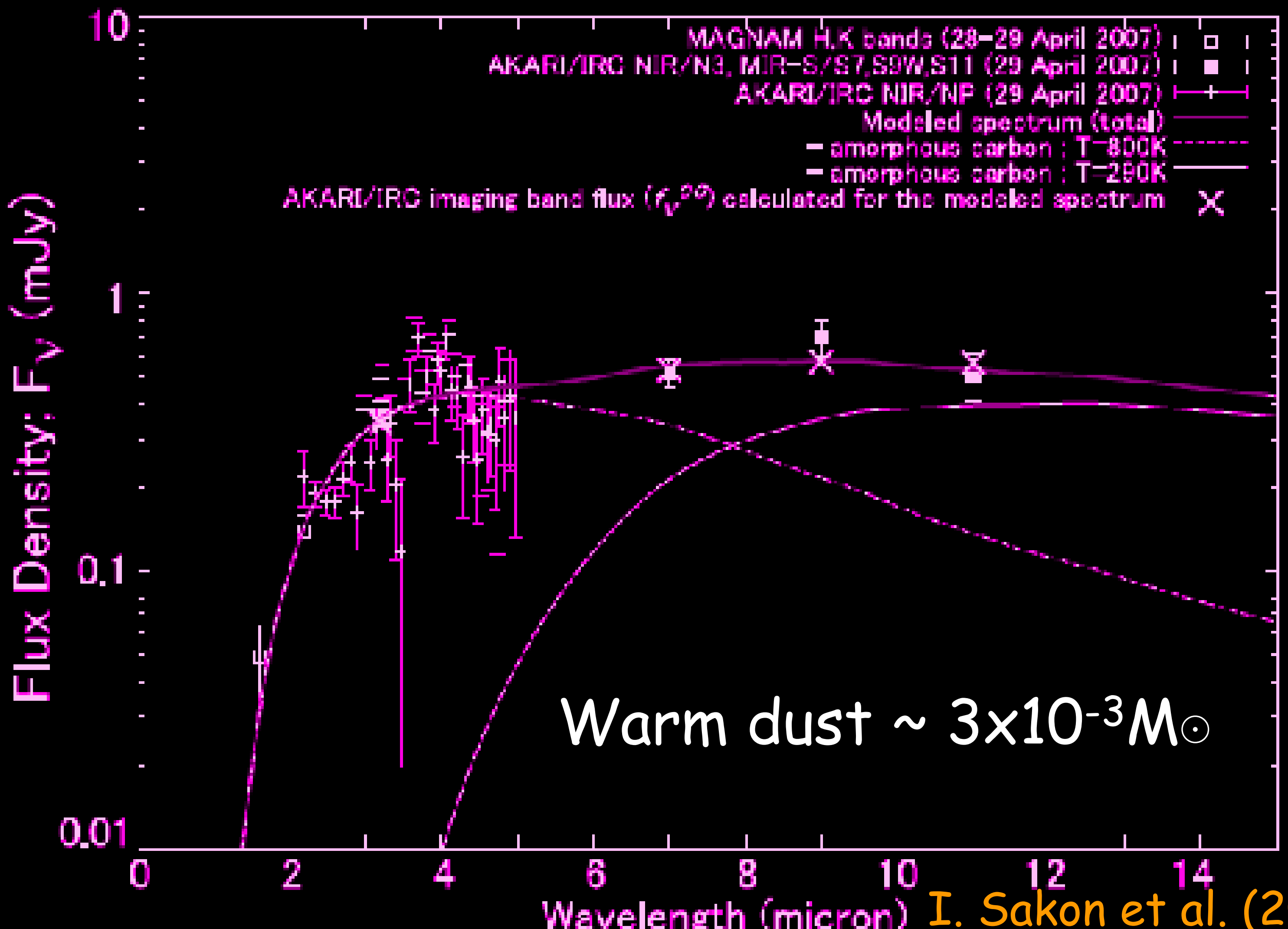

Few ($<10^{-4} M_\odot$) dust grains (hot component) formed in SN 2006jc

Dust formation in SNe is inefficient?

I. Sakon et al. (2009) ApJ in press

Dust associated with SN remnants

SNe are a source of dust and also destroy IS dust

Observations of SNRs in our Galaxy are difficult because of confusion -> Go to Large Magellanic Cloud

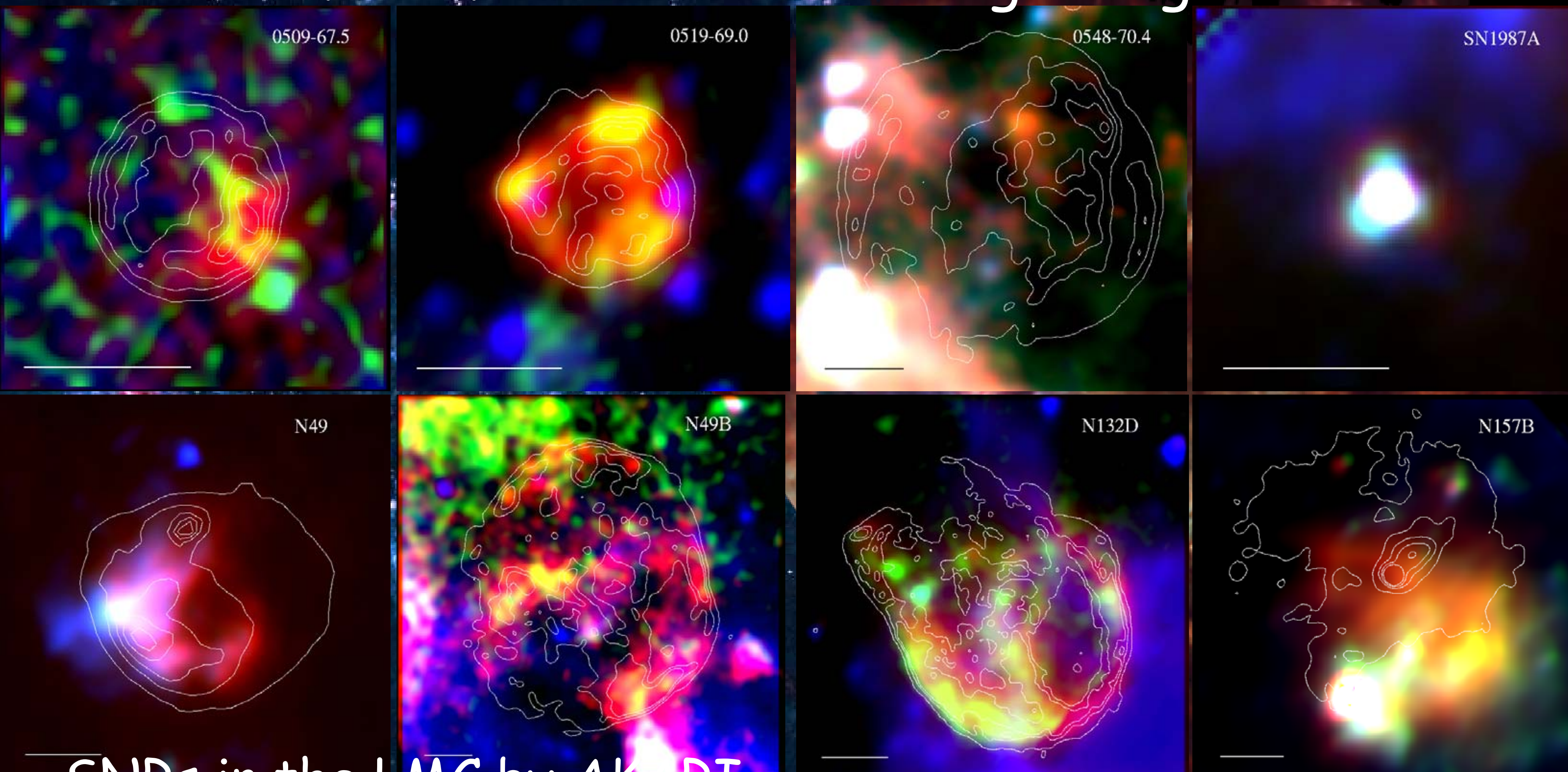

SNRs in the LMC by AKARI

(Seok et al. 2008, PASJ, 60, S453)

LMC@AKARI 9, 18, 65, 90, &140μm

Multi-component spectrum of SNRs

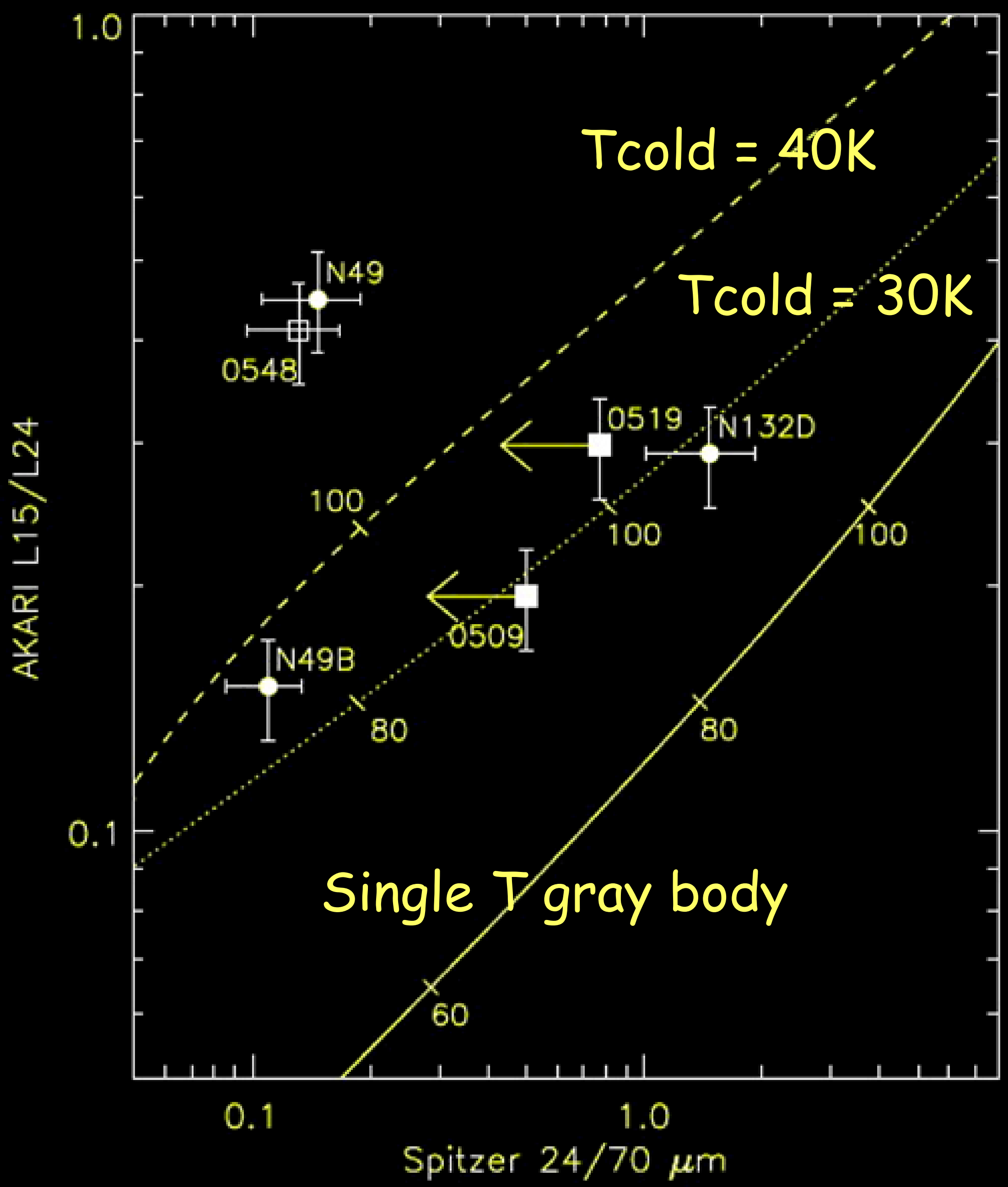

Seok et al. 2008 PASJ 60, S453

24 and 70μm flux is well fit by dust destruction model of SNR shocks (Borkowski et al. 2006, ApJ, 642, L141; Williams et al. 2006, ApJ, 652, L33)

15, 24, & 70μm flux can not be fit with a single temperature gray body, suggesting a cold dust component of large mass

More dust associated with SNRs in LMC, indicating less efficient dust destruction in SNRs

IRS Spectra of SNRs

Cas A

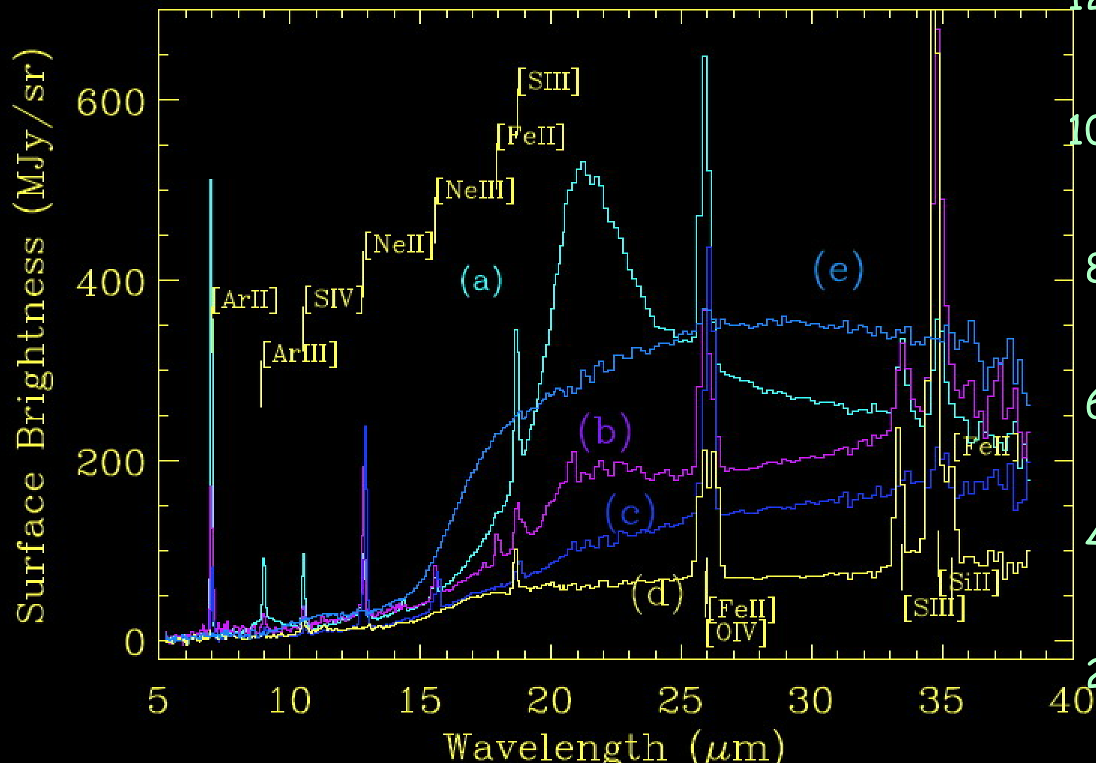

Rho et al. 2008, ApJ,. 673, 271

Kepler

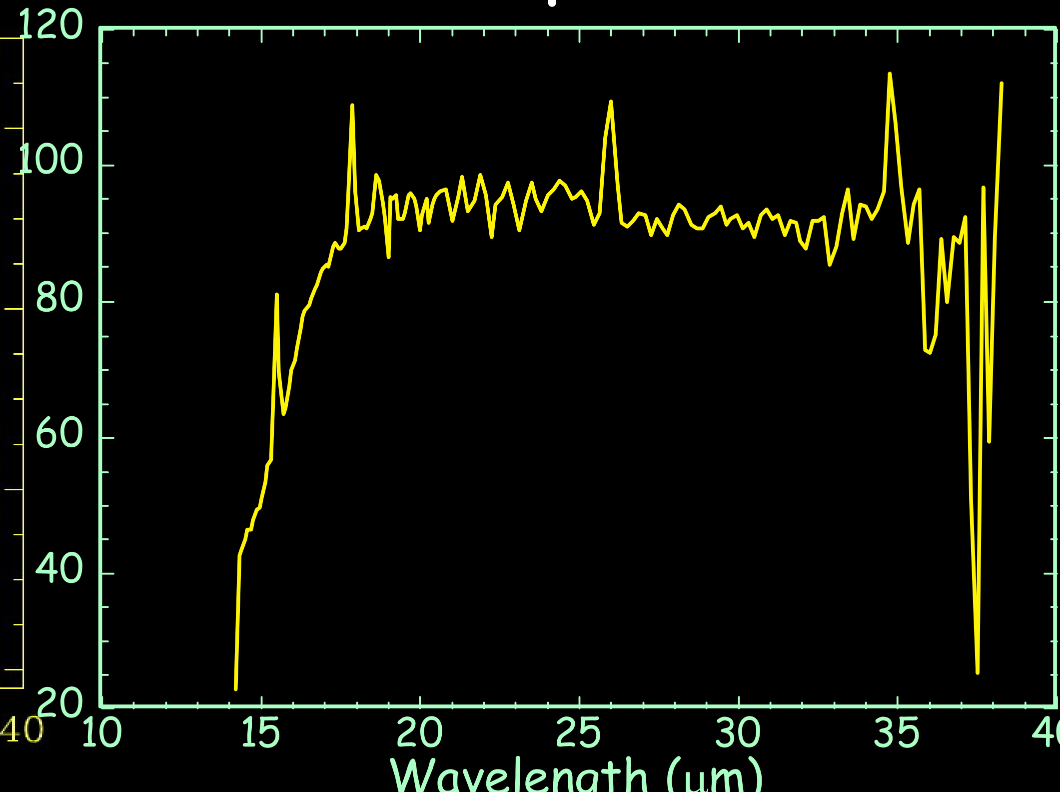

original schematics

SNR spectra have dust features + line emission cannot be fit by a single temperature gray body

Spectroscopic study is important

Dust processing in the ISM

Variations of the UIR bands provide significant information on the ISM processing of carbonaceous grains

A systematic trend is seen only in the 6.2/11.3 and 7.7/11.3 in particular environments

Role of SNe for dust supply and destruction is yet to be investigated observationally

Spectroscopic observations are indispensable to correctly understand the IR emission from SNRs

IR line spectroscopy has a great potential to study gas abundance of dense regions

Cyg X @AKARI 90 & 140μm

PASJ, 60

http://www.akari2009.com

AKARI All-Sky Survey

9μm source (~700,000)

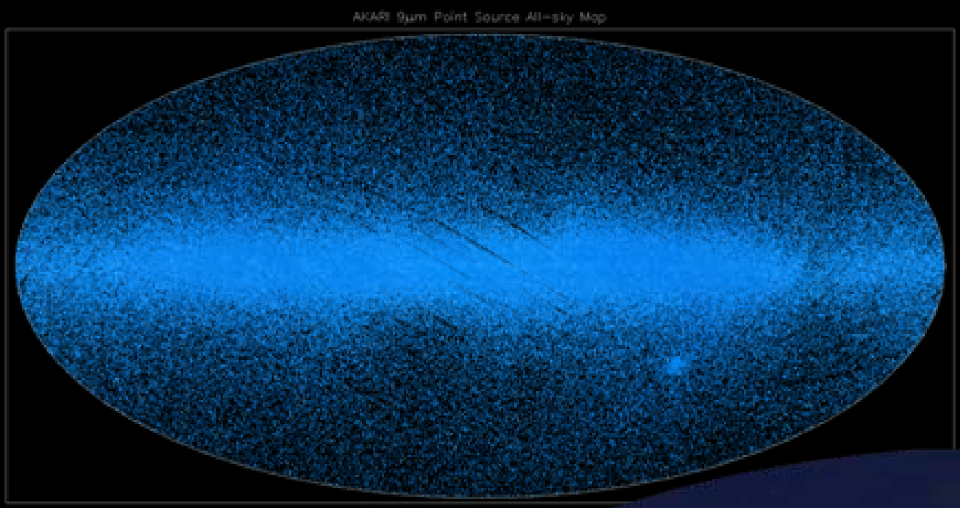

90μm source (~60,000)

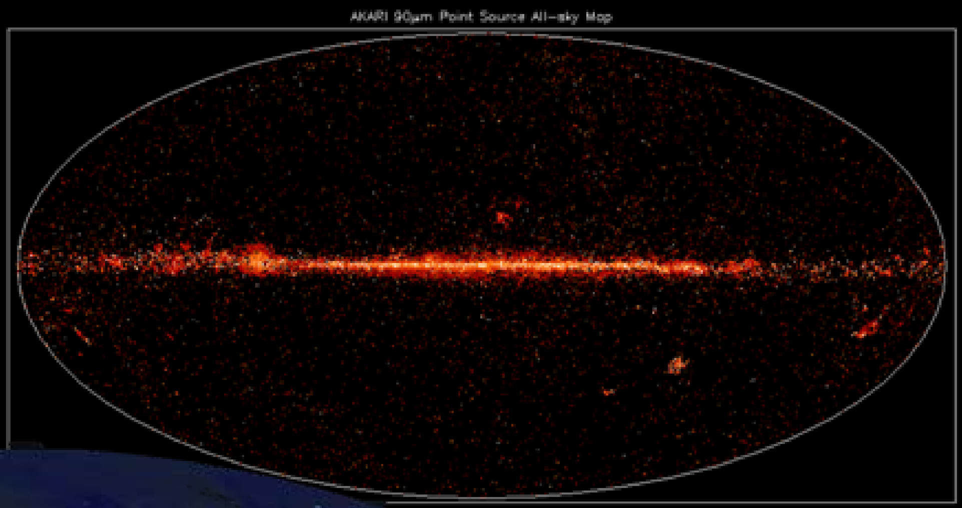

9 & 18μm

65, 90, 140, & 160μm

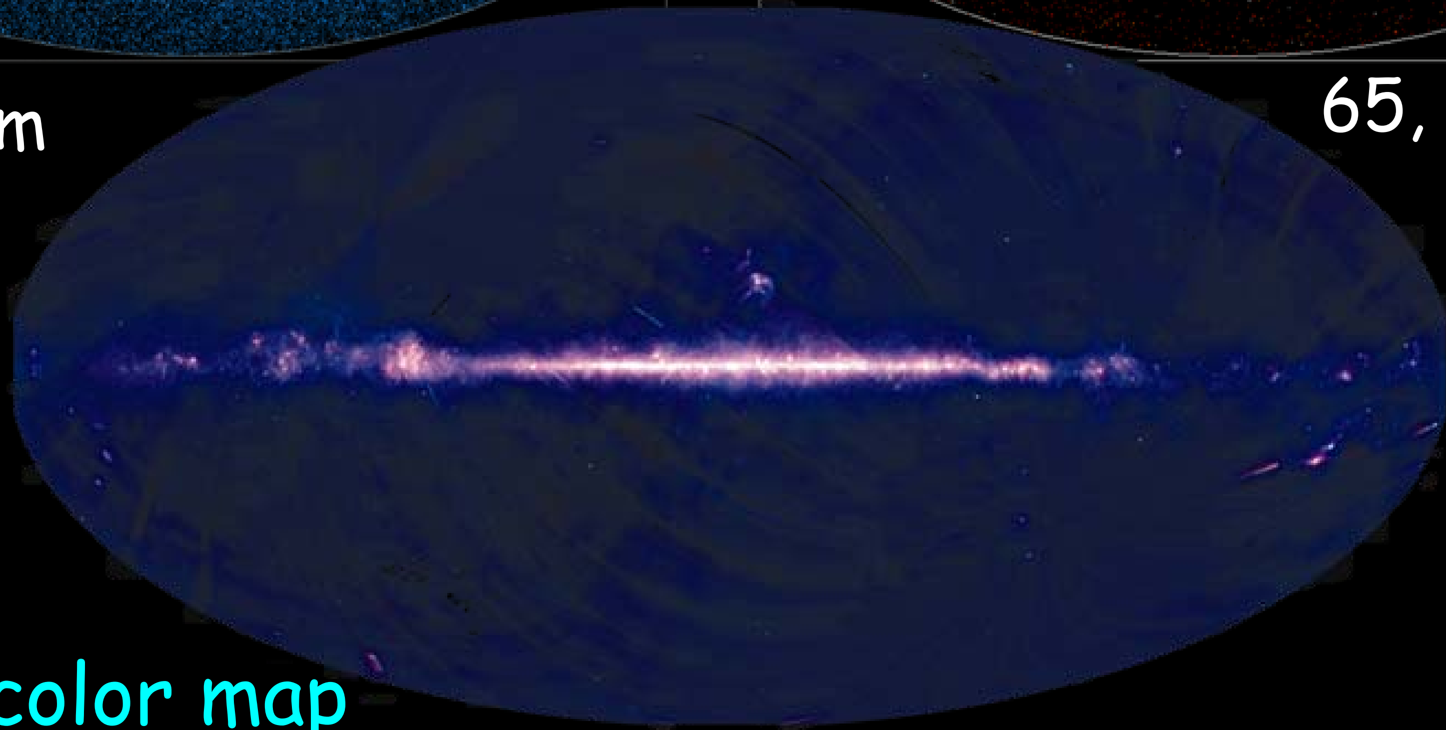

9-18μm color map

http://www.ir.isas.jaxa.jp/ASTRO-F/Outreach/results/PR081119/pr081119_1.html

AKARI All-Sky Survey Performance

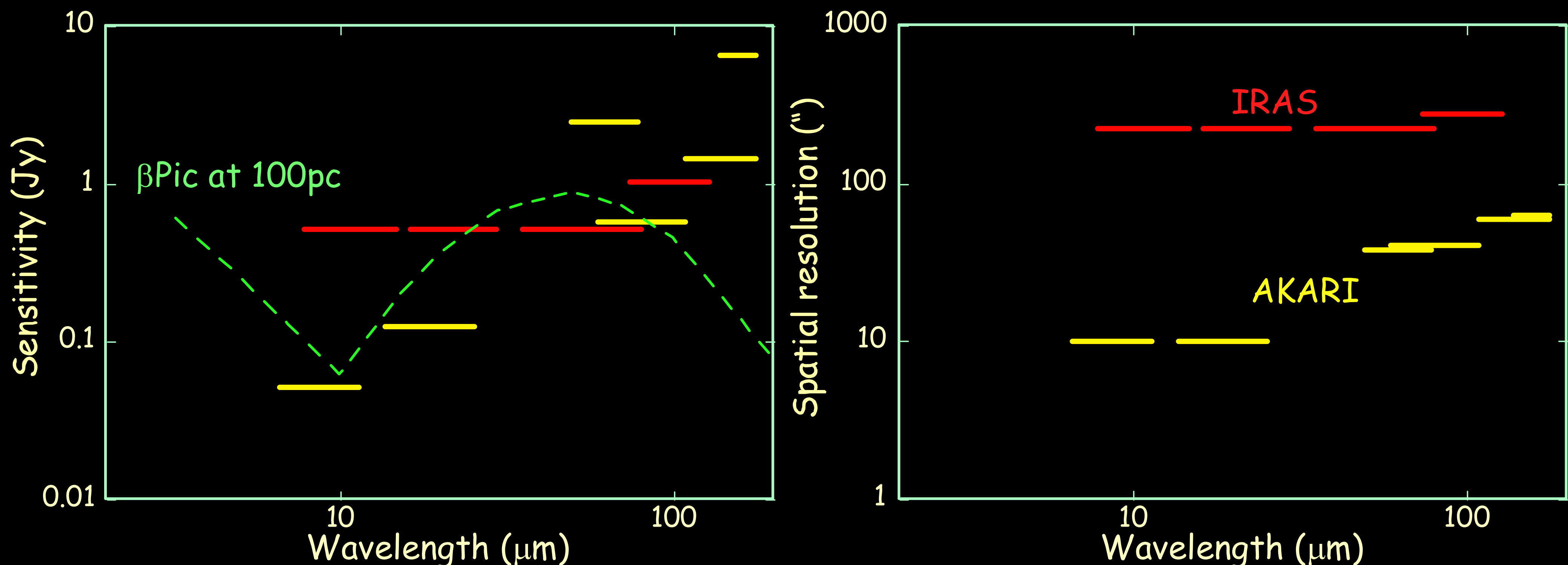

尾中 & 石原 2009, 天文月報, 102, 103

Higher sensitivity in 9-18μm than IRAS
Higher spatial resolution than IRAS

Point Source Catalogues will be released
to the public in 2009

Herschel & Planck (ESA) (2009)

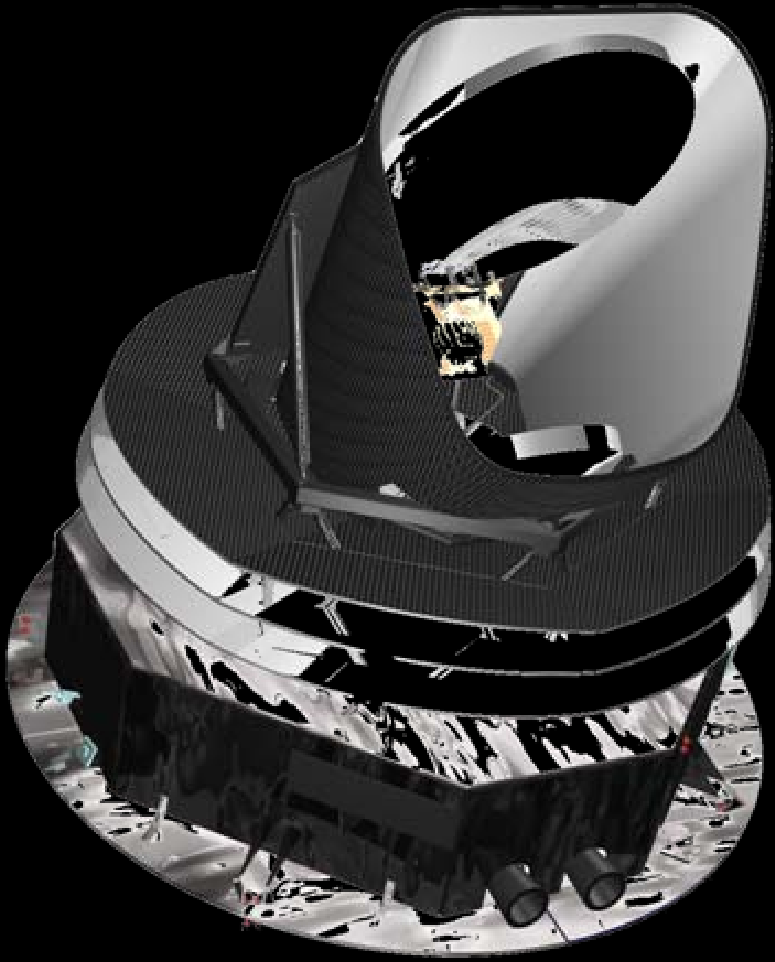

Herschel (3.5m) (55-672μm)

Planck (1.5m) (350μm – 9mm)

WISE & JWST (NASA)

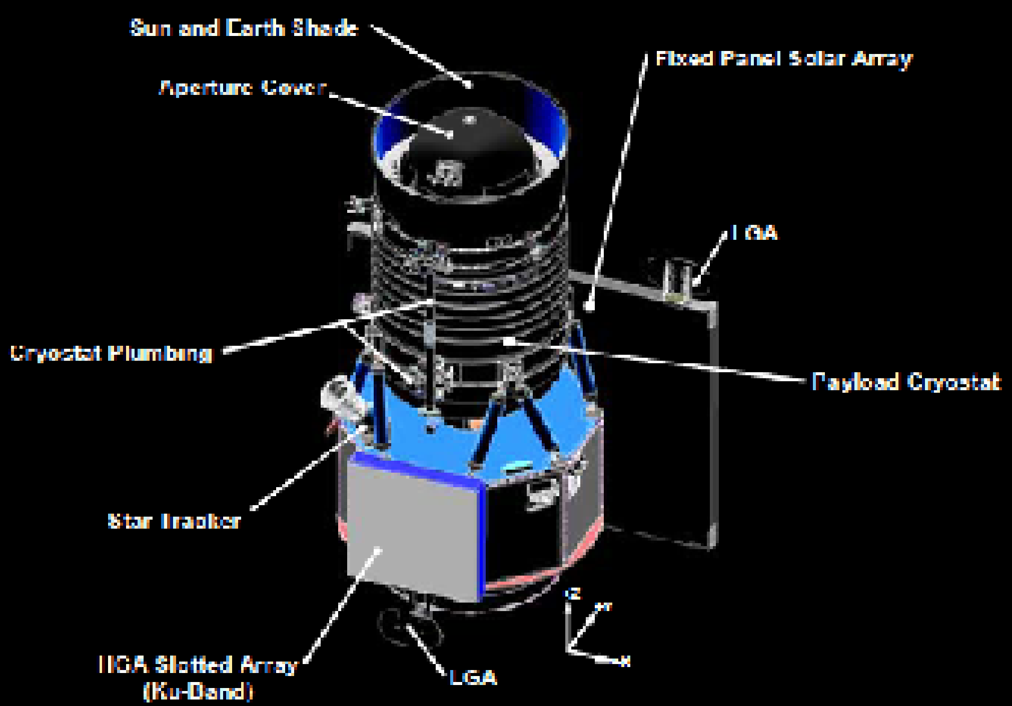

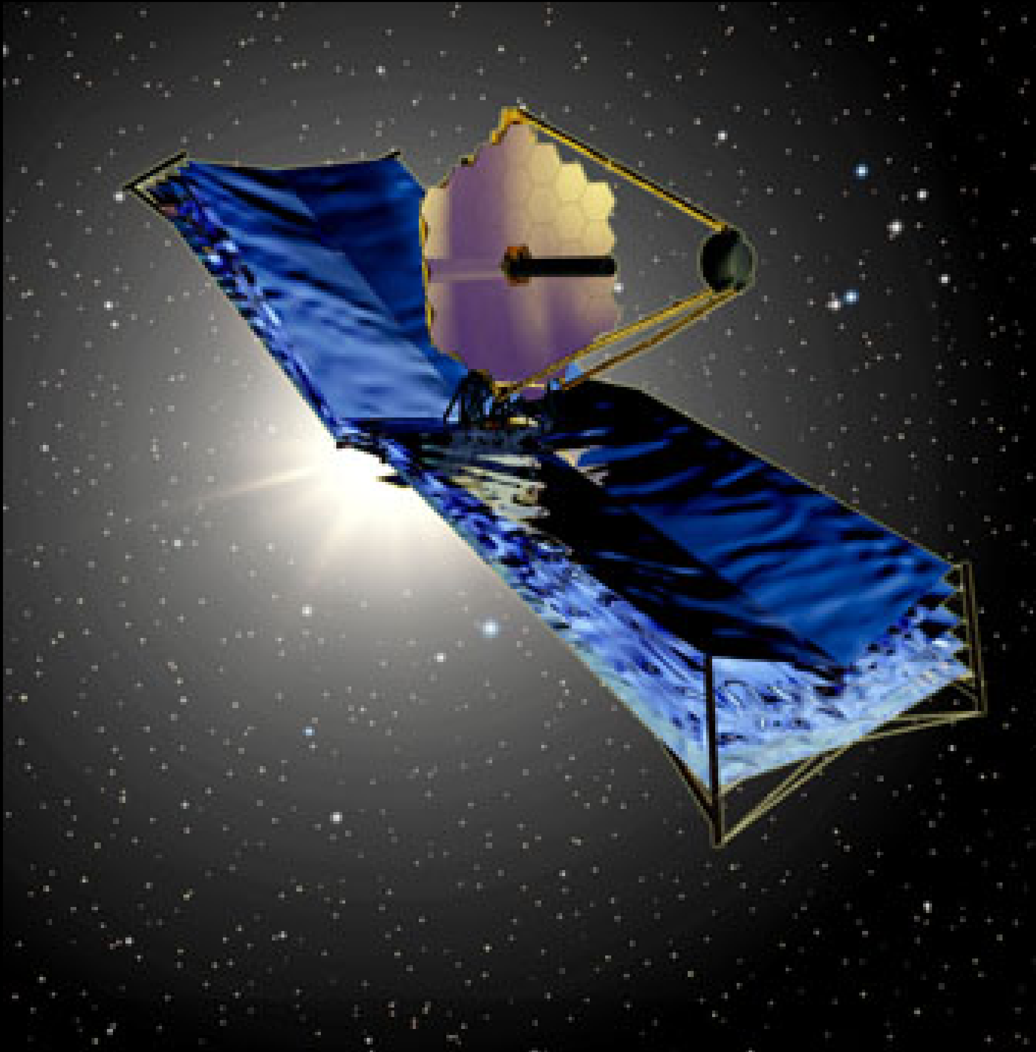

WISE (2009) 40cm
3-24μm

JWST (2013) 6.5m
<28μm

Space Infrared Telescope for Cosmology and Astrophysics (SPICA)

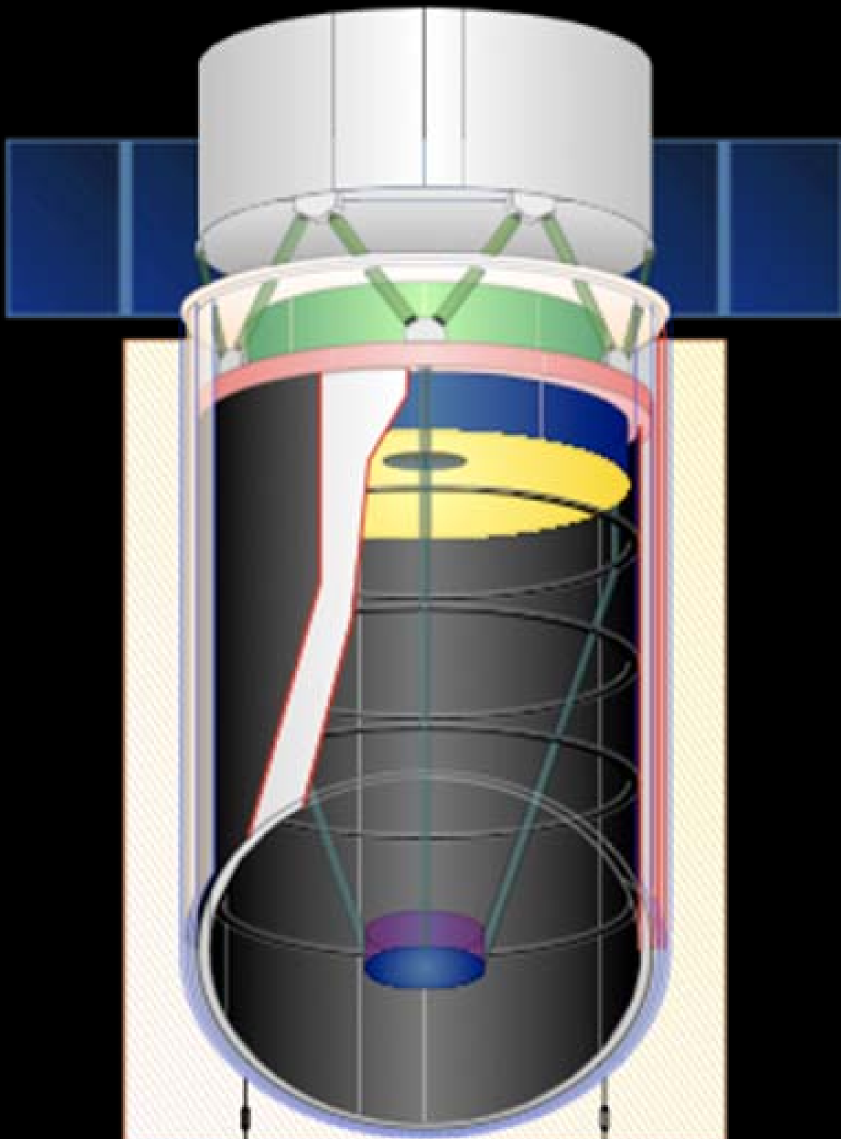

SPICA 3.5m ISAS/JAXA
Cooled telescope by mechanical coolers
for wavelengths 5 -200μm

Approved to
phase-A study by JAXA
ESA contribution approved
aiming at 2017 launch

http://www.ir.isas.jaxa.jp/SPICA/index.html

Thank you for your attention

Many thanks to the LOC

Reference

- Fitzpatrick, E. L., & Massa, D. 1986, ApJ, 307, 286
- Bradley, J., Dai, Z. R., Erni, R., et al. 2005, Science, 307, 244
- Steel, T. M., & Duley, W. W. 1987, ApJ, 315, 337
- Savage, B. D., & Sembach, K. R. 1996, ARA&A, 34,279
- Predehl, P., & Schmitt, J. H. M. M. 1995, A&A, 293, 889
- Henke, B. L., Lee. P., Tanaka, T. J., et al. 1982, Atomic Data and Nuclear Data Tables, 27, 1
- Takei, Y., Fujimoto, R., Mitsuda, K., & Onaka, T. 2002, ApJ, 581, 307
- Costantini, E., Freyberg, M. J., & Predehl, P. 2005, A&A, 444, 187
- Draine, B. T. 2003, ApJ, 598, 1026
- Ueda, Y., Mitsuda, K., Murakami, H., & Matsushita, K. 2005, ApJ, 620, 274

Reference

- Kaneda, H., Onaka, T., Nakagawa, T., et al. 2005, Appl. Opt., 44, 6823
- 尾中 & 石原 2009, 天文月報, 102, 103
- Onaka, T., Yamamura, I., Tanabe, T., et al. 1996, PASJ, 48, 59
- Onaka, T., Mizutani, M., Chen, K. W., et al. 2000, ESASP, 456, 55
- Kahanpaa, J., Mattila, K., Lehtinen, K., et al. 2003, A&A, 405, 999
- Sakon, I., Onaka, T., Ishihara, D., et al. 2004, ApJ, 609, 203
- Kaneda, H., Onaka, T., & Sakon, I. 2005, ApJ, 632, 83
- Kaneda, H., Onaka, T., & Sakon, I. 2007, ApJ, 666, 21
- Kaneda, H., Onaka, T., Sakon, I., et al. 2008, ApJ, 684, 270
- Sakon, I., Onaka, T., Wada, T., et al. 2007, PASJ, 59, 483

The 1st CPS International School of Planetary Sciences
Dust in Space
January 5 - 9, 2009
Kobe, Japan

Reference

- Engelbracht, C. W., Kundurthy, P., Gordon, K. D., et al. 2006, ApJ, 642, 127
- Galliano, F., Madden, S. C., Tielens, A. G. G. M., et al. 2008, ApJ, 679, 310
- Matsumoto, H., et al. 2009, Proc. of IAU, 251, 249
- Gordon, K. D., Engelbracht, C. W., Rieke, G. H., et al. 2008, ApJ, 682, 336
- Mizutani, M., Onaka, T., & Shibai, H. 2004, A&A, 423, 579
- Okada, Y., Onaka, T., Miyata, T., et al. 2008, ApJ, 682, 416
- Koo, B.-C., Lee, H.-G., Moon, D.-S., et al. 2007, PASJ, 59S, 455
- Sakon, I., et al. 2009, ApJ in press
- Seok, J. Y., Koo. B.-C., Onaka, T., et al. 2008, PASJ, 60, 453